2. Structure of wall-bounded flows

Alexander J. Smits

Department of Mechanical and Aerospace Engineering
Princeton University

Lecture 2, 23 August 2023
Les Houches School of Physics

ÉCOLE DE PHYSIQUE DES HOUCHES

Turbulent flows and Reynolds number

- As the Reynolds number increases, so does the range of scales

$$Re_\tau = \frac{\delta}{\nu/u_\tau} = \frac{\delta u_\tau}{\nu}$$

- That is, the spectrum broadens
- We will focus primarily on the one-dimensional spectrum of u’

$$\overline{u^2} = \int_0^\infty E(k)dk = \int_0^\infty kE(k)d\log k$$

$Re_\tau \approx 150$

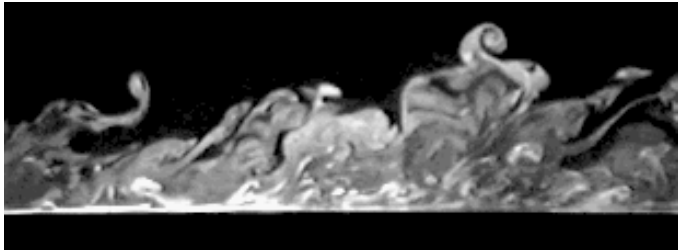

Delo, Kelso & Smits (2004)

$Re_\tau \approx 2000$

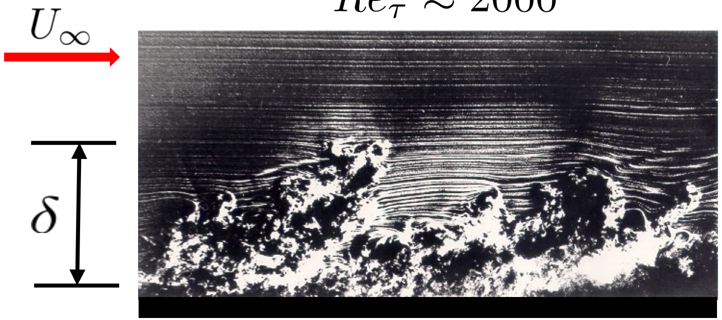

Corke, Guezennec & Nagib (1980)

Turbulent spectra

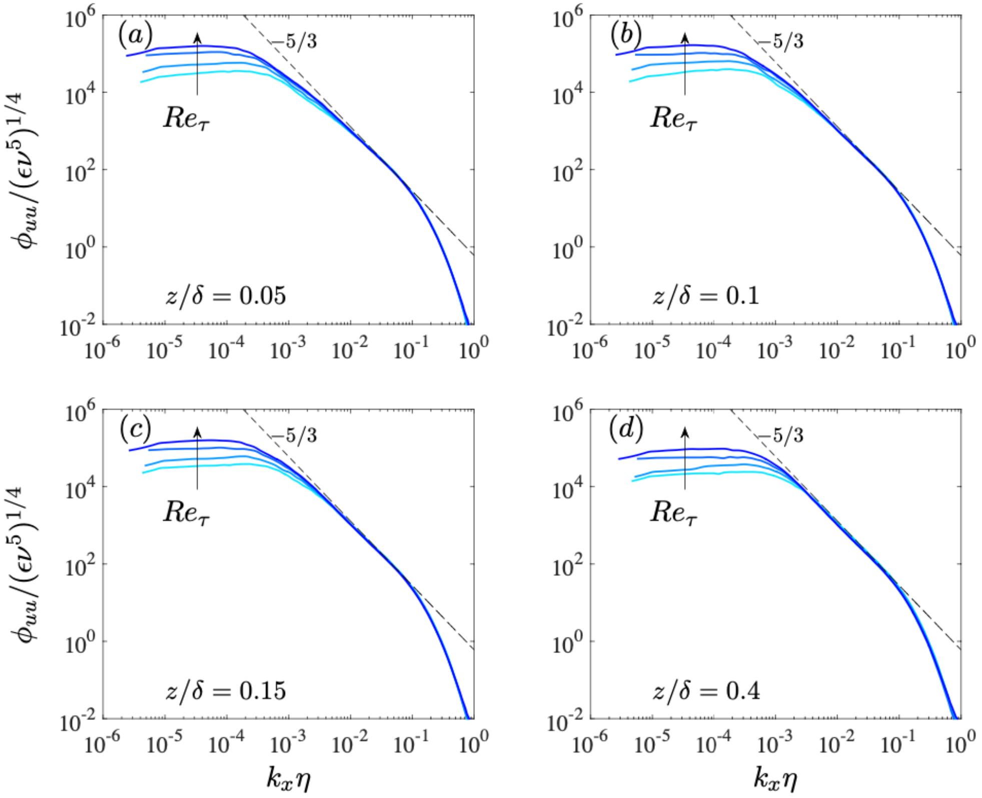

Boundary layer:

$Re_\tau = 6000;\ 10{,}000;\ 14{,}500;\ 20{,}000$

Dissipation from isotropic estimate:

$$\varepsilon = 15\nu \int_0^\infty k_x^2 \phi_{uu} dk$$

$$\eta = (\nu^3/\varepsilon)^{1/4}$$

Inertial region grows with Reynolds number and with distance from the wall

Samie et al. (2018)

Premultiplied spectra

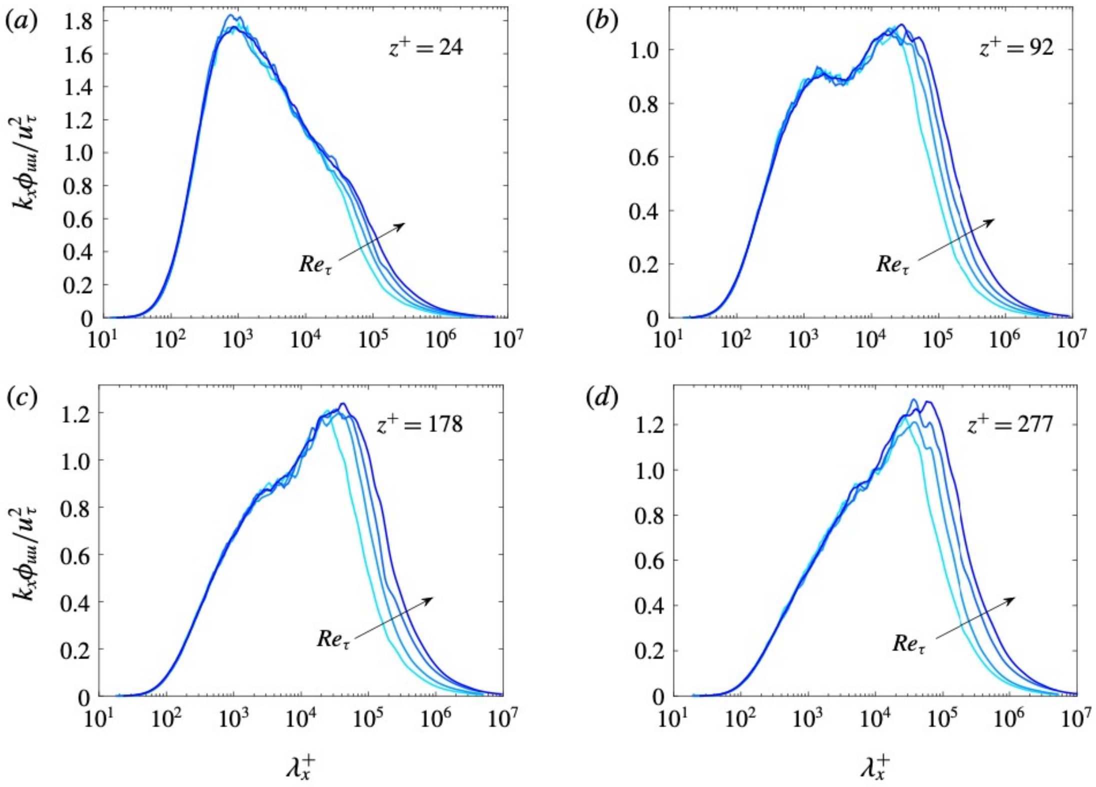

Boundary layer:

$Re_\tau = 6000;\ 10{,}000;\ 14{,}500;\ 20{,}000$

$$\overline{u^2} = \int_0^\infty E(k)dk = \int_0^\infty kE(k)d\log k$$

- Small scale motions independent of Reynolds number
- Large scales present even very close to the wall
- Energy in large scales grows with Reynolds number

Samie et al. (2018)

Comparing pipe and boundary layer

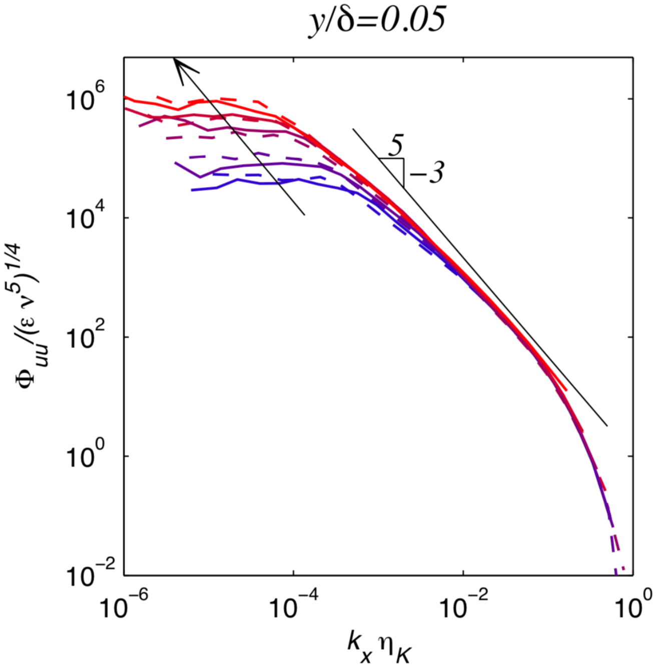

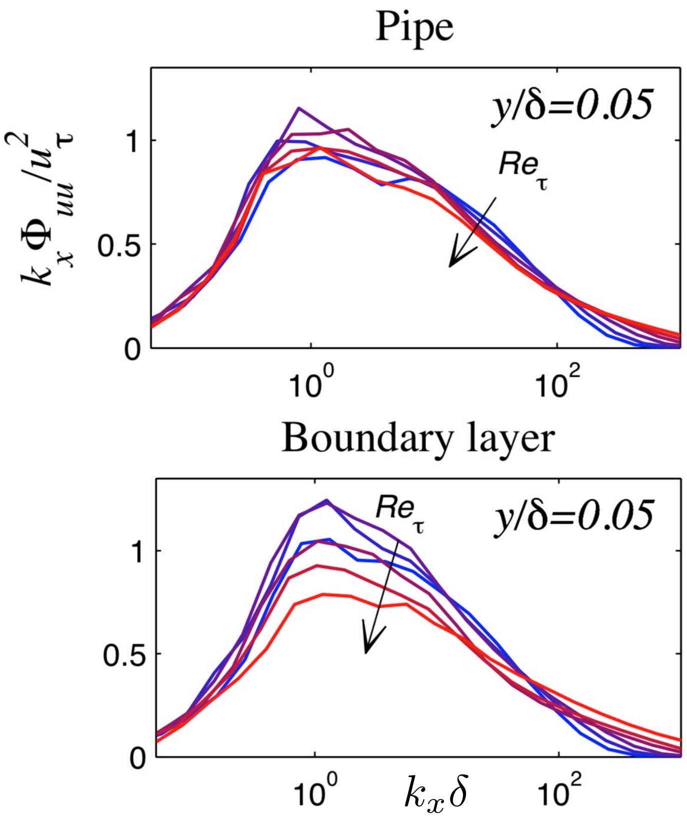

Margit Vallikivi

Vallikivi, Ganapathasubramani & Smits (2015)

Comparing boundary layer and pipe

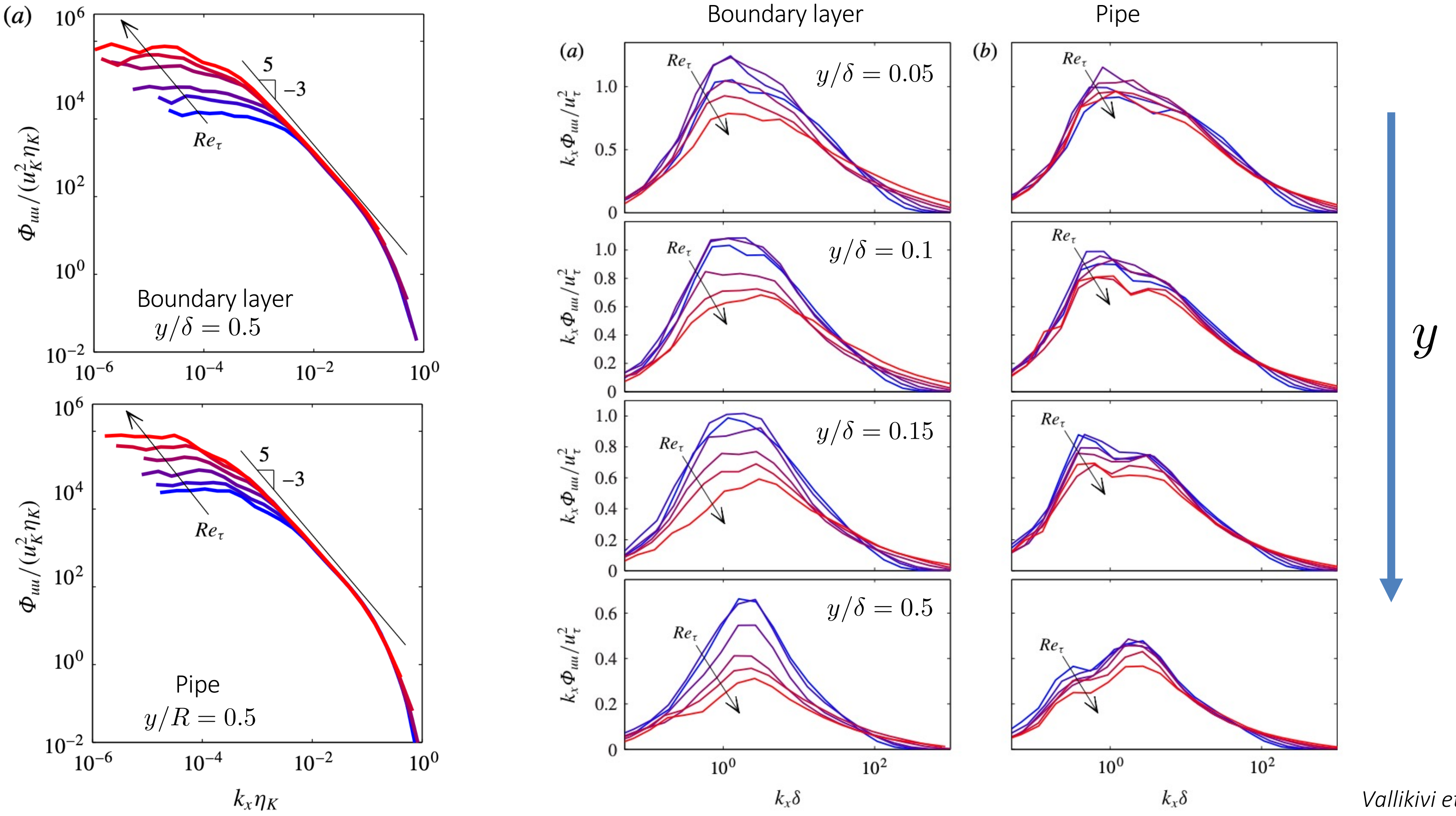

Vallikivi et al. (2015)

Premultiplied energy and dissipation spectra

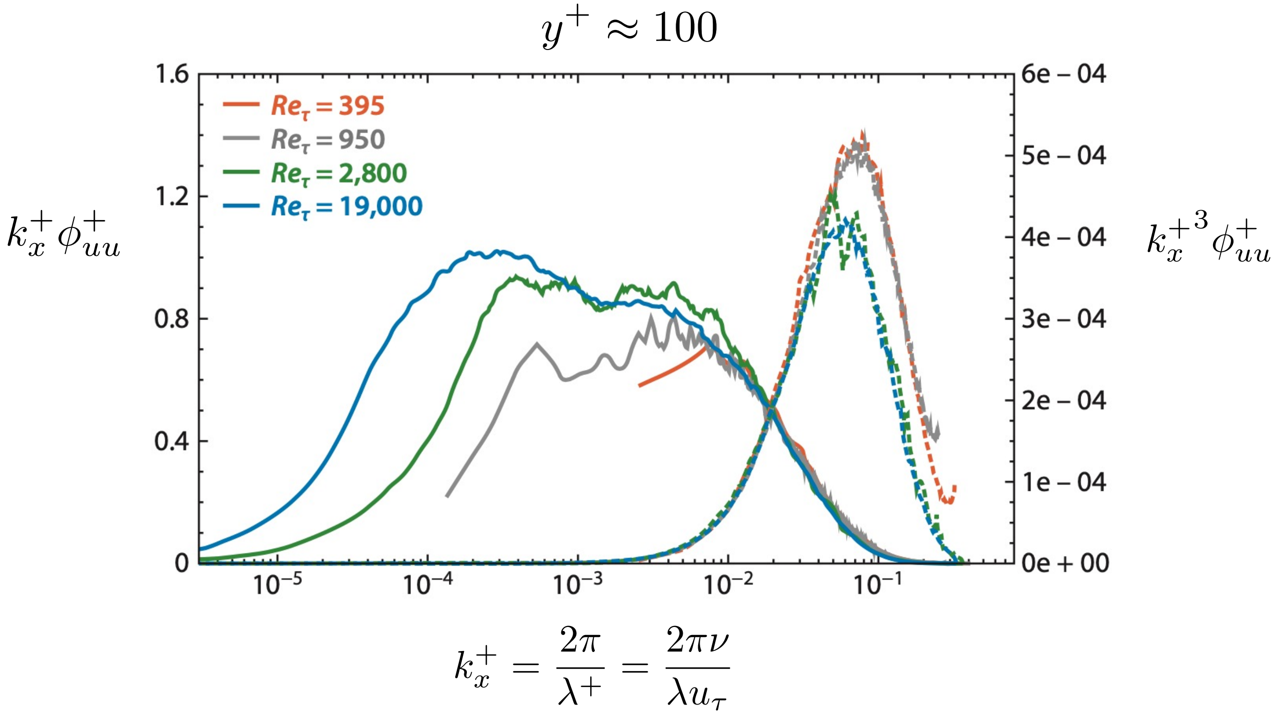

Smits, McKeon & Marusic (2011)

Premultiplied spectral maps

Re_τ = 5000, boundary layer

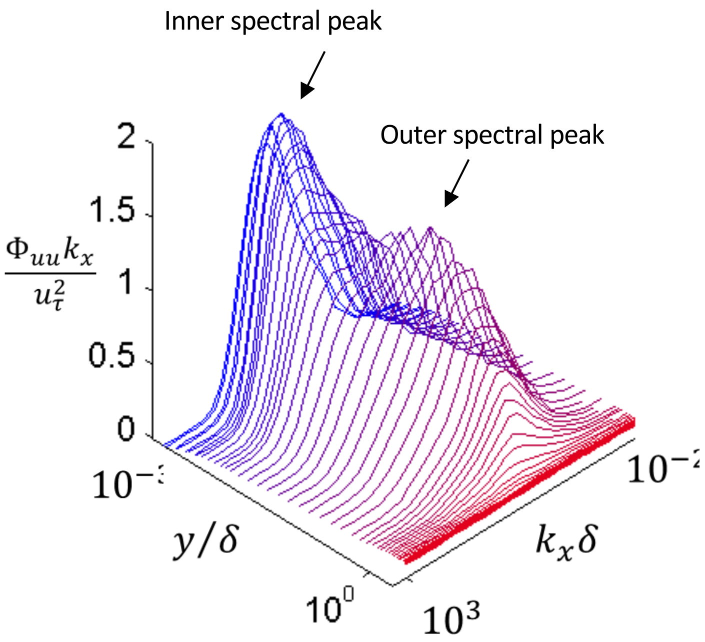

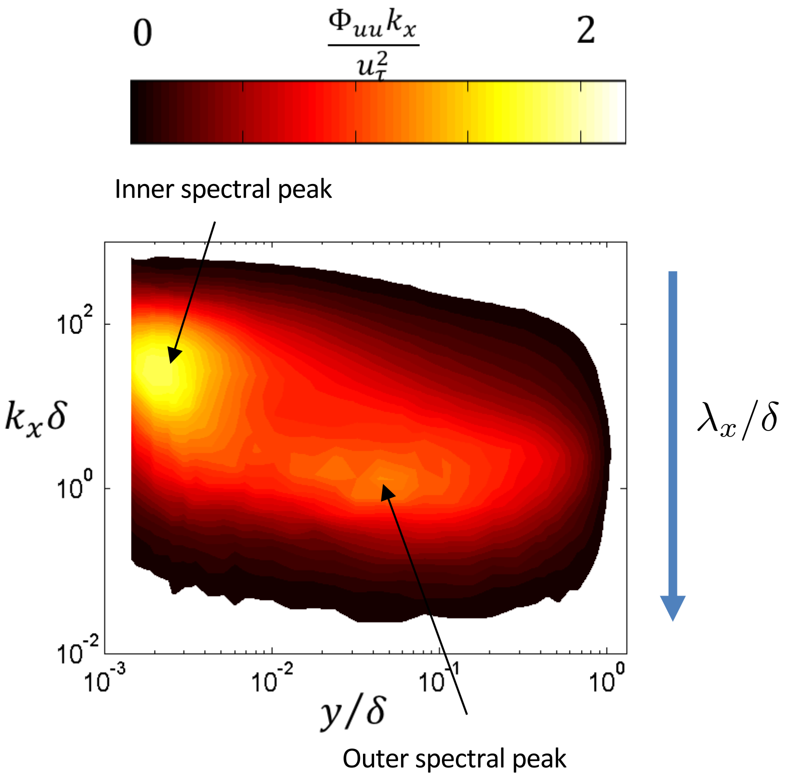

With thanks to Nick Hutchins

Premultiplied spectral maps

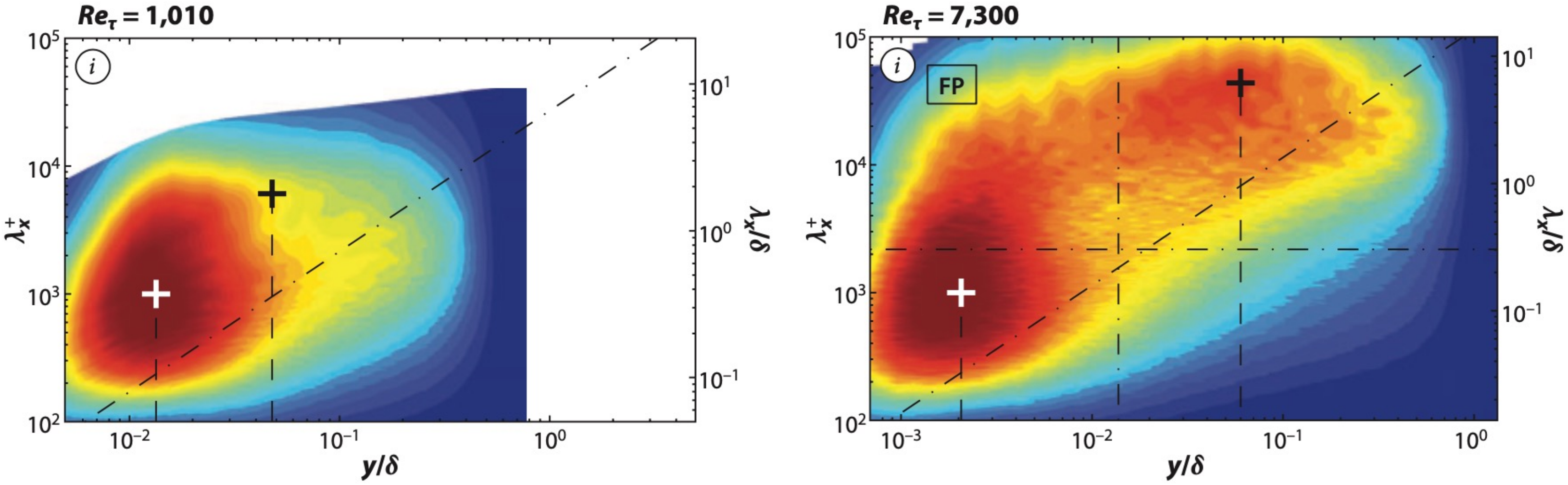

Smits, McKeon & Marusic (2011)

Boundary layer

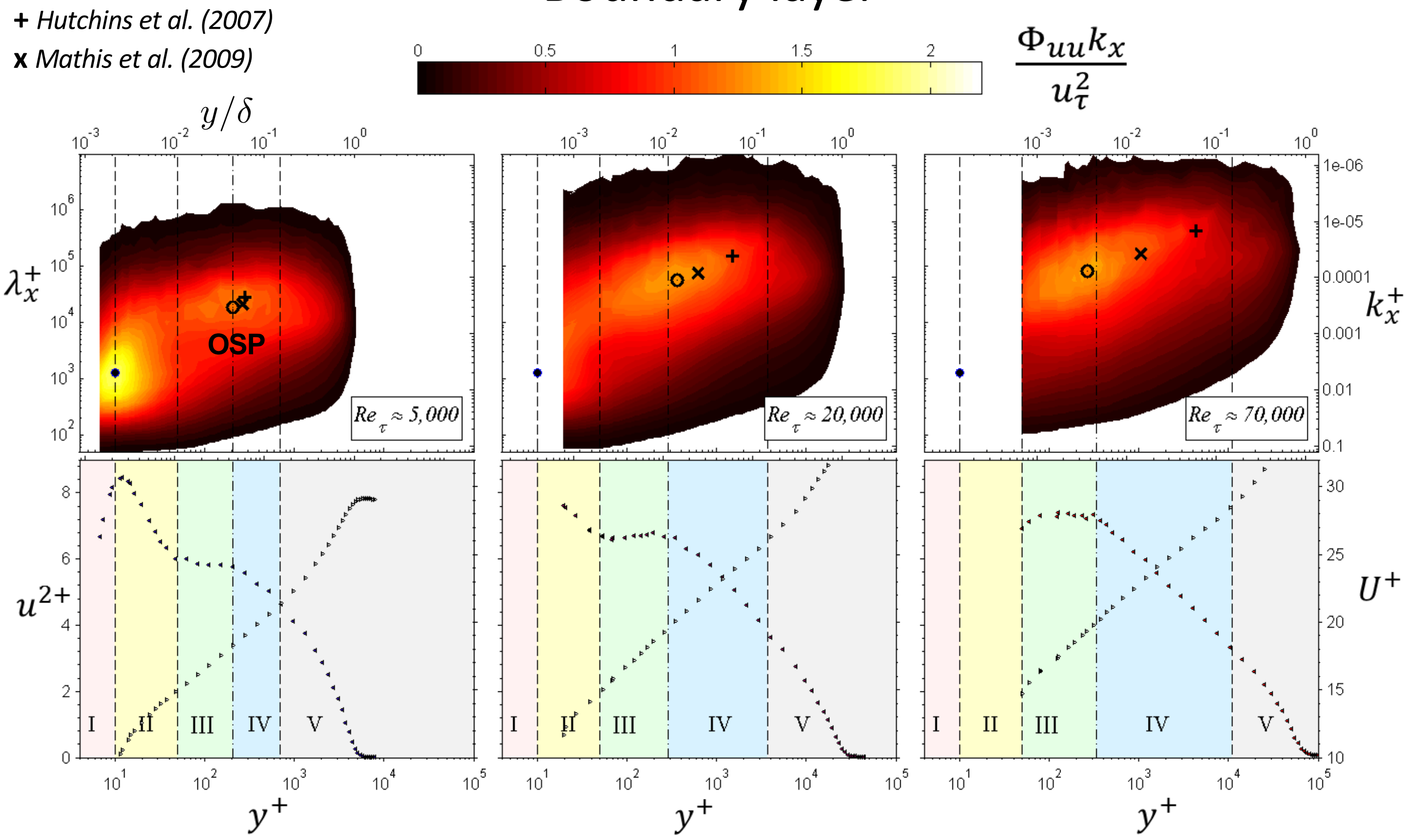

I – Linear Sublayer
II – Buffer Layer
III – Mesolayer
IV – Inertial Sublayer
V – Wake Region

Pipe

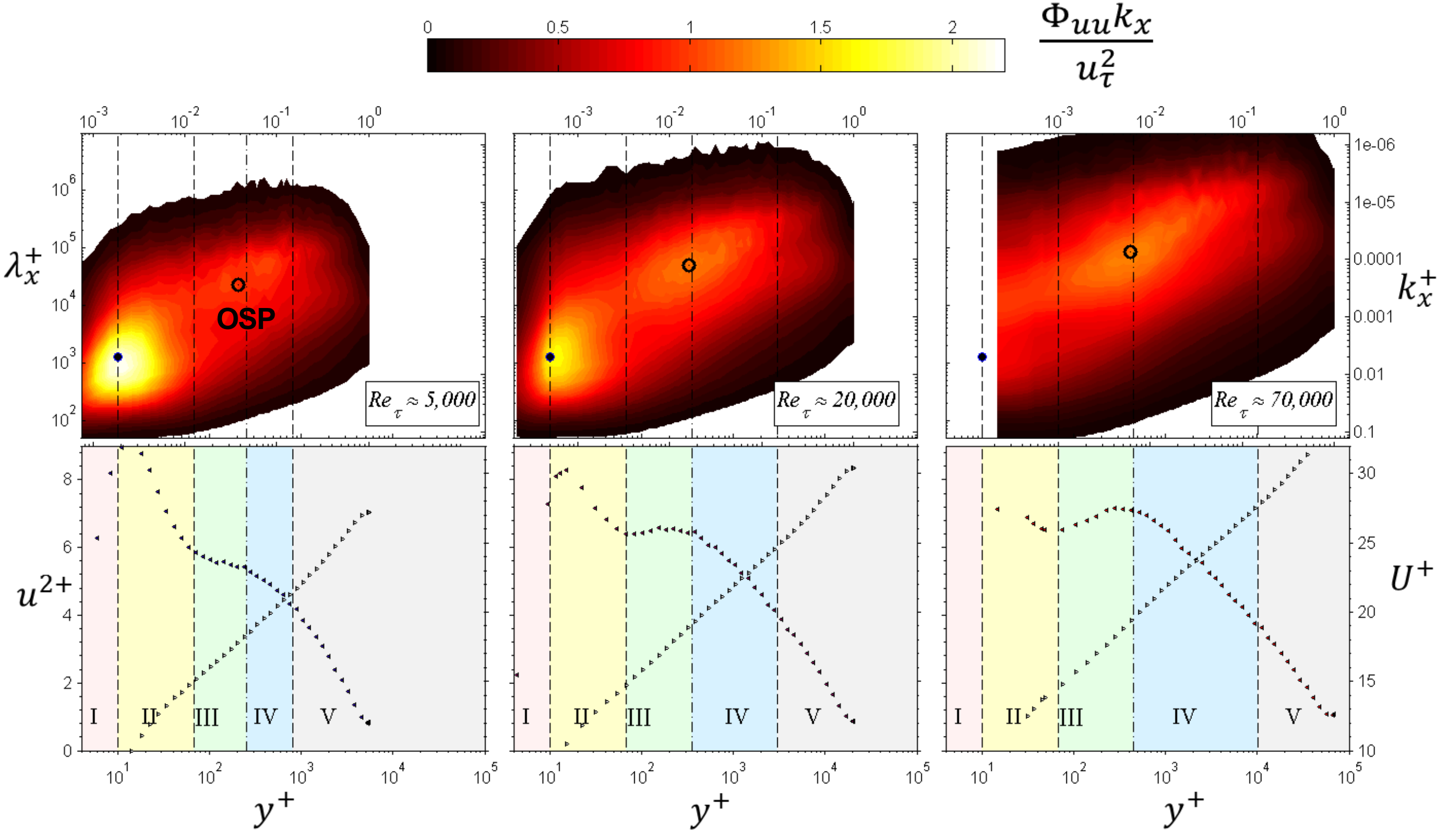

I – Linear Sublayer
II – Buffer Layer
III – Mesolayer
IV – Inertial Sublayer
V – Wake Region

The structure of wall-bounded turbulence

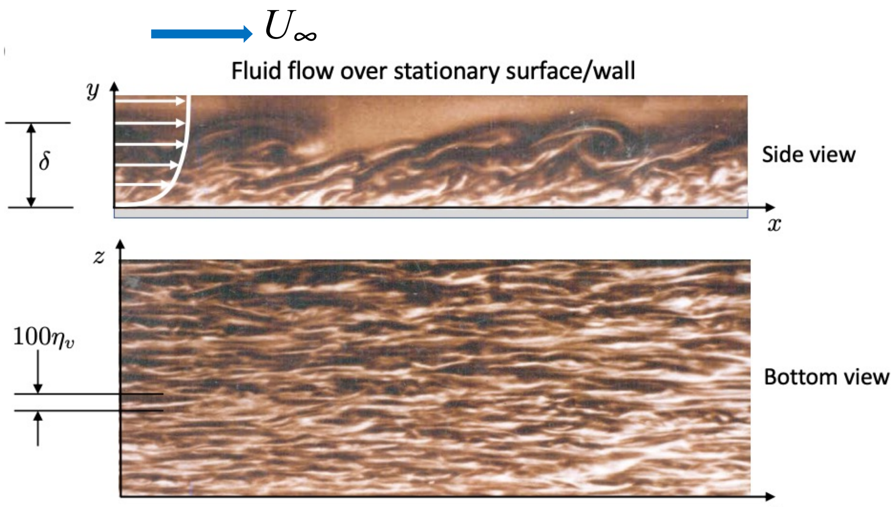

Cantwell, Coles & Dimotakis (1978)

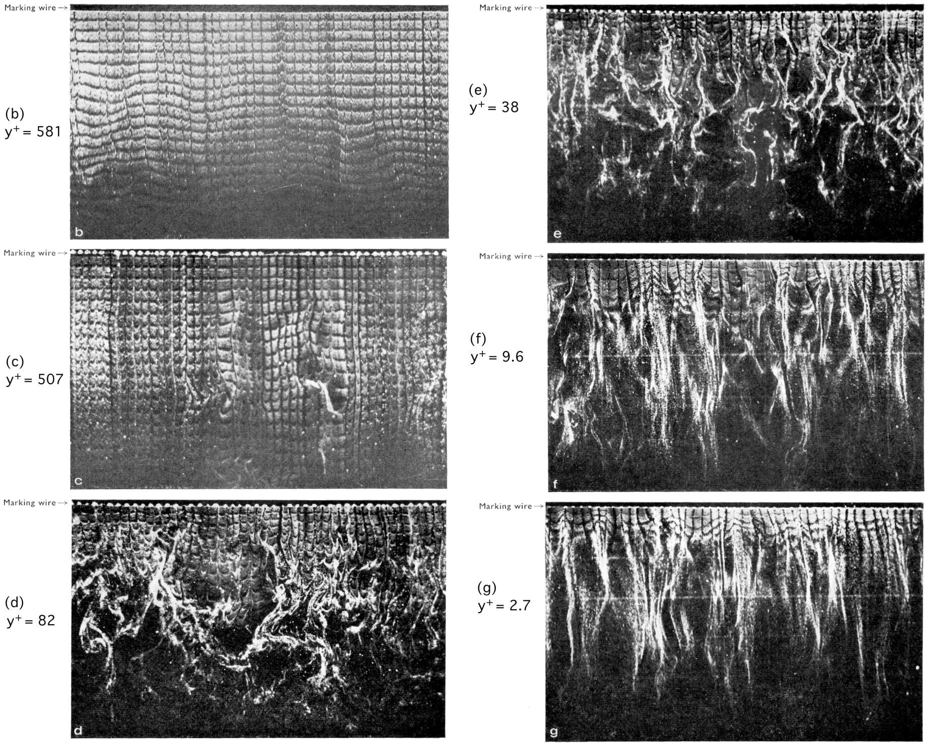

Kline et al. (1967)

The structure of wall-bounded turbulence

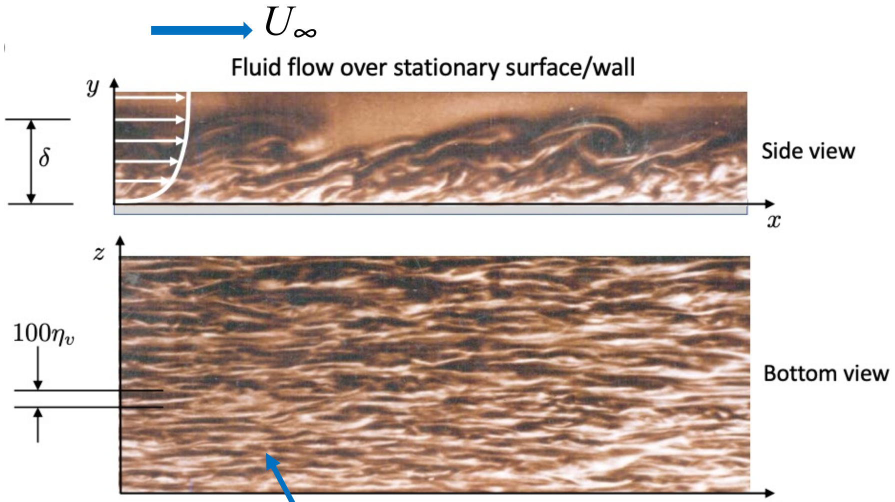

Cantwell, Coles & Dimotakis (1978)

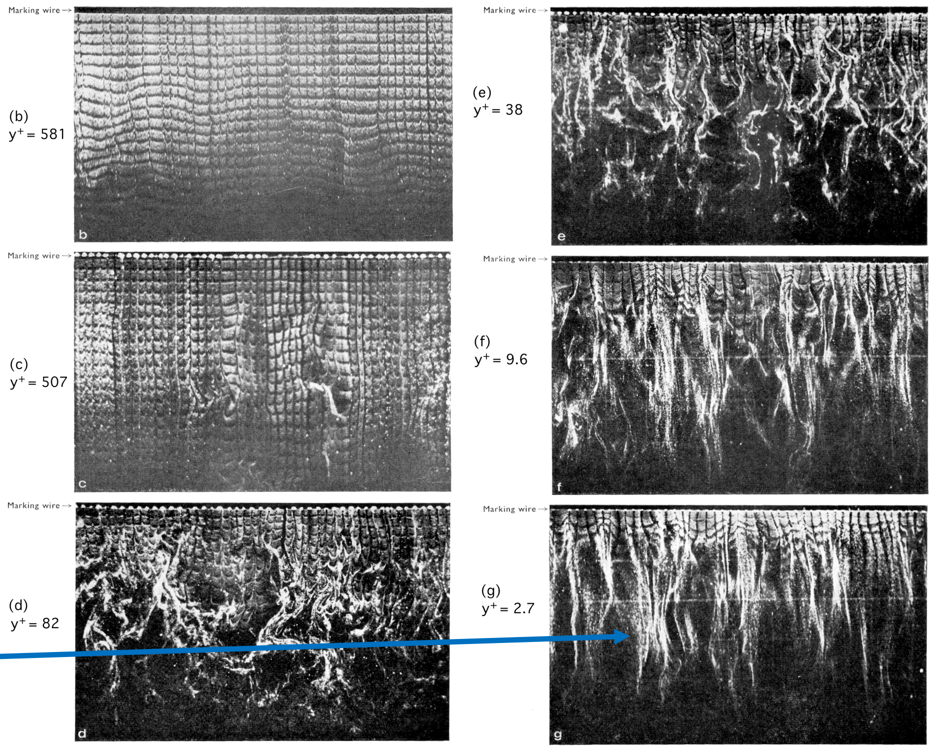

Kline et al. (1967)

Hairpin vortices

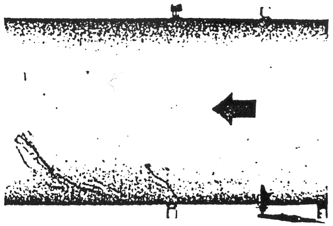

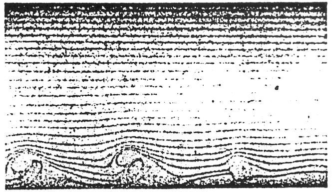
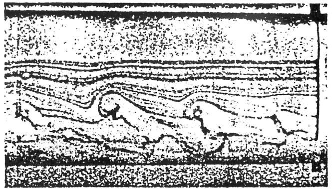
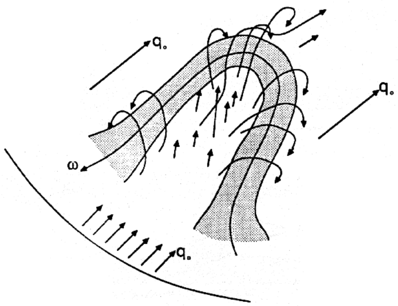

Theodorson (1952, 1955)

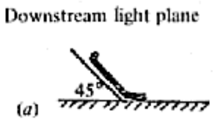

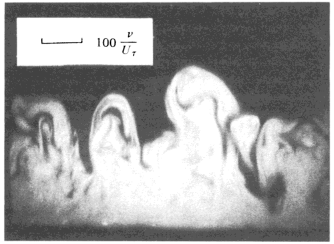

Re_θ = 600

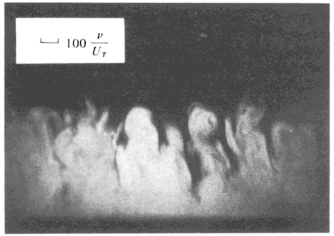

Re_θ = 1700

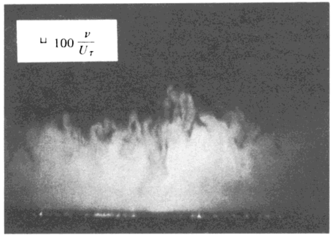

Re_θ = 9400

Head & Bandyopadhay (1981)

Vortex packets

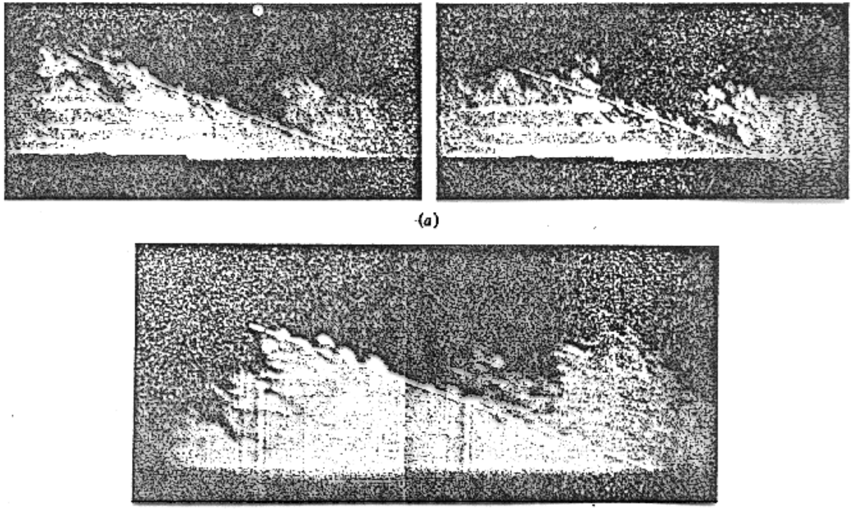

(a)

(b)

(a) Examples of features with interface inclined at approximately 20° to surface.
(b) Example of 20° interface at $Re_\theta = 17\,500$ (this is a composite of two frames because of the restricted length of the light plane).

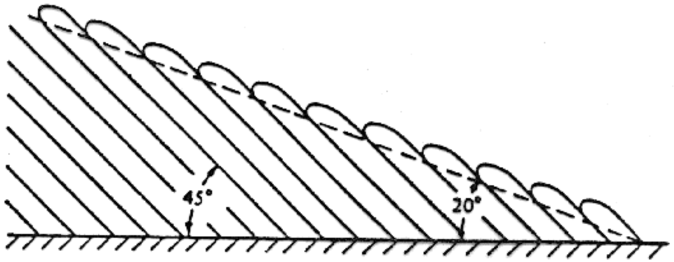

Head and Bandyopadhyay [1981].

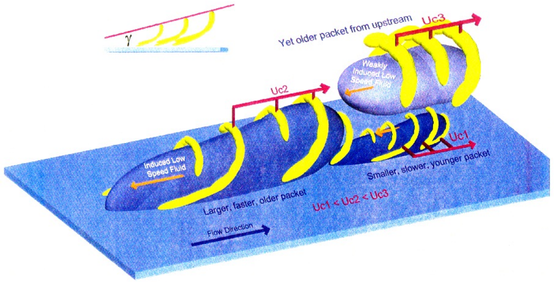

Adrian, Meinhart & Tomkins (1991)

Visualizations of coherent motions

Adrian, Meinhart, Tomkins (1999)

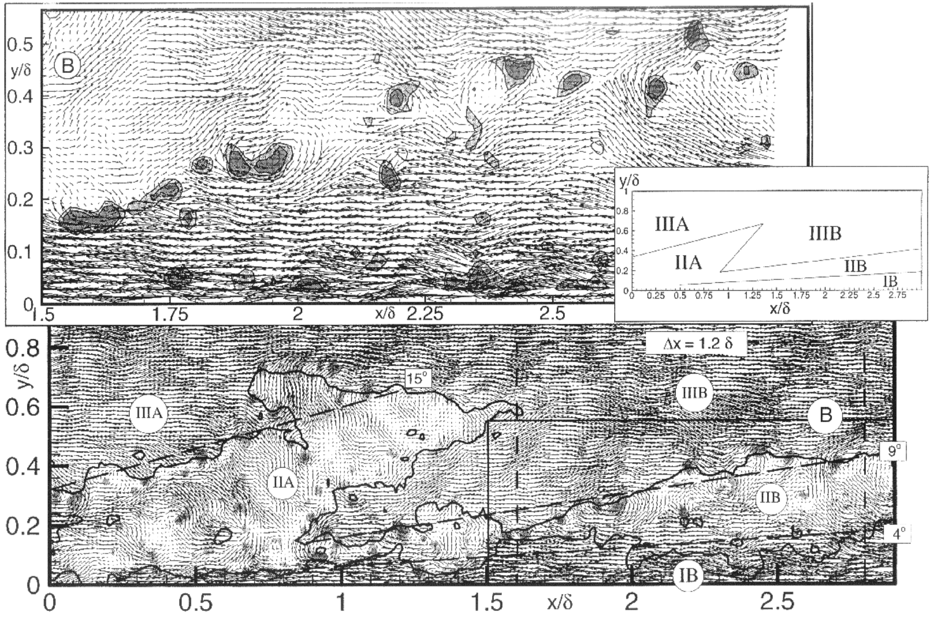

Figure 19 Illustrative example of large-scale structure of hairpin vortex packets at $Re_\theta = 7705$. The solid lines are contours of constant streamwise velocity at 61% and 79% of the free stream velocity. The velocity field in the lower plot has $U_c = 0.75U_\infty$ subtracted and gray levels indicate swirling strength. The upper plot of the inset region has $U_c = 0.75U_\infty$ subtracted, and gray-levels indicate fluctuating spanwise vorticity.

Wu & Moin (2009)

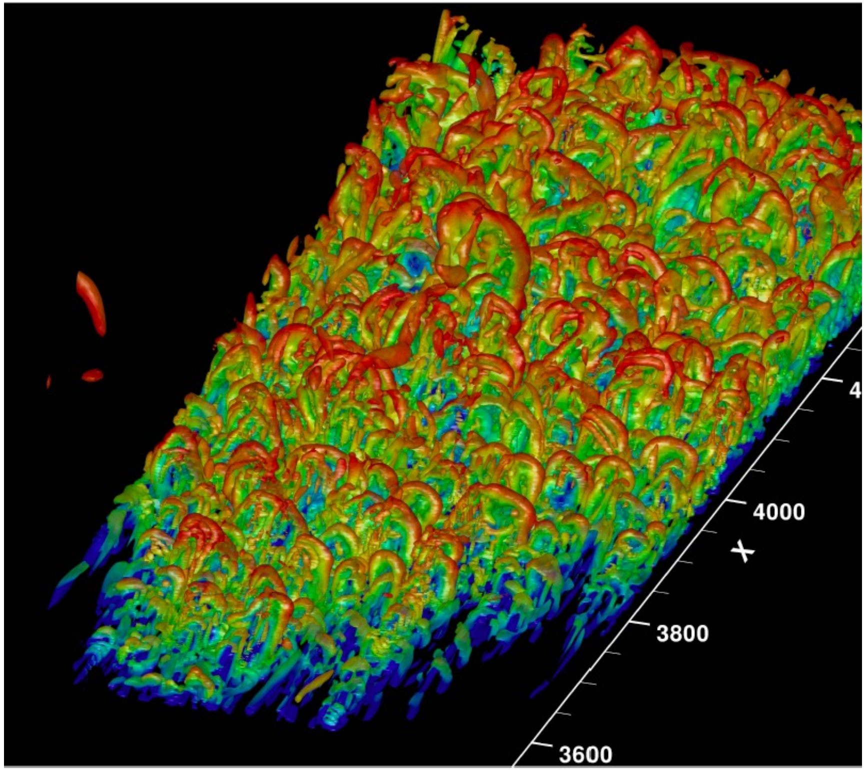

Uniform momentum zones (UMZ)

$Re_\tau \approx 2600$

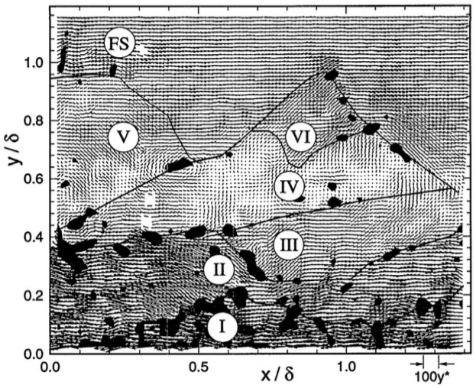

Meinhart & Adrian (1995)

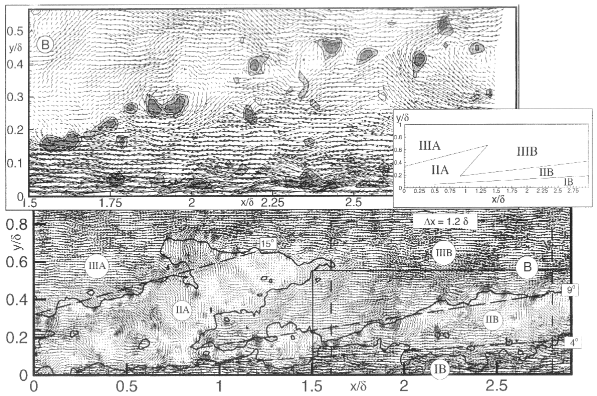

Adrian, Meinhart & Tomkins (1999)

- Number of UMZ's scales logarithmically with Re+
- But not as fast as the number of hierarchies

$Re_\tau \approx 8000$

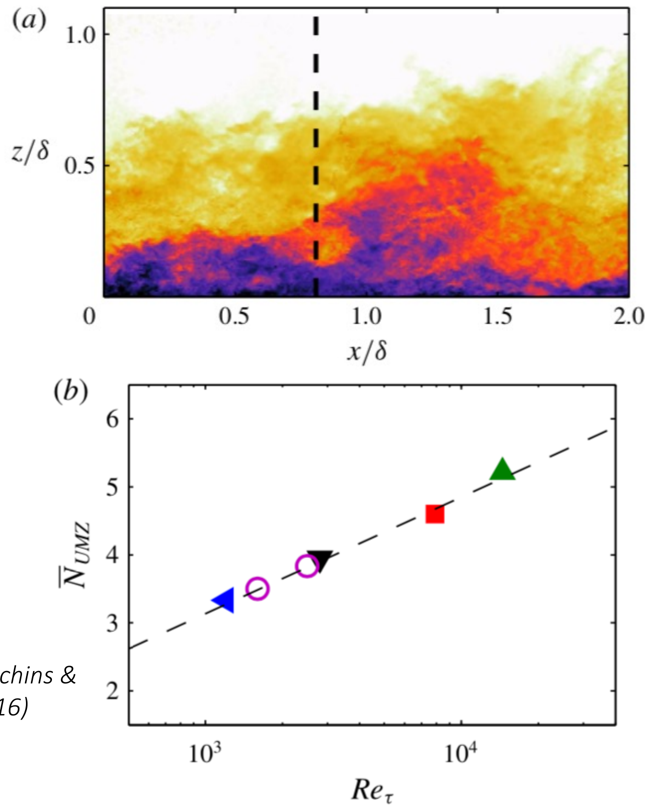

de Silva, Hutchins & Marusic (2016)

Uniform momentum zones (UMZ)

$Re_\tau \approx 2600$

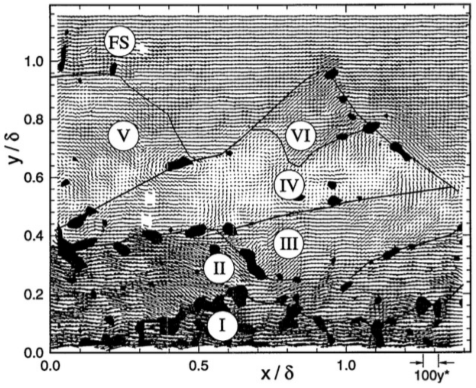

Meinhart & Adrian (1995)

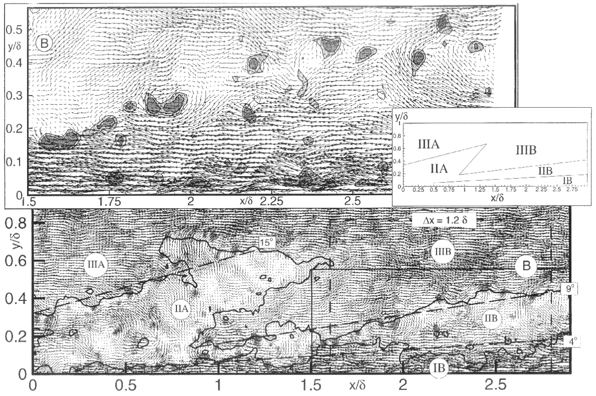

Adrian, Meinhart & Tomkins (1999)

Incompressible flow
Mach = 0

$Re_\tau \approx 8000$

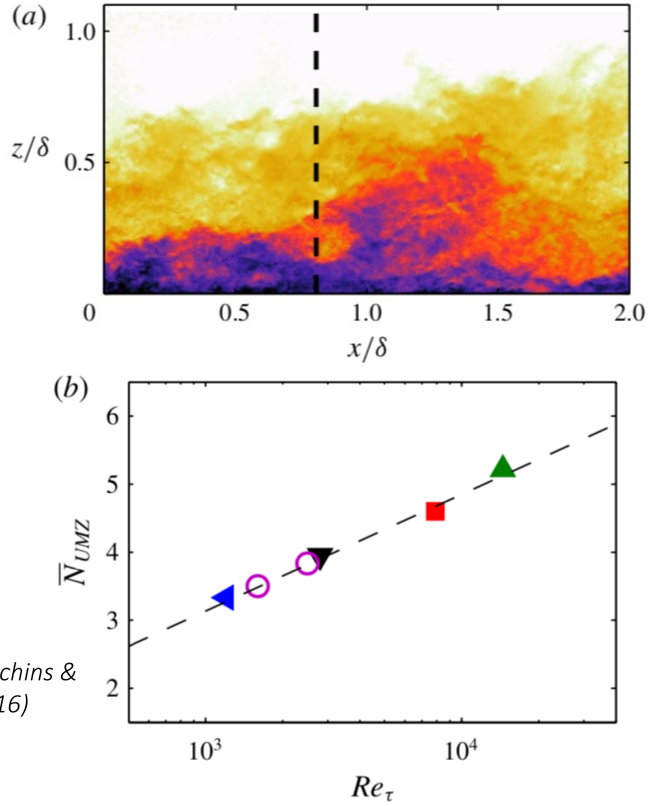

de Silva, Hutchins & Marusic (2016)

Coherent motions in wall-bounded turbulence

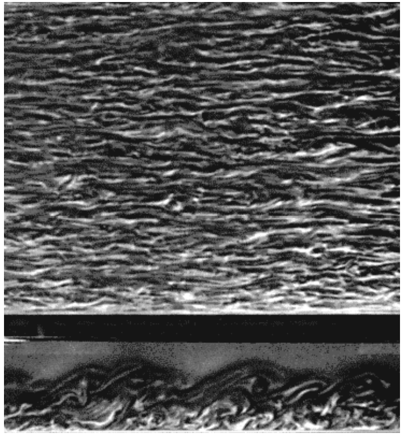

Cantwell, Coles & Dimotakis (1978)

Sublayer streaks

$y^+ < 10$

$x^+ \approx 1000$

$100\nu/u_\tau$

Inner scaling

Coherent motions in wall-bounded turbulence

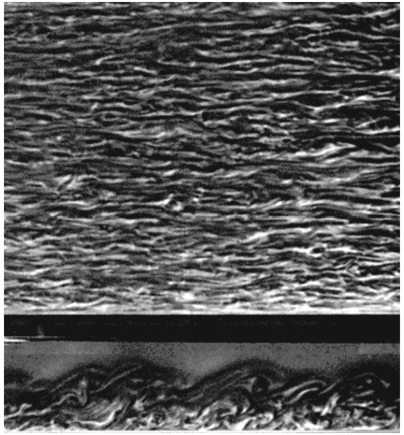

Cantwell, Coles & Dimotakis (1978)

Sublayer streaks
$y^+ < 10$
$x^+ \approx 1000$

Hairpin vortices
$y^+ > 100,\ 45^\circ$

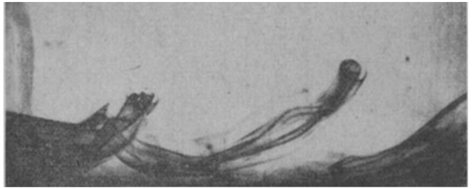

Theodorsen (1952)

Coherent motions in wall-bounded turbulence

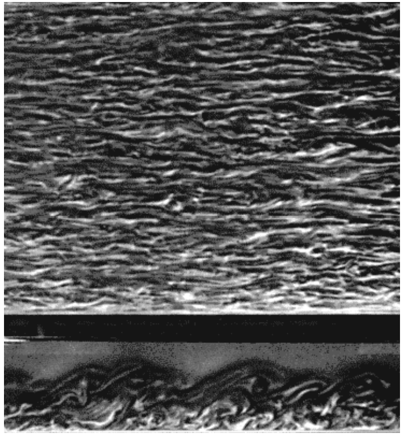

Cantwell, Coles & Dimotakis (1978)

Sublayer streaks
$y^+ < 10$
$x^+ \approx 1000$

Hairpin vortices
$y^+ > 100, \;\; 45^\circ$

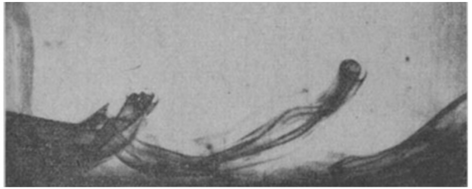

Theodorsen (1952)

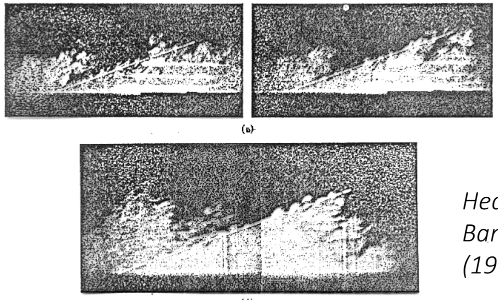

Head & Bandyopadhyay (1981)

Vortex packets
or LSM, $15 - 20^\circ$

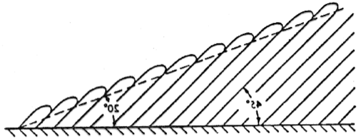

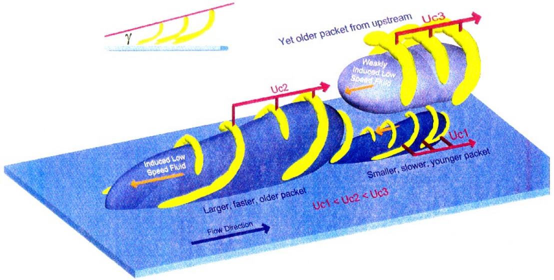

Adrian, Meinhart & Tomkins (1991)

Coherent motions in wall-bounded turbulence

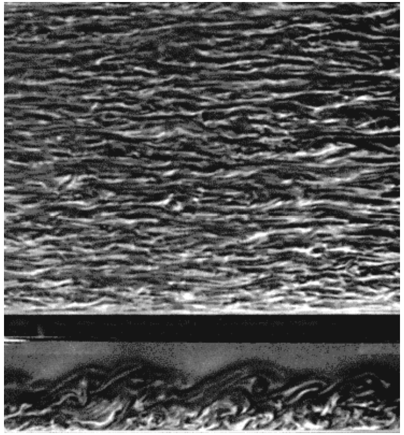

Cantwell, Coles & Dimotakis (1978)

Sublayer streaks
$y^+ < 10$
$x^+ \approx 1000$

Hairpin vortices
$y^+ > 100,\ 45^\circ$

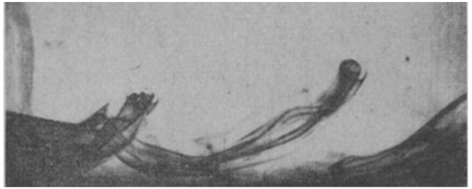

Theodorsen (1952)

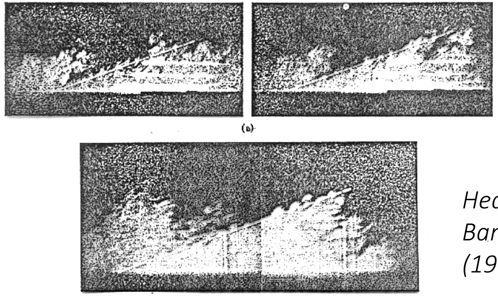

Head & Bandyopadhyay (1981)

Vortex packets or LSM, $15-20^\circ$

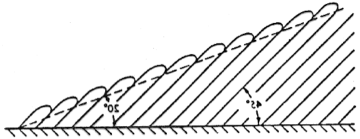

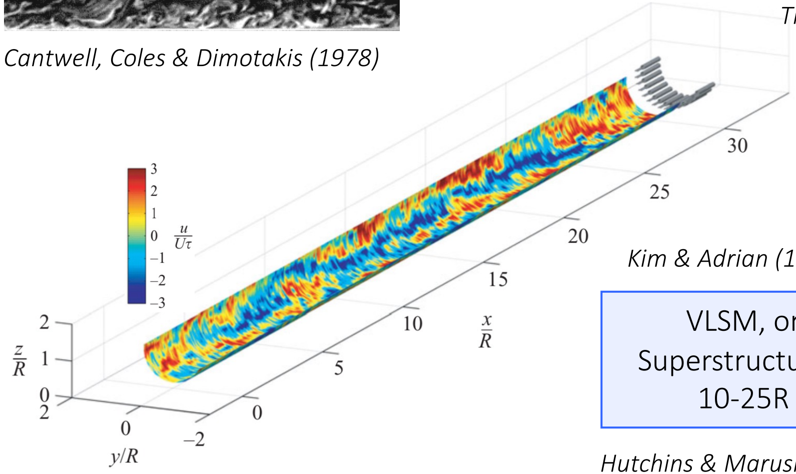

Kim & Adrian (1999)

Monty, Stewart, Williams & Chong (2007)

VLSM, or Superstructures, 10-25R

Hutchins & Marusic (2007)

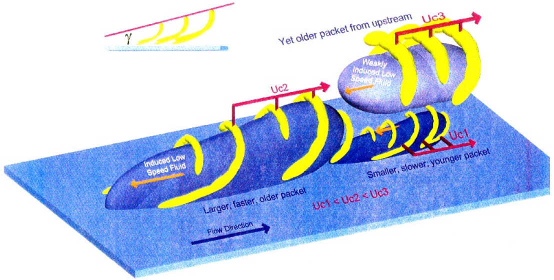

Adrian, Meinhart & Tomkins (1991)

Attached eddy concepts

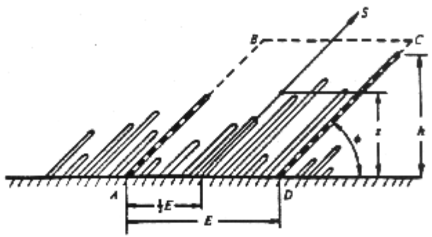

Random distribution of horseshoe vortices, from Perry and Chong's (1982) model of a turbulent boundary layer.

Hierarchical model of outer layer turbulence using Λ-eddies

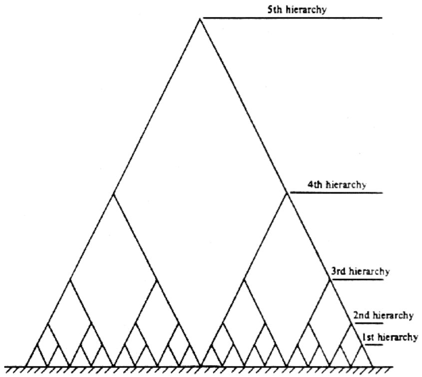

Symbolic representation of a discrete system of geometrically similar eddy hierarchies from Perry and Chong [1982].

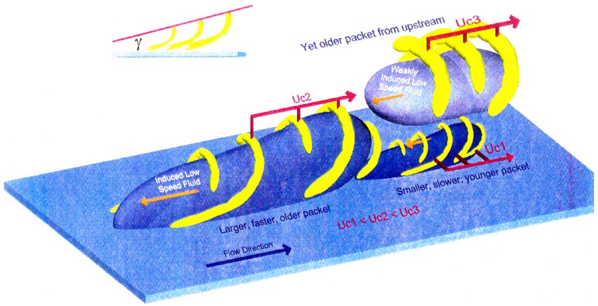

Adrian, Meinhart & Tomkins (1999)

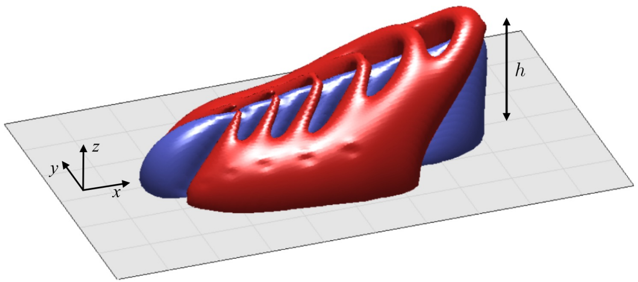

Woodcock & Marusic (2015)

Scaling the turbulence: the Attached Eddy Hypothesis

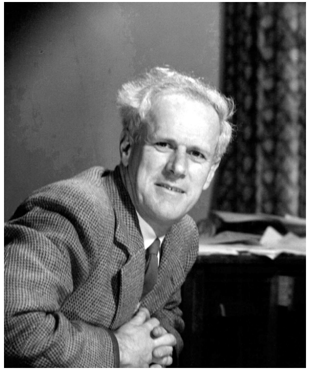

Townsend: "It is difficult to imagine how the presence of the wall could impose a dissipation length-scale proportional to distance from it unless the main eddies of the flow have diameters proportional to distance of their "centres" from the wall, because their motion is directly influenced by its presence. In other words, the velocity fields of the main eddies, regarded as persistent, organized flow patterns, extend to the wall and, in a sense, they are attached to the wall."

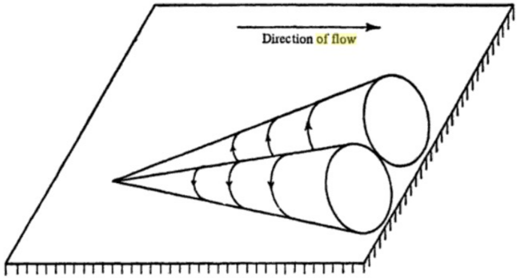

Townsend (1976)

Scaling the turbulence: the Attached Eddy Hypothesis

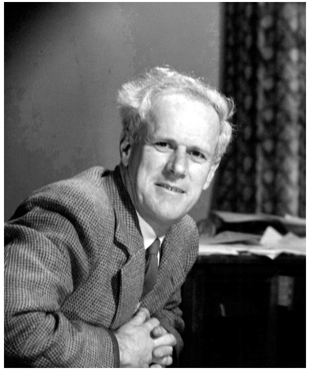

Townsend: "It is difficult to imagine how the presence of the wall could impose a dissipation length-scale proportional to distance from it unless the main eddies of the flow have diameters proportional to distance of their "centres" from the wall, because their motion is directly influenced by its presence. In other words, the velocity fields of the main eddies, regarded as persistent, organized flow patterns, extend to the wall and, in a sense, they are attached to the wall."

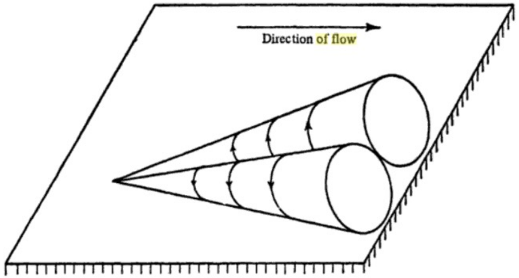

Townsend (1976)

Perry: In this theory, wall turbulence is considered to consist of a 'forest' of randomly positioned horseshoe, hairpin or Λ-shaped vortices that lean in the streamwise direction and have their legs extending to the wall.

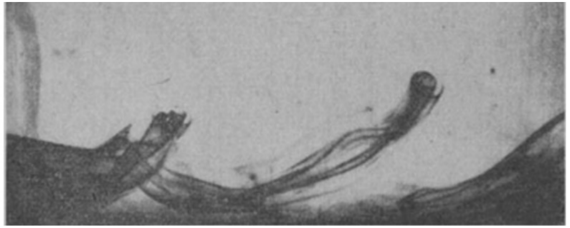

Theodorsen (1952)

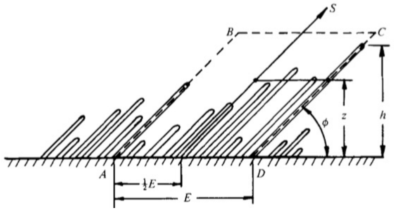

Perry & Chong (1982)

Townsend Attached Eddy Model

- The model is inviscid (high Reynolds number), and considers a superposition of geometrically self-similar, attached eddies
- The eddies cover a wide range of scales, but each scale is proportional to the distance from the wall
- The eddies have the same characteristic velocity scale
- At high enough Reynolds number, the model is designed to give $-\overline{uv}/u_\tau^2 = 1$
- Model applies in the constant stress (logarithmic) region

Townsend Attached Eddy Model

- The model is inviscid (high Reynolds number), and considers a superposition of geometrically self-similar, attached eddies
- The eddies cover a wide range of scales, but each scale is proportional to the distance from the wall
- The eddies have the same characteristic velocity scale
- At high enough Reynolds number, the model is designed to give $-\overline{uv}/u_\tau^2 = 1$
- Model applies in the constant stress (logarithmic) region

The model then predicts:

$$\frac{\overline{u^2}}{u_\tau^2} = B_1 - A_1 \ln\left(\frac{y}{\delta}\right)$$

$$\frac{\overline{v^2}}{u_\tau^2} = A_2$$

$$\frac{\overline{w^2}}{u_\tau^2} = B_3 - A_3 \ln\left(\frac{y}{\delta}\right)$$

Perry & Chong Attached Eddy Model

- The model is largely similar to Townsend's, but eddy shapes can be specified
- The eddies are grouped into hierarchies, and each hierarchy scales with the distance from the wall
- The number of eddies per unit area scales with $1/y^2$

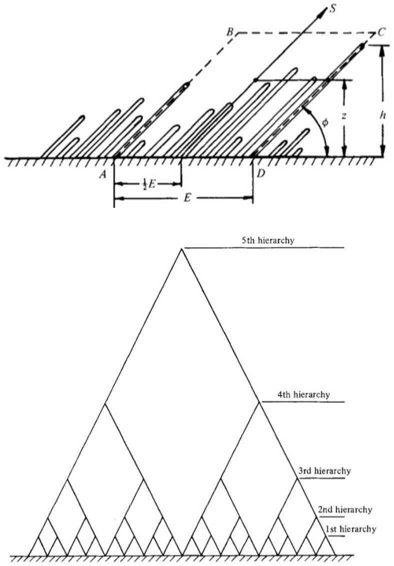

Perry & Chong (1982)

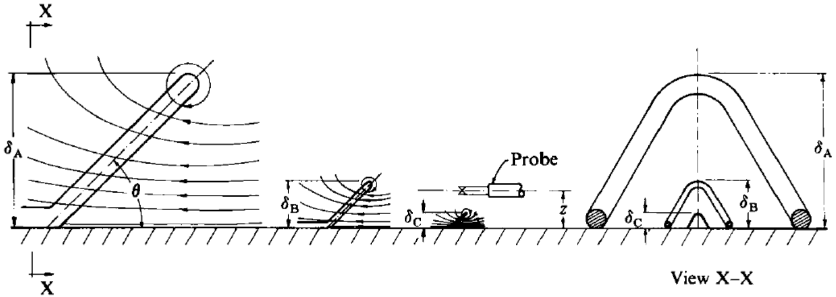

Perry, Henbest & Chong (1986)

Perry & Chong Attached Eddy Model

- The model is largely similar to Townsend’s, but eddy shapes can be specified
- The eddies are grouped into hierarchies, and each hierarchy scales with the distance from the wall
- The number of eddies per unit area scales with $1/y^2$

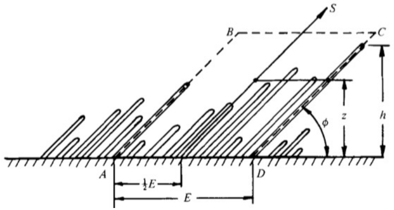

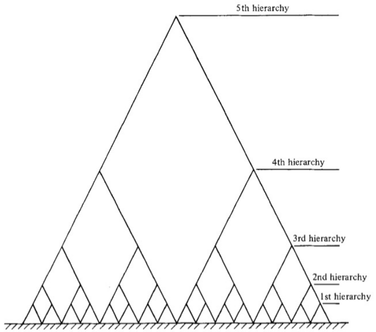

The model then predicts: $$\frac{dU}{dy} = \frac{u_\tau}{\kappa y} \longrightarrow \text{log-law}$$

And it is consistent with:

$$\frac{\overline{u^2}}{u_\tau^2} = B_1 - A_1 \ln\left(\frac{y}{\delta}\right)$$

$$\frac{\overline{v^2}}{u_\tau^2} = A_2$$

$$\frac{\overline{w^2}}{u_\tau^2} = B_3 - A_3 \ln\left(\frac{y}{\delta}\right)$$

(see also Marusic and Monty, Annual Reviews, 2019)

Connection to the spectrum

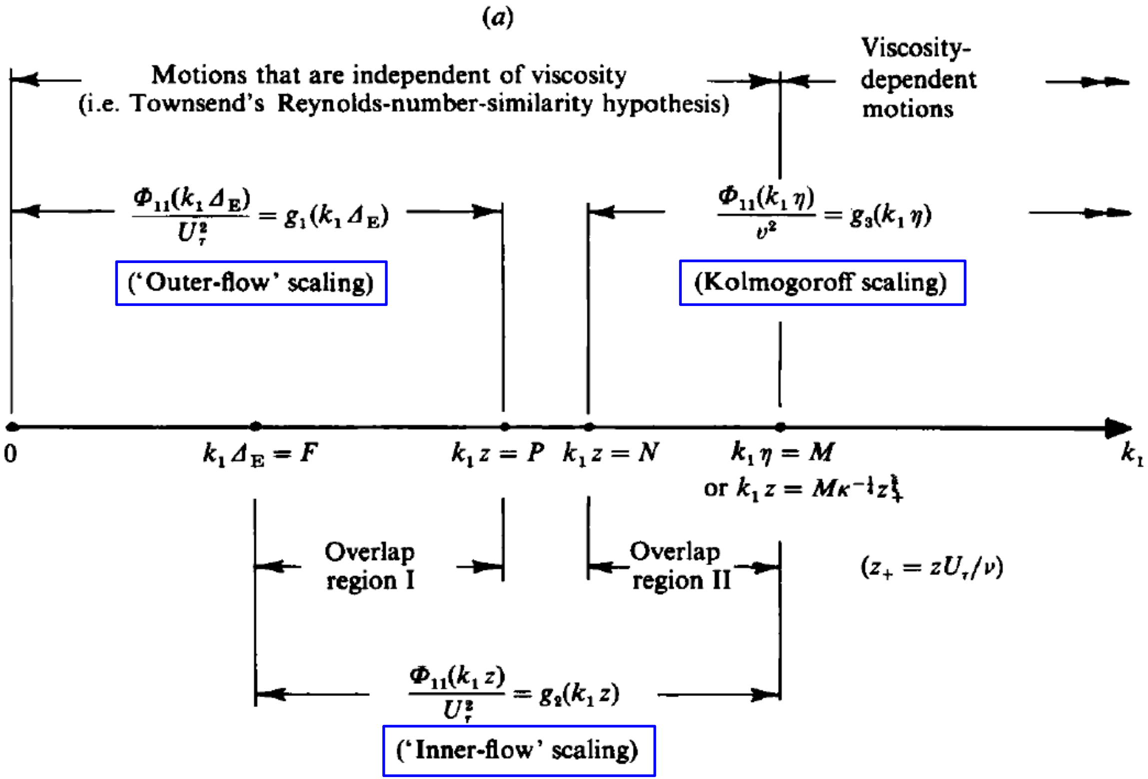

Perry & Abell (1977), Perry, Henbest & Chong (1986)

Connection to the spectrum

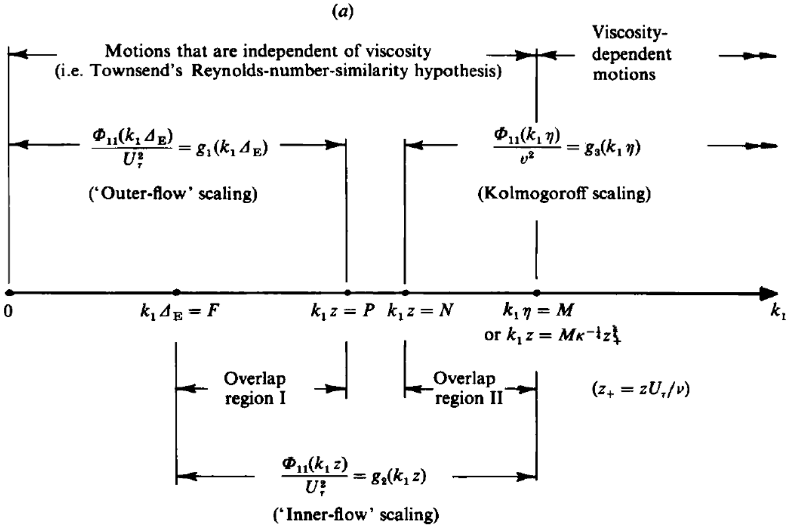

Outer scaling

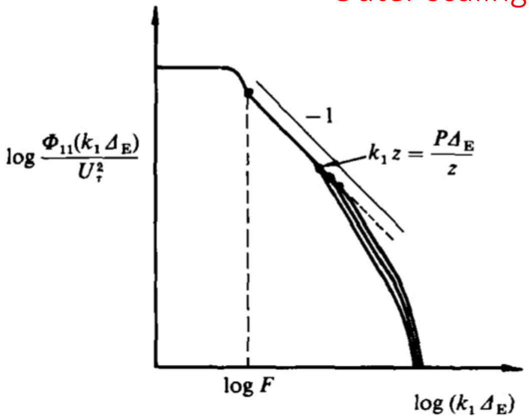

Log-log

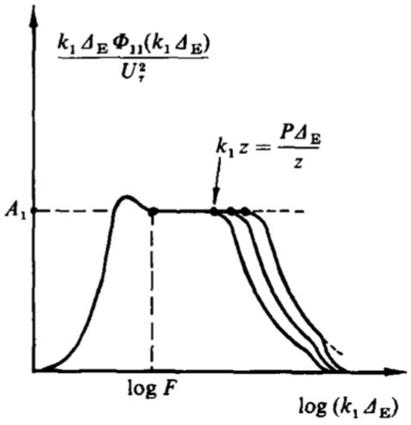

Premultiplied

Connection to the spectrum

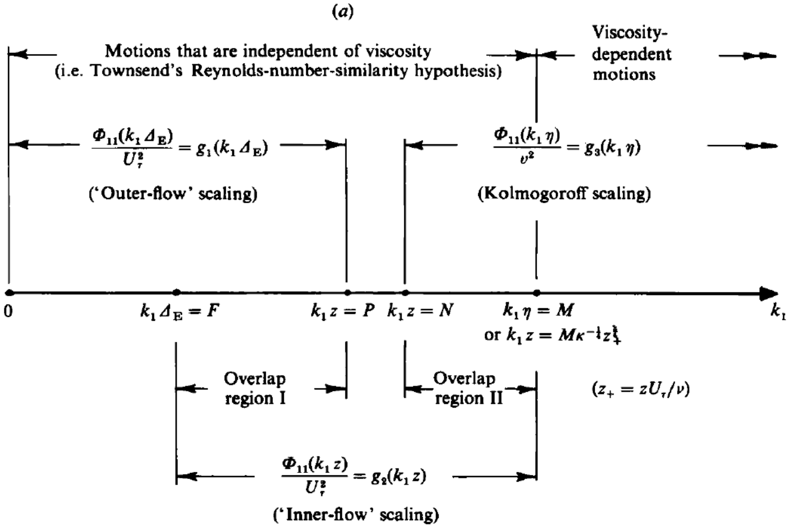

Outer scaling

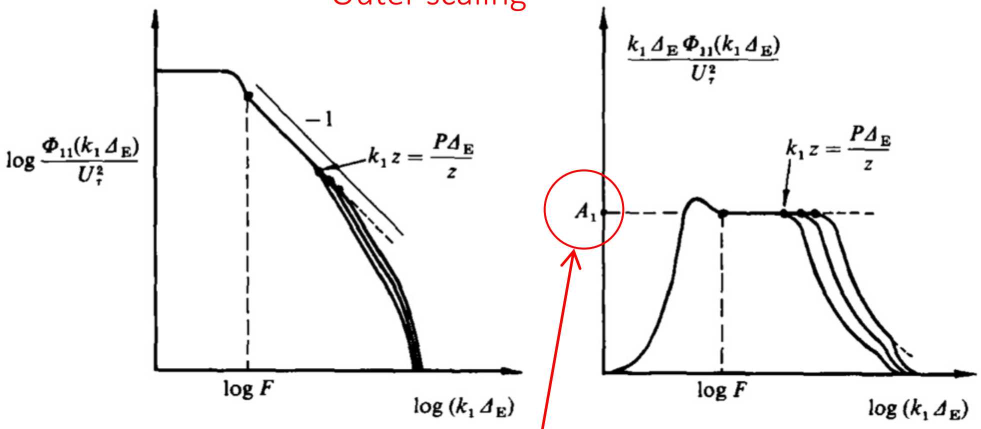

Log-log

Premultiplied

$$\frac{\overline{u^2}}{u_\tau^2} = B_1 - A_1 \ln\left(\frac{y}{\delta}\right)$$

Connection to the spectrum

spectrum → integrate

$$\frac{\overline{u^2}}{u_\tau^2} = B_1 - A_1 \ln\left(\frac{y}{\delta}\right) - V_1(y^+)$$

$$\frac{\overline{v^2}}{u_\tau^2} = A_2 - V_2(y^+)$$

$$\frac{\overline{w^2}}{u_\tau^2} = B_3 - A_3 \ln\left(\frac{y}{\delta}\right) - V_3(y^+)$$

For high Reynolds numbers, $V(y^+) \to 0$

Superpipe turbulence data (NSTAP)

Inner Scaling

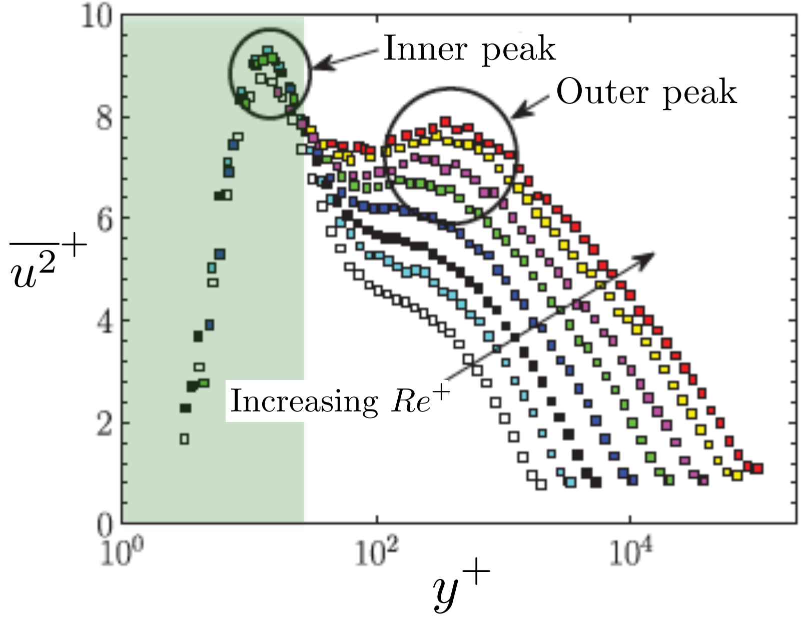

Outer Scaling

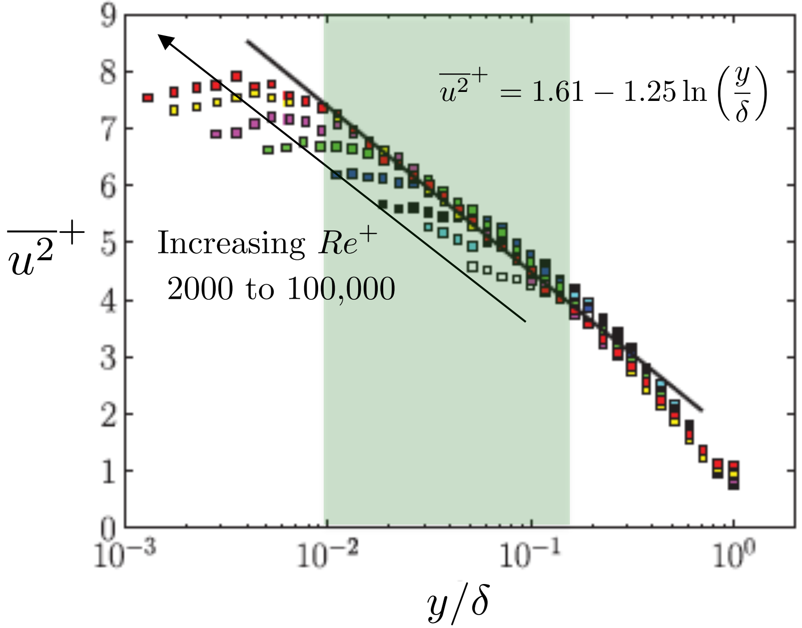

Hultmark , Vallikivi, Bailey & Smits (2012)

Growth of the inner peak

Inner Scaling

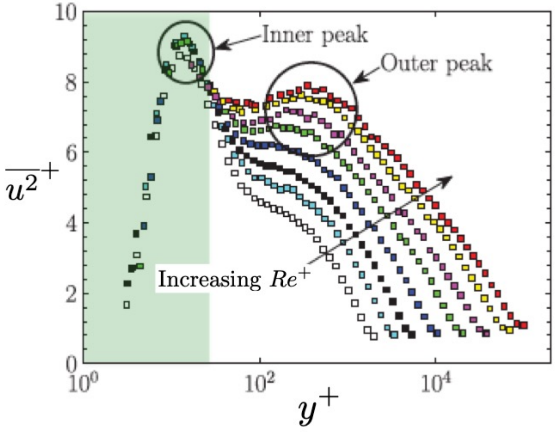

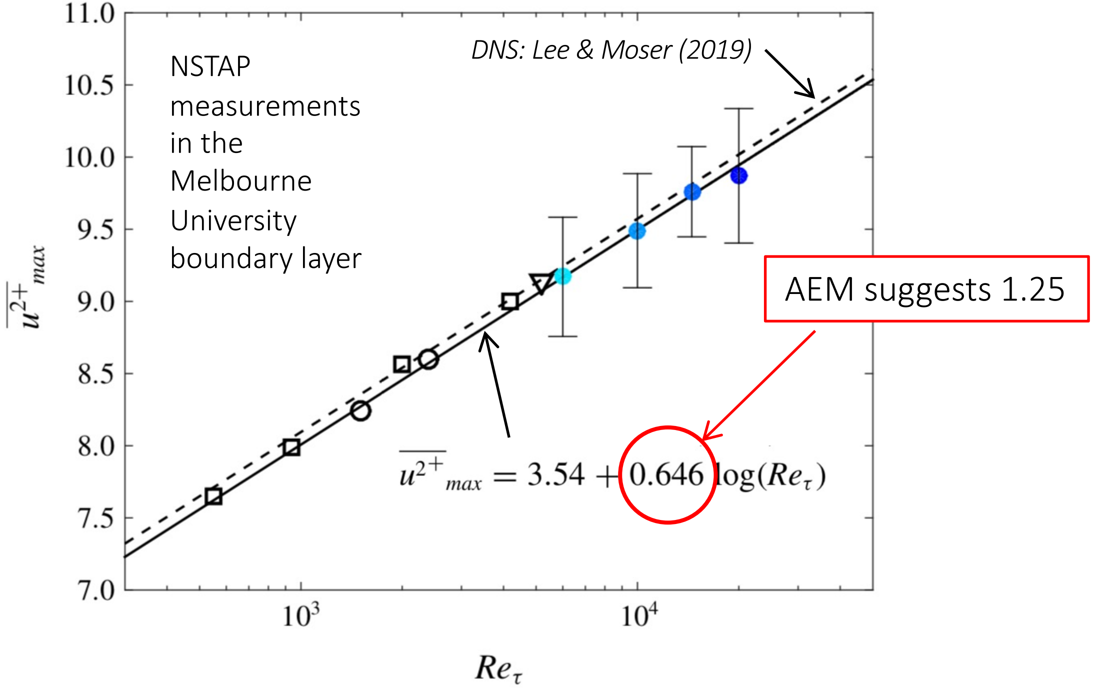

Samie , Marusic, Hutchins, Fan, Fu, Hultmark & Smits (2018)

A universal log law for turbulence

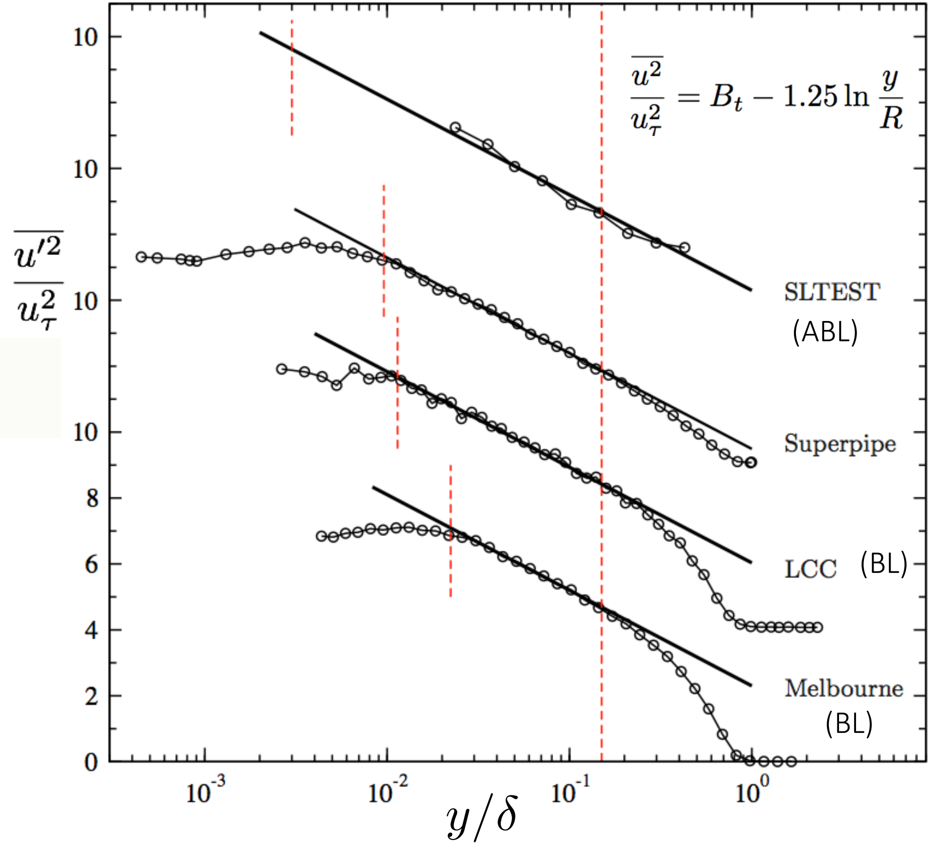

Marusic, Monty, Hultmark & Smits (2012)

A universal log law for turbulence

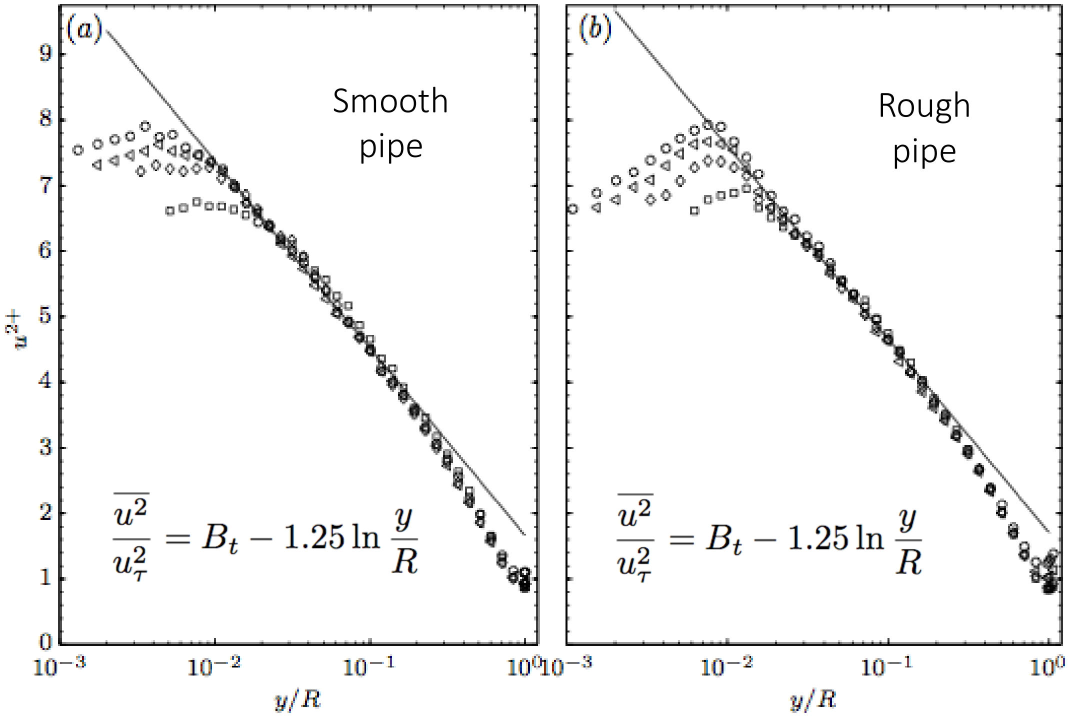

Second order moments of u'

Hultmark, Bailey, Vallikivi & Smits (2013)

A universal log law for turbulence

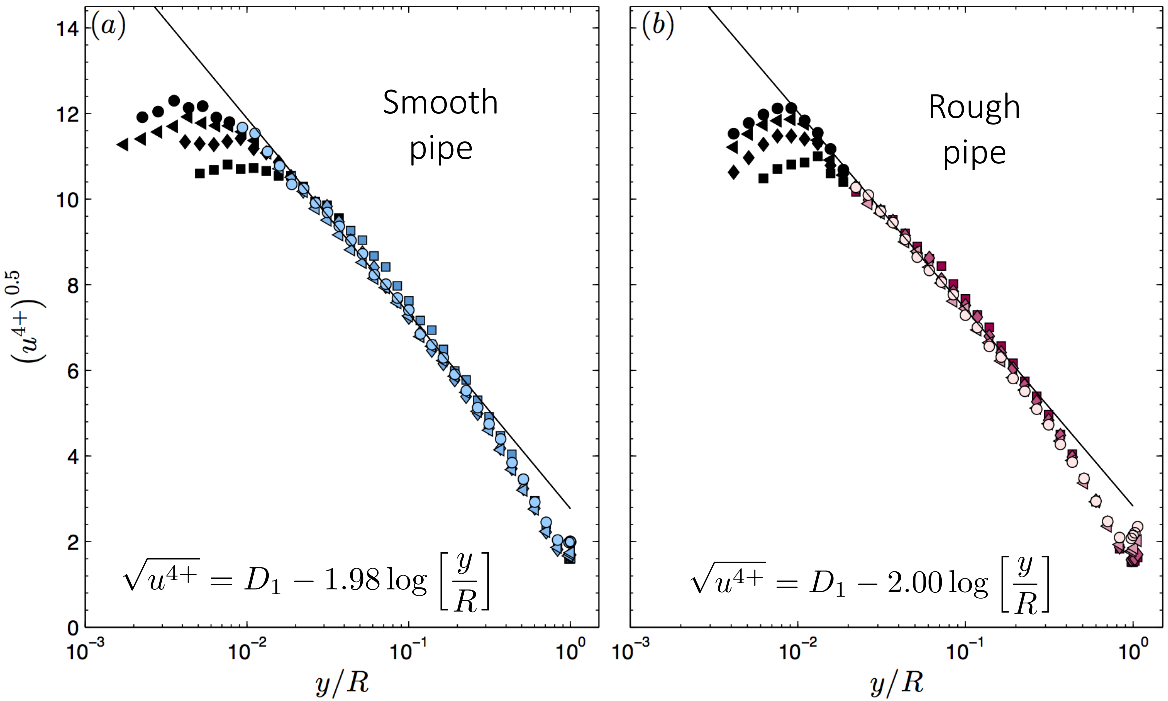

$$1.25\sqrt{3} = 2.16$$ (Gaussian expectation)

Meneveau & Marusic (2013)

Hultmark, Vallikivi, Bailey & Smits (2013)

What about the other stresses?

Spanwise component

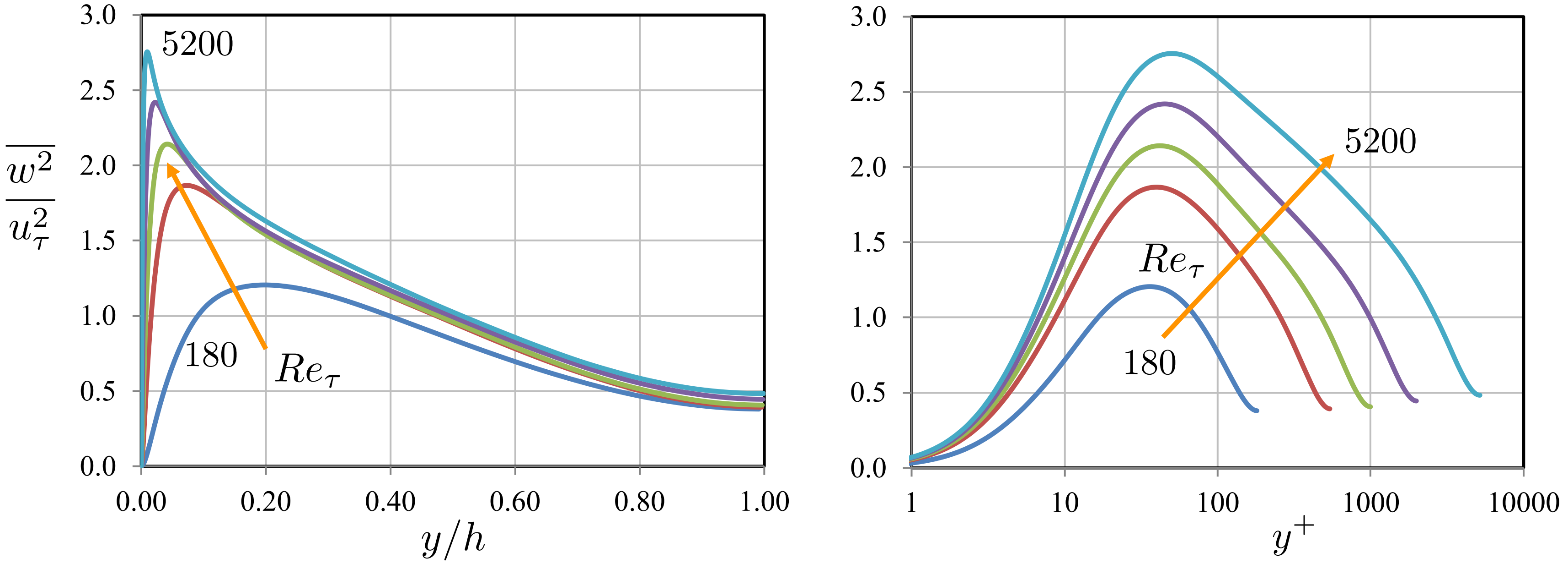

Channel flow DNS (Lee & Moser 2019)

Spanwise component: channel

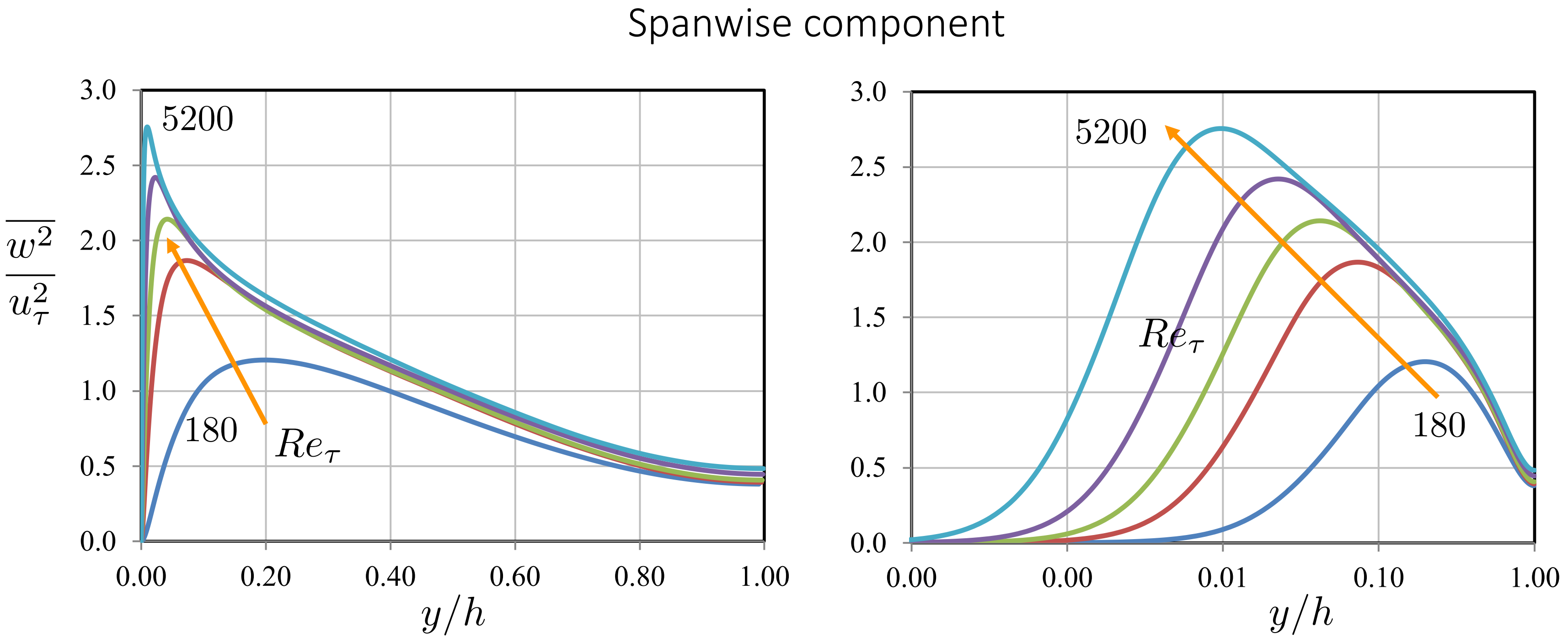

Channel flow DNS (Lee & Moser 2019)

Spanwise component: channel

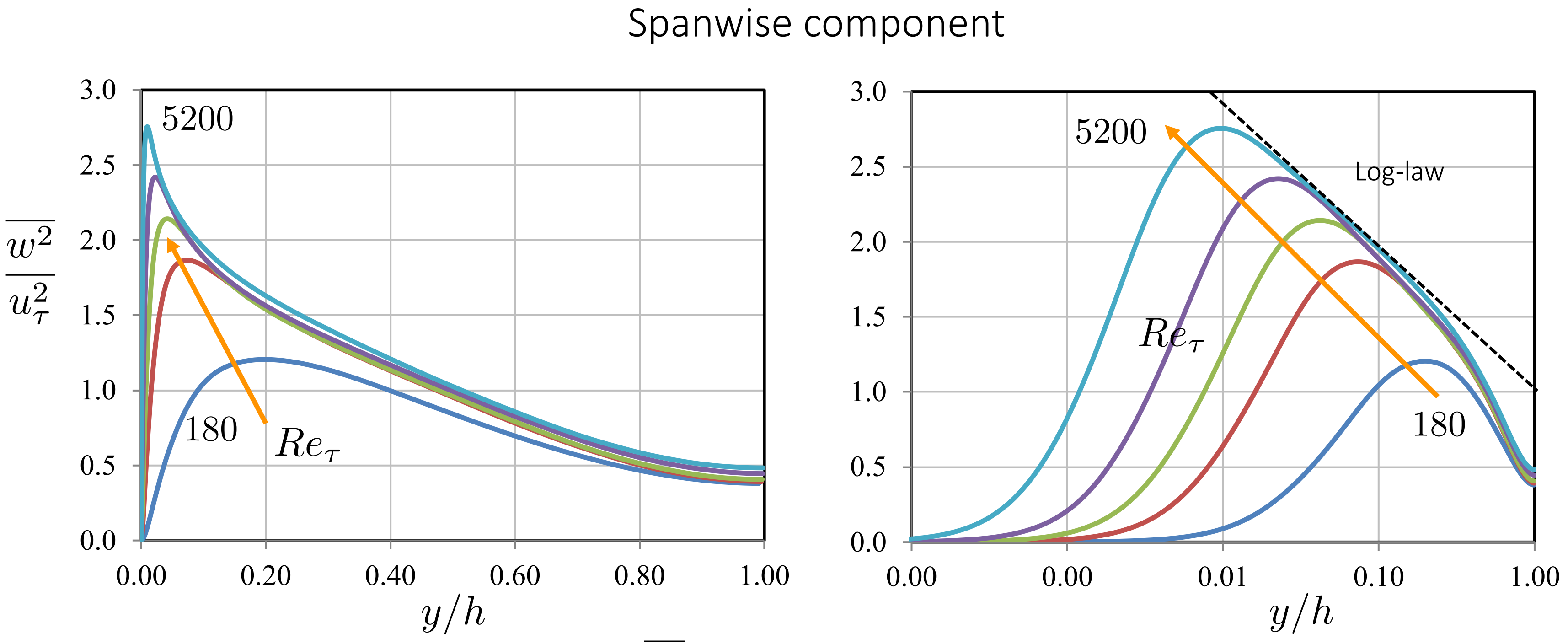

$$\frac{\overline{w^2}}{u_\tau^2} = 1.08 - 0.387 \ln \frac{y}{h}$$

Channel flow DNS (Lee & Moser 2019)

Wall-normal component: channel

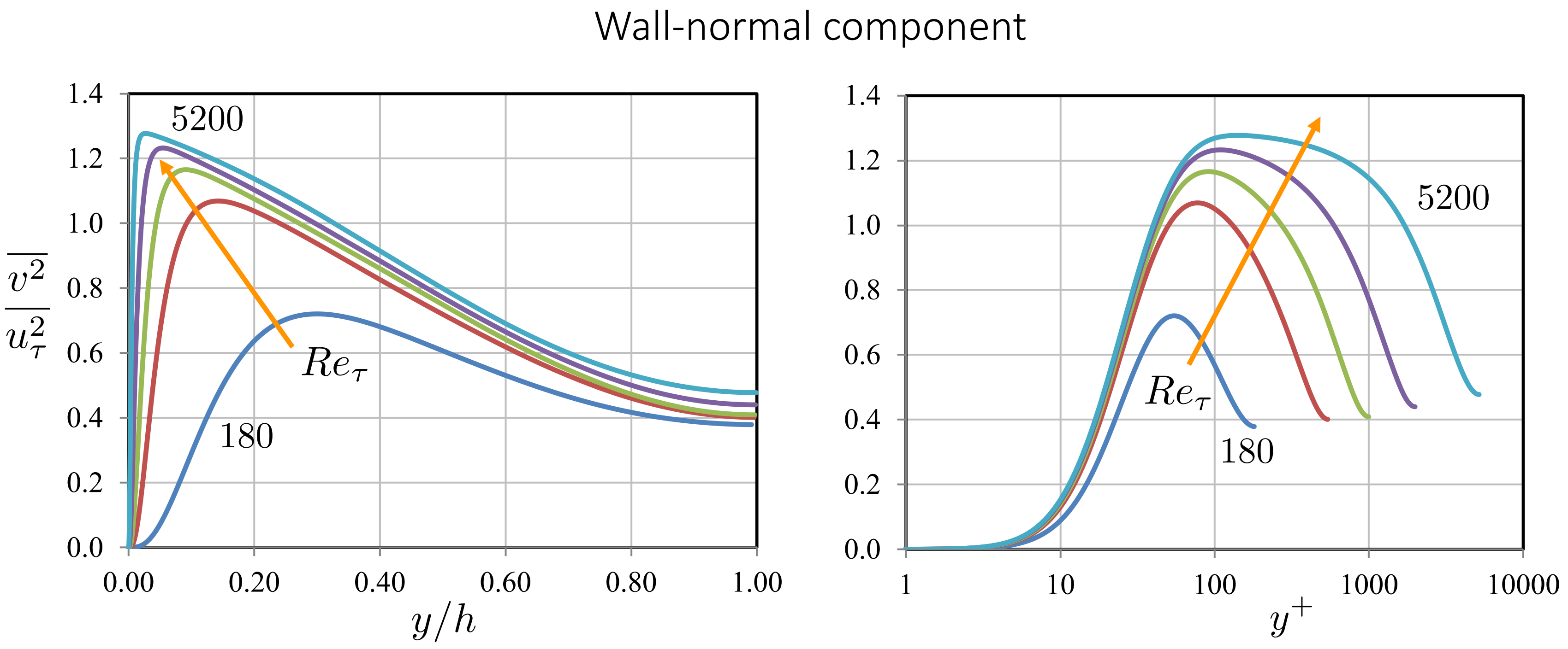

Channel flow DNS (Lee & Moser 2019)

Shear stress: channel

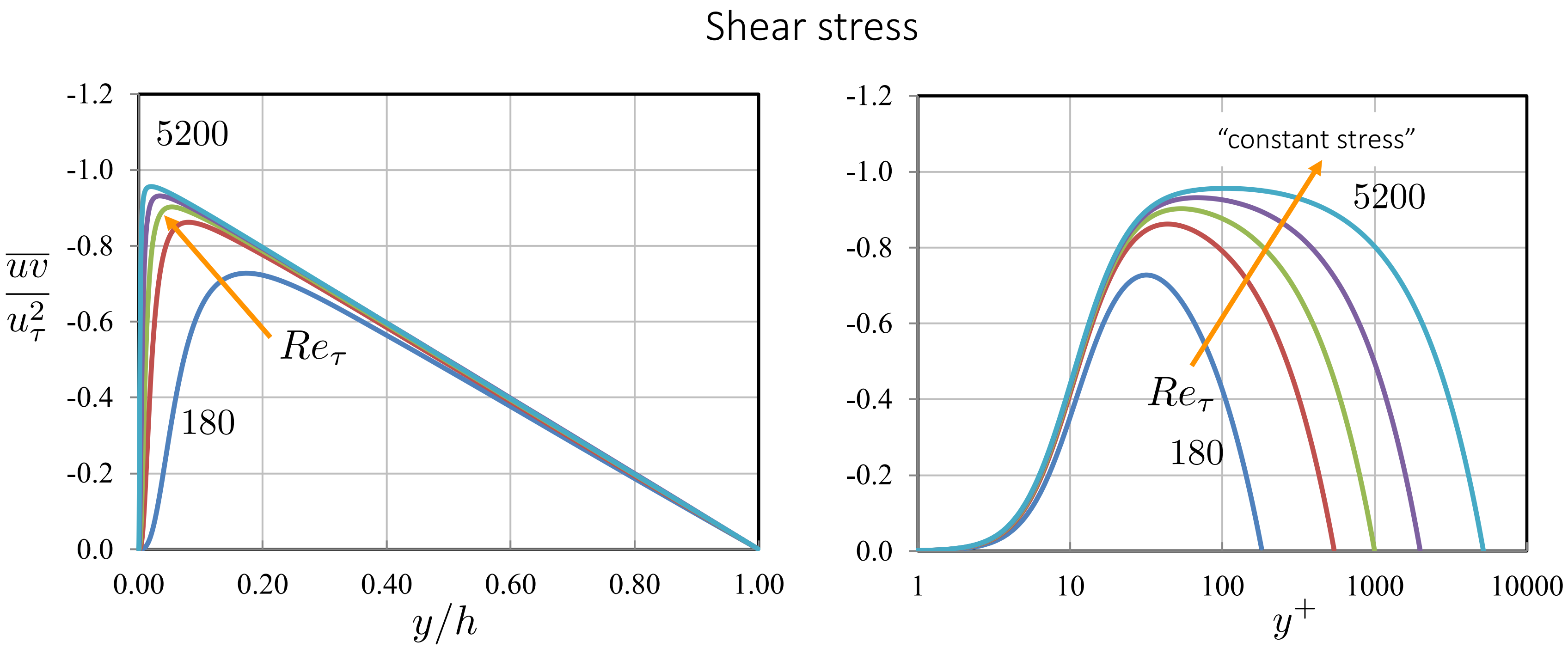

For fully-developed channel flow: $$-\overline{uv} + \nu \frac{dU}{dy} = u_\tau^2 \left(1 - \frac{y}{h}\right)$$

Channel flow DNS (Lee & Moser 2019)

Shear stress: boundary layer

Shear stress

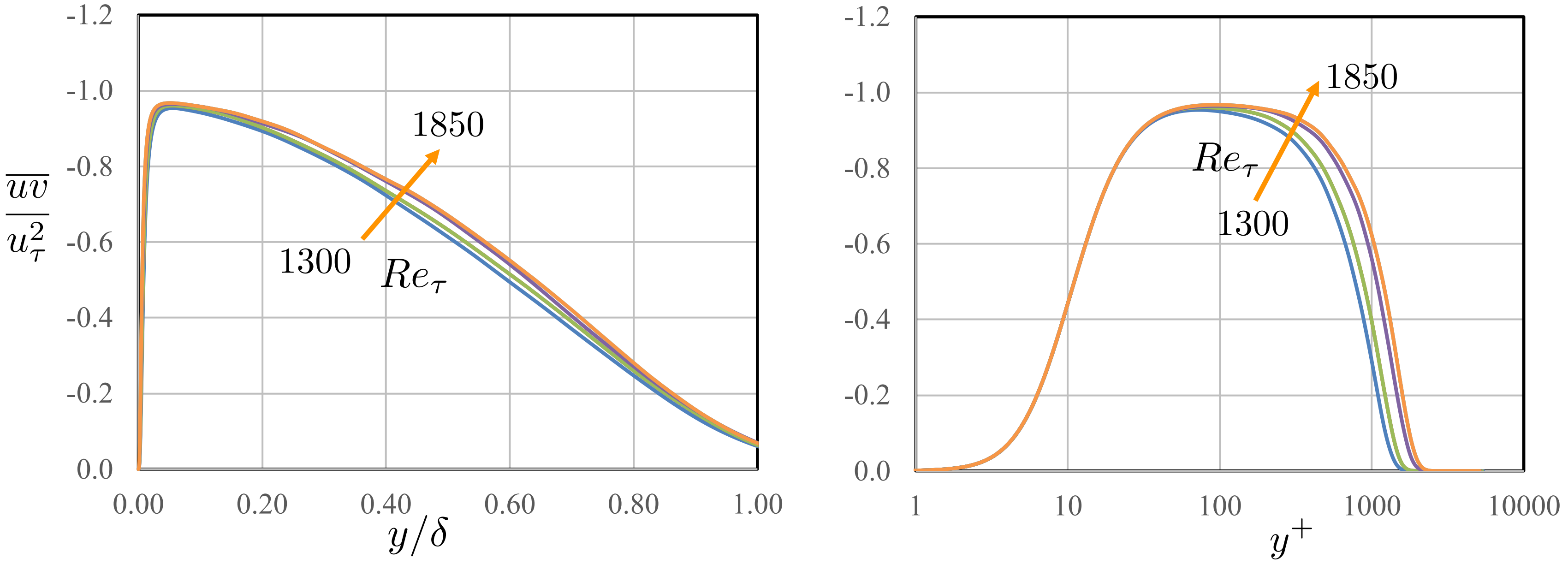

Boundary layer DNS (Sillero et al. 2013)

Spectral scaling: what about -5/3?

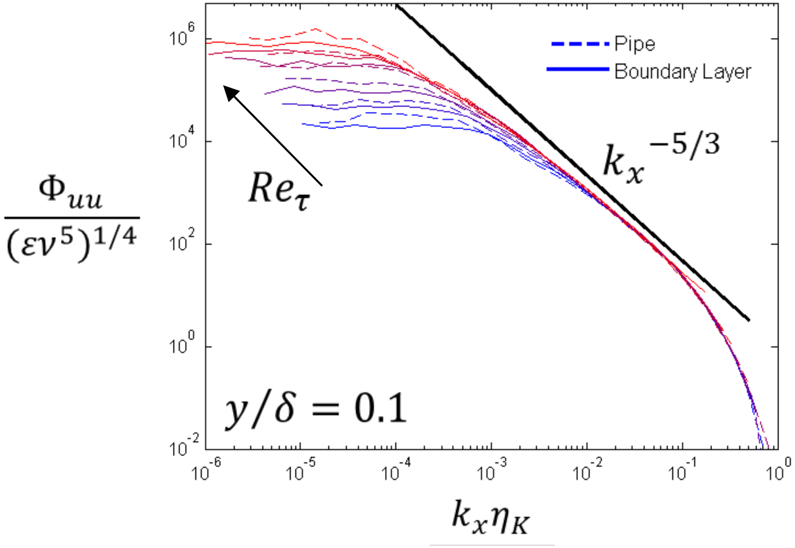

Overlap region II:

$k_x^{-5/3}$ region

$$\Phi_{uu} \sim k_x^{-5/3}$$

Spectral scaling: what about -5/3?

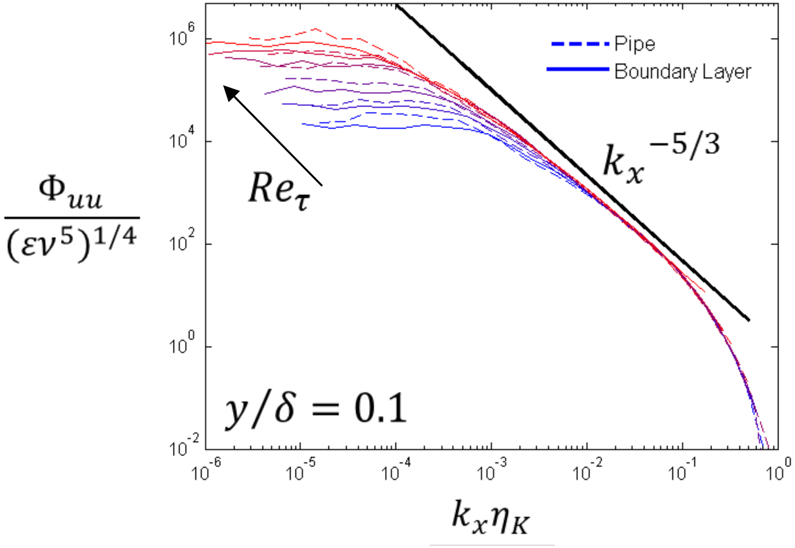

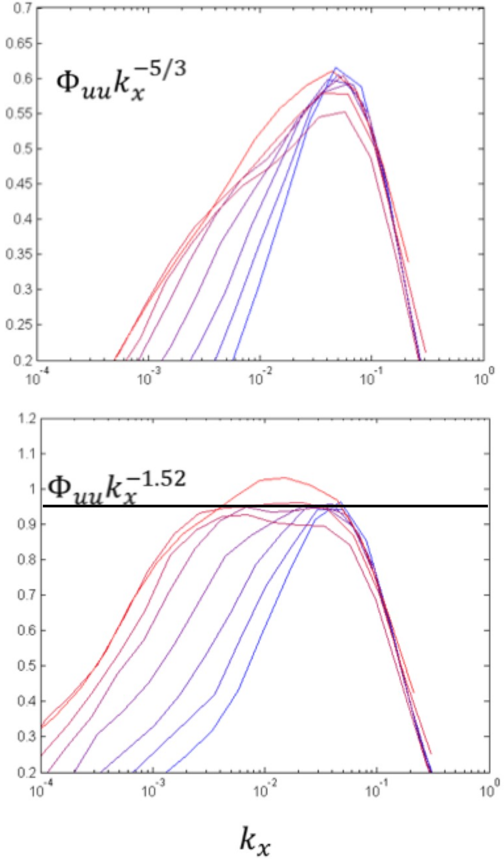

Pre-multiplied spectra

$k^{-1.52}$

Overlap region II:

$k_x^{-5/3}$ region

$\Phi_{uu} \sim k_x^{-5/3}$

Spectral scaling: what about -5/3?

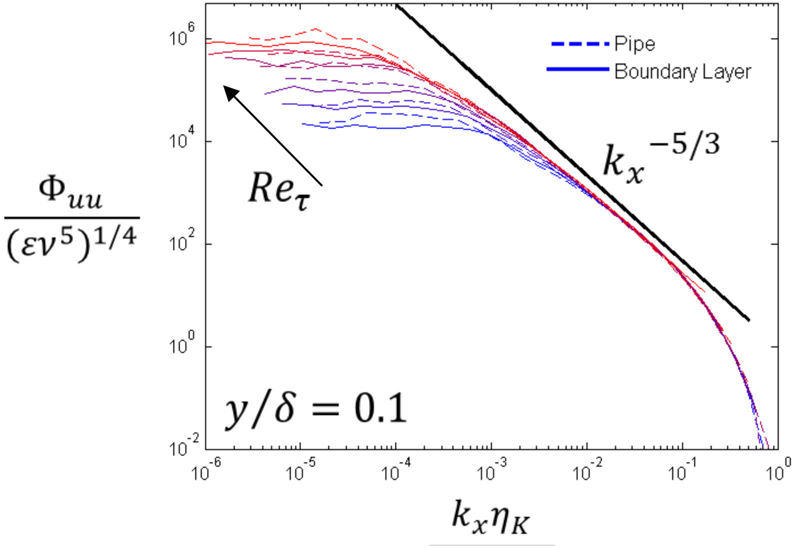

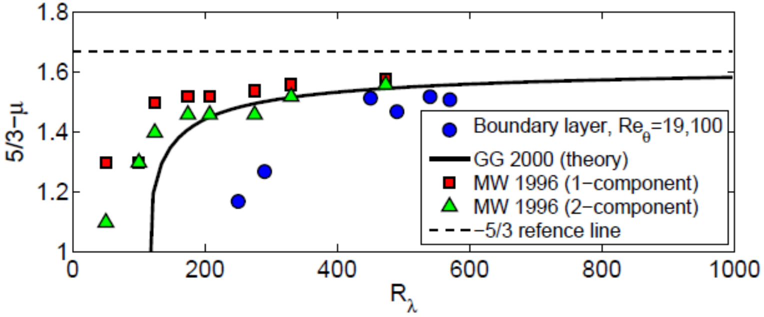

Mydlarski and Warhaft (1996), Gamard and George (2000):

$$\Phi_{uu} \sim k_x^{-\frac{5}{3}+\mu}, \qquad \mu \sim \frac{1}{\ln Re}$$

Overlap region II:

$k_x^{-5/3}$ region

$$\Phi_{uu} \sim k_x^{-5/3}$$

Spectral scaling: what about -5/3?

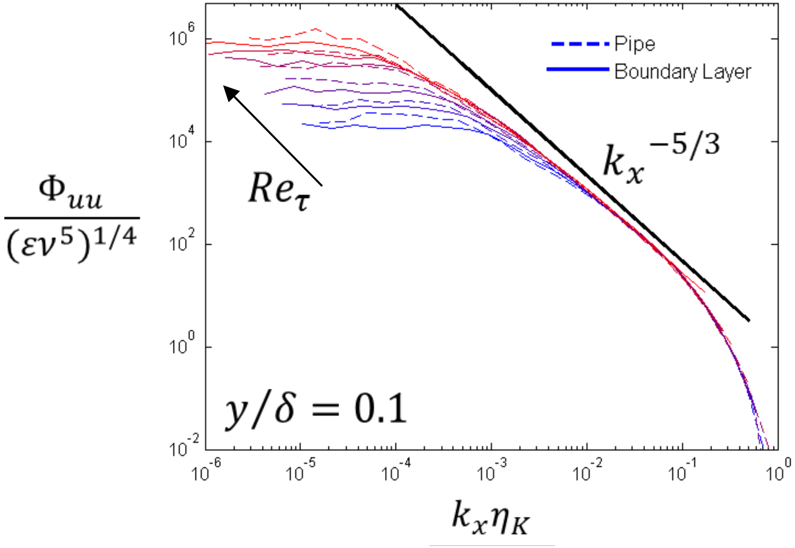

Overlap region II:

$k_x^{-5/3}$ region

$\Phi_{uu} \sim k_x^{-5/3}$

Our data

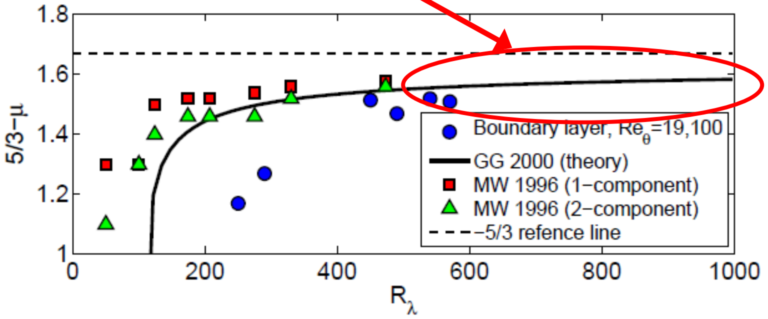

Mydlarski and Warhaft (1996), Gamard and George (2000):

$$\Phi_{uu} \sim k_x^{-\frac{5}{3}+\mu}, \qquad \mu \sim \frac{1}{\ln Re}$$

What about -1?

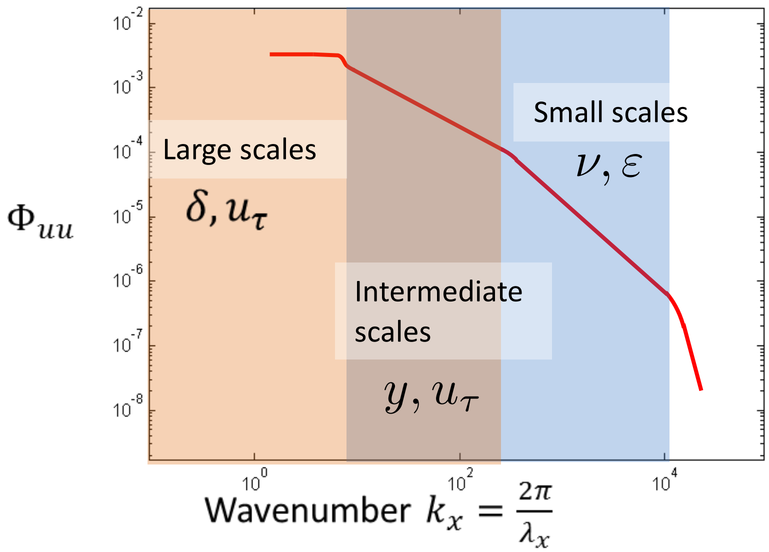

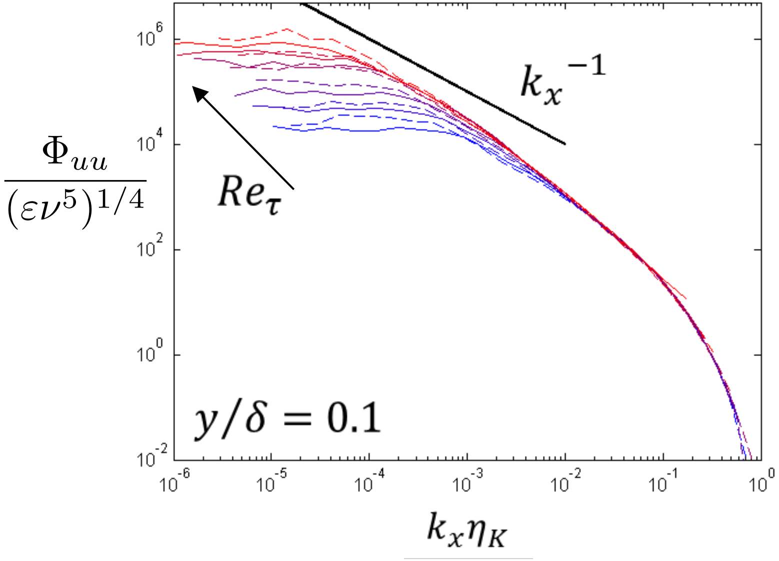

Overlap region I:

$$k_x^{-1} \text{ region}$$

$$\Phi_{uu} \sim k_x^{-1}$$

Pre-multiplied-1 spectra: $Re_\tau \approx 5000$

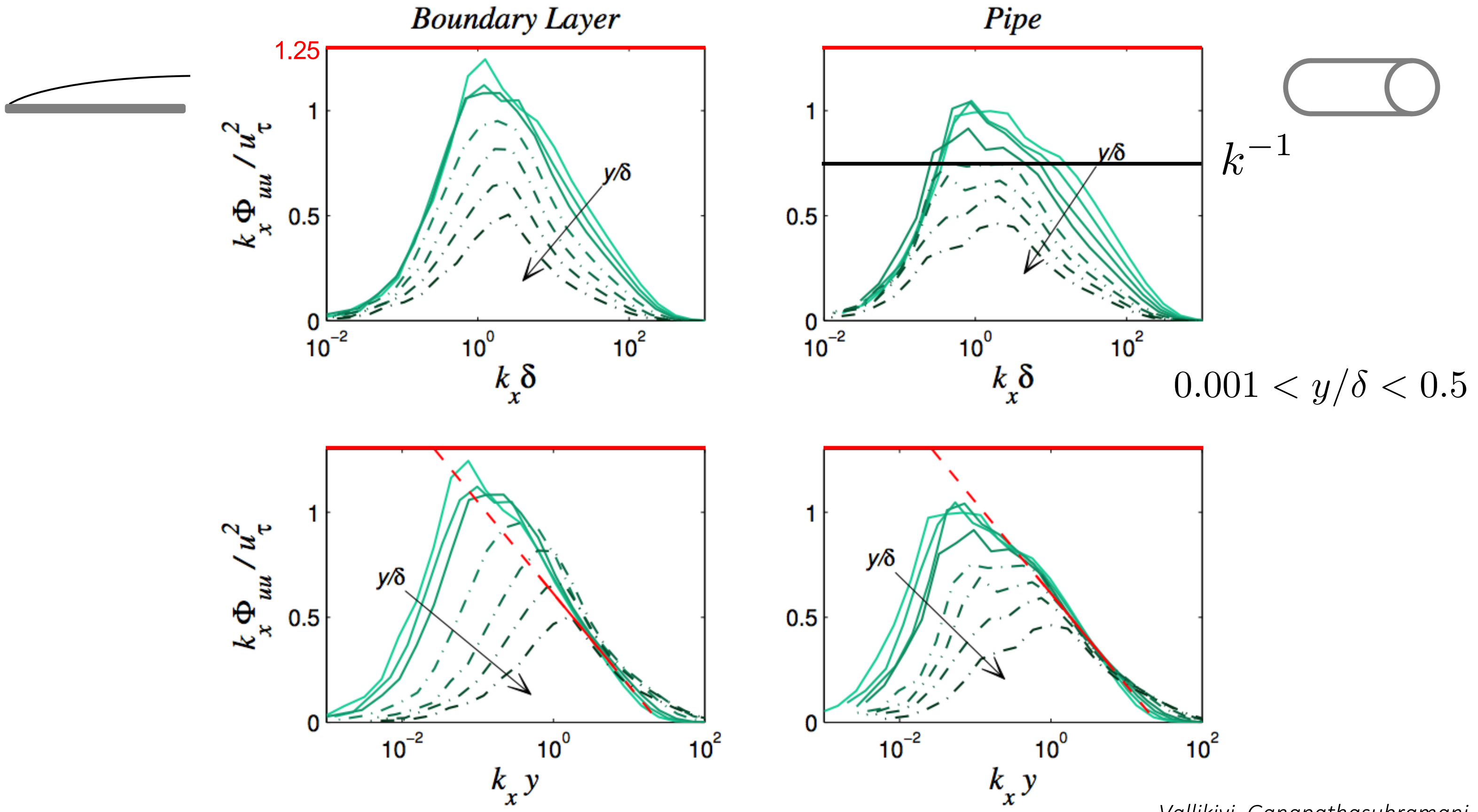

Vallikivi, Ganapathasubramani & Smits (2015)

Pre-multiplied-1 spectra: $Re_\tau \approx 5000$

$$\frac{\overline{u^2}}{u_\tau^2} = B_1 - A_1 \ln\left(\frac{y}{\delta}\right)$$

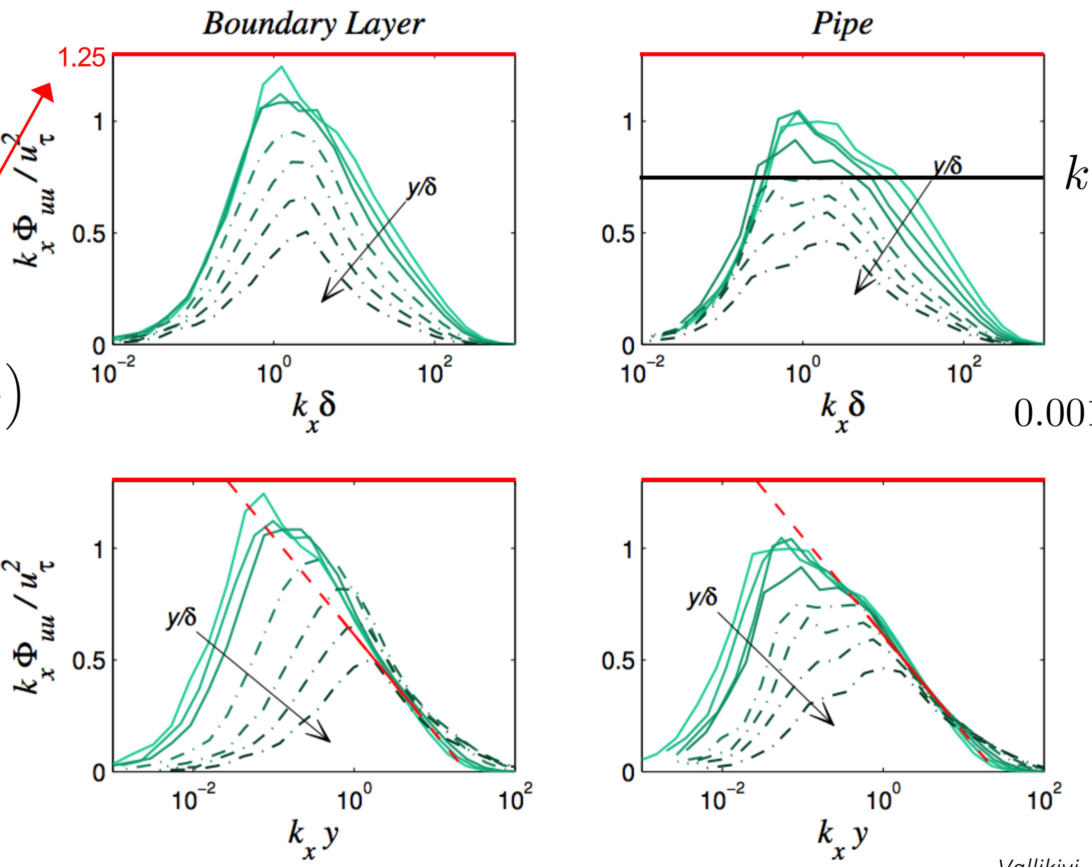

k^{-1}

$0.001 < y/\delta < 0.5$

Vallikivi, Ganapathasubramani & Smits (2015)

Pre-multiplied-1 spectra: $Re_\tau \approx 70{,}000$

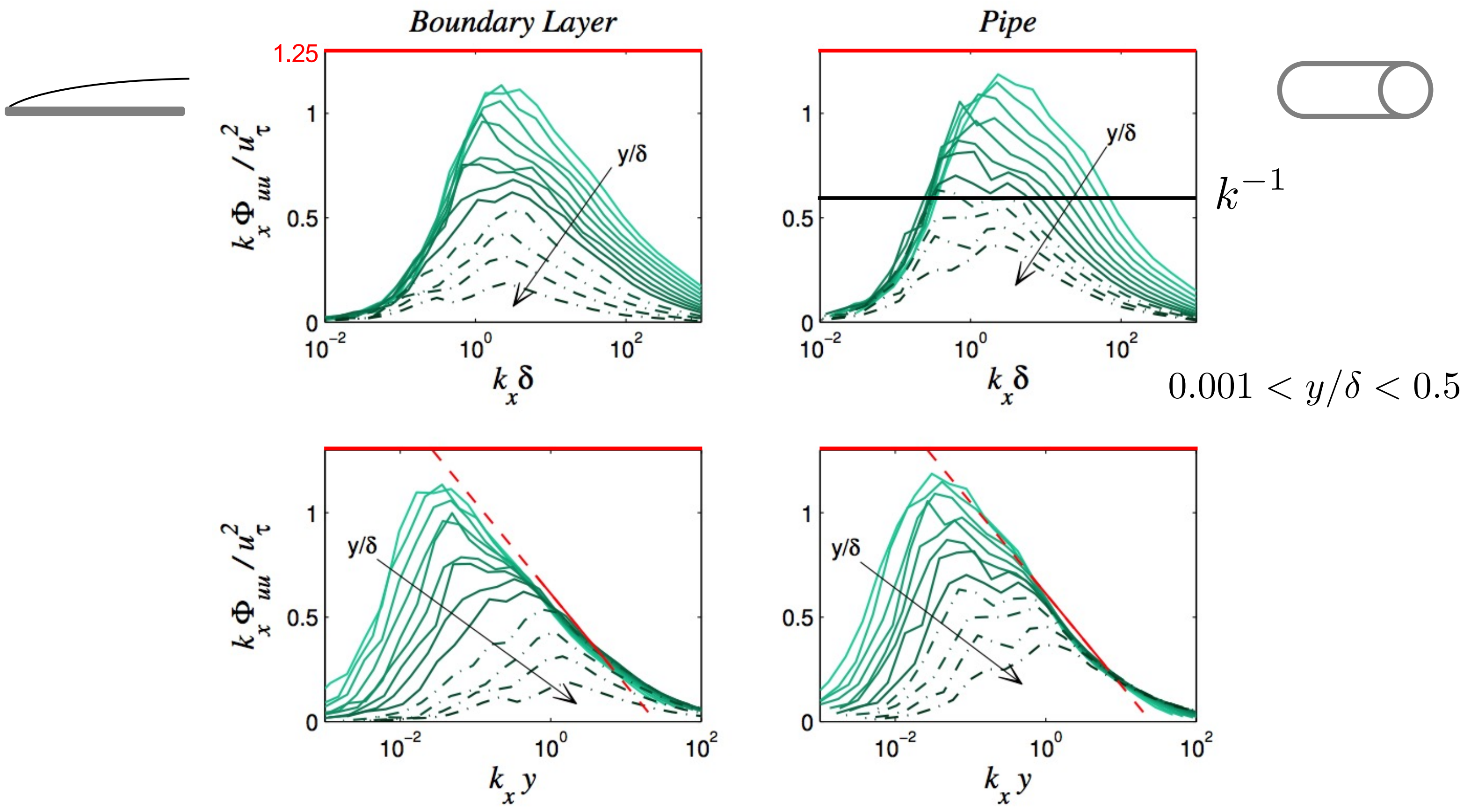

Growth of the inner peak

Inner Scaling

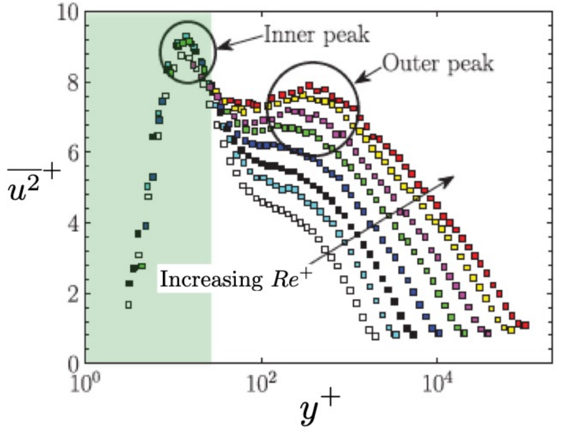

Something else is going on

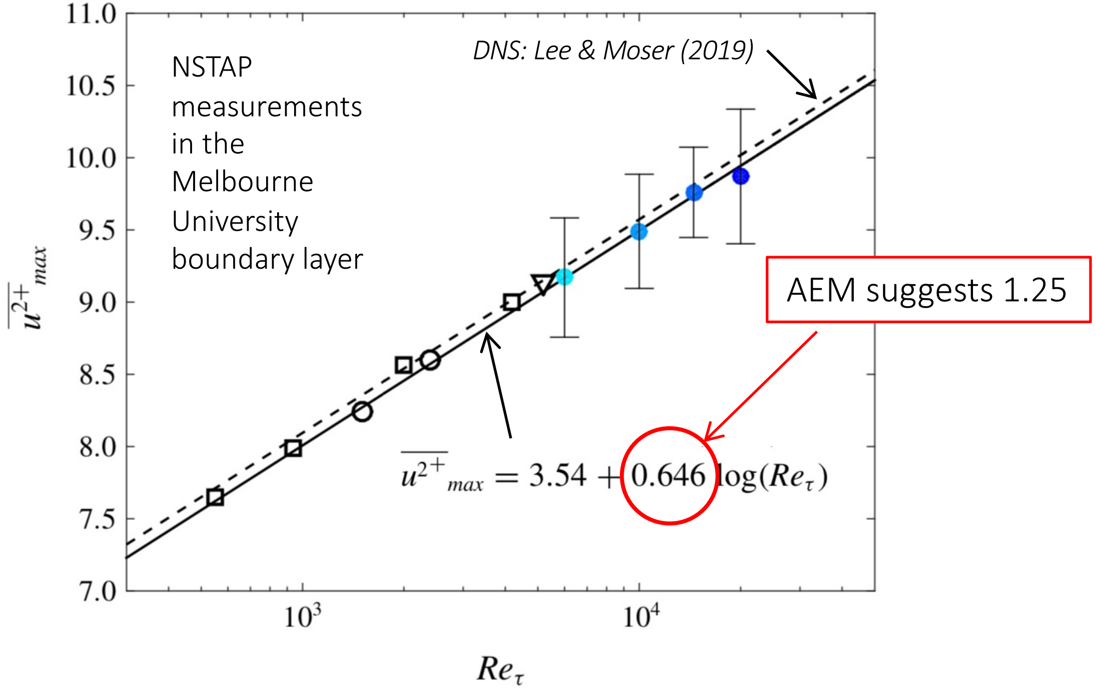

VLSMs and superstructures

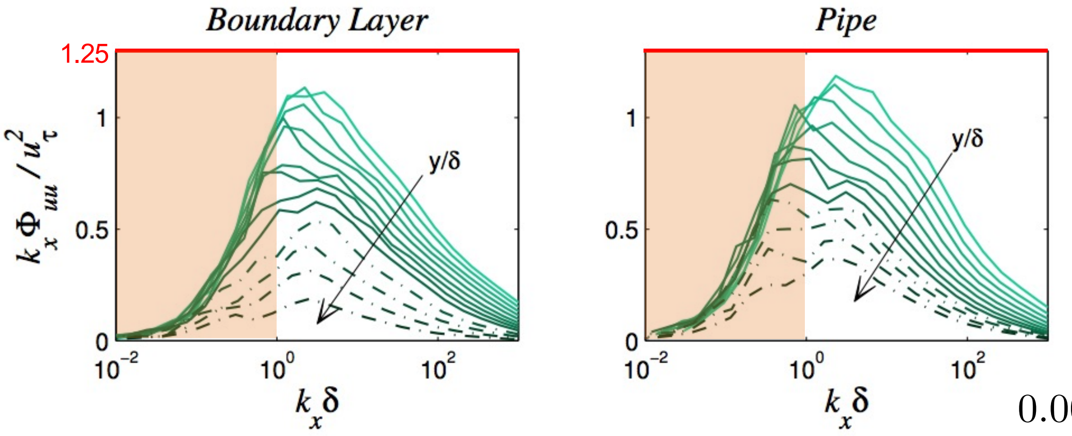

$0.001 < y/\delta < 0.5$

- Significant fraction of the energy is contained in region λ < δ
- Energy associated with these motions in pipe flow called “Very Large Scale Motions”
- In boundary layers they are often called “superstructures”

$u'/u_\tau, \ Re_\tau = 3472$

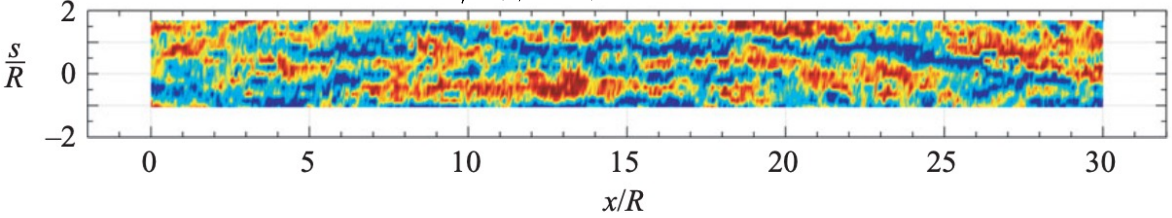

Kim & Adrian (1999)
Hutchins & Marusic (2007)
Monty et al. (2007)

Influence of outer layer motions on inner layer motions

- The outer region in the turbulent stress distributions scale with the outer length scale *δ, h, R*
- The inner region has a mixed scaling, indicating the influence of outer scale motions on inner scale motions
- The outer scale motions modulate and superimpose on the inner scale motions

Rao, Narasimha & Badri Narayanan (1971)
Blackwelder & Kovasznay (1972)
Brown & Thomas (1977)
Alfredsson & Johansson (1984)
Bandyophadyay & Hussain (1986)
Wark & Nagib (1991)
DeGraaff & Eaton (2000)
Metzger & Klewicki (2001)
Abe, Kawamura & Choi (2004)
Hoyas & Jimenez (2006)
Hutchins & Marusic (2007)
Schlatter et al (2009)
George & Tutkun (2009)
Chung & McKeon (2010)
Buschmann & Gad-el-Hak (2010)
and others..

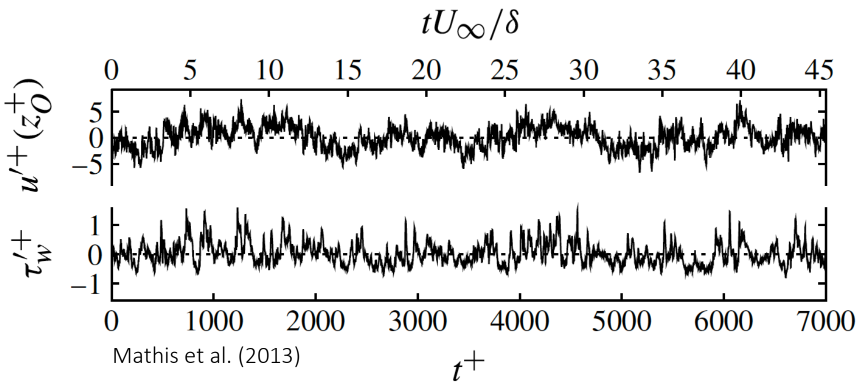

Log region

At the wall

Mathis et al. (2013)

$Re_\tau = 4480$

Outer scale motions modulate and superimpose on near-wall motions

Marusic et al. (2010)

DNS: $Re_\tau = 2003$; Hoyas & Jimenez (2006)

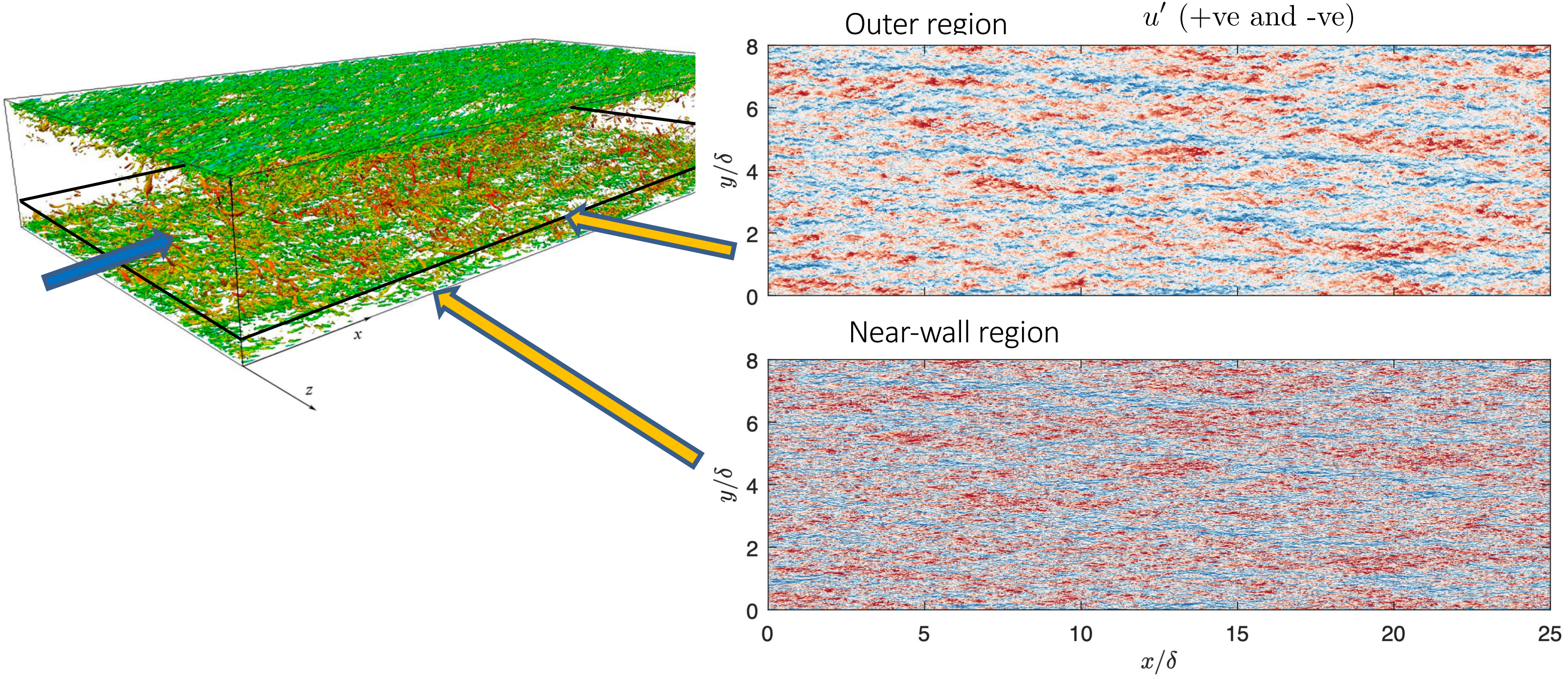

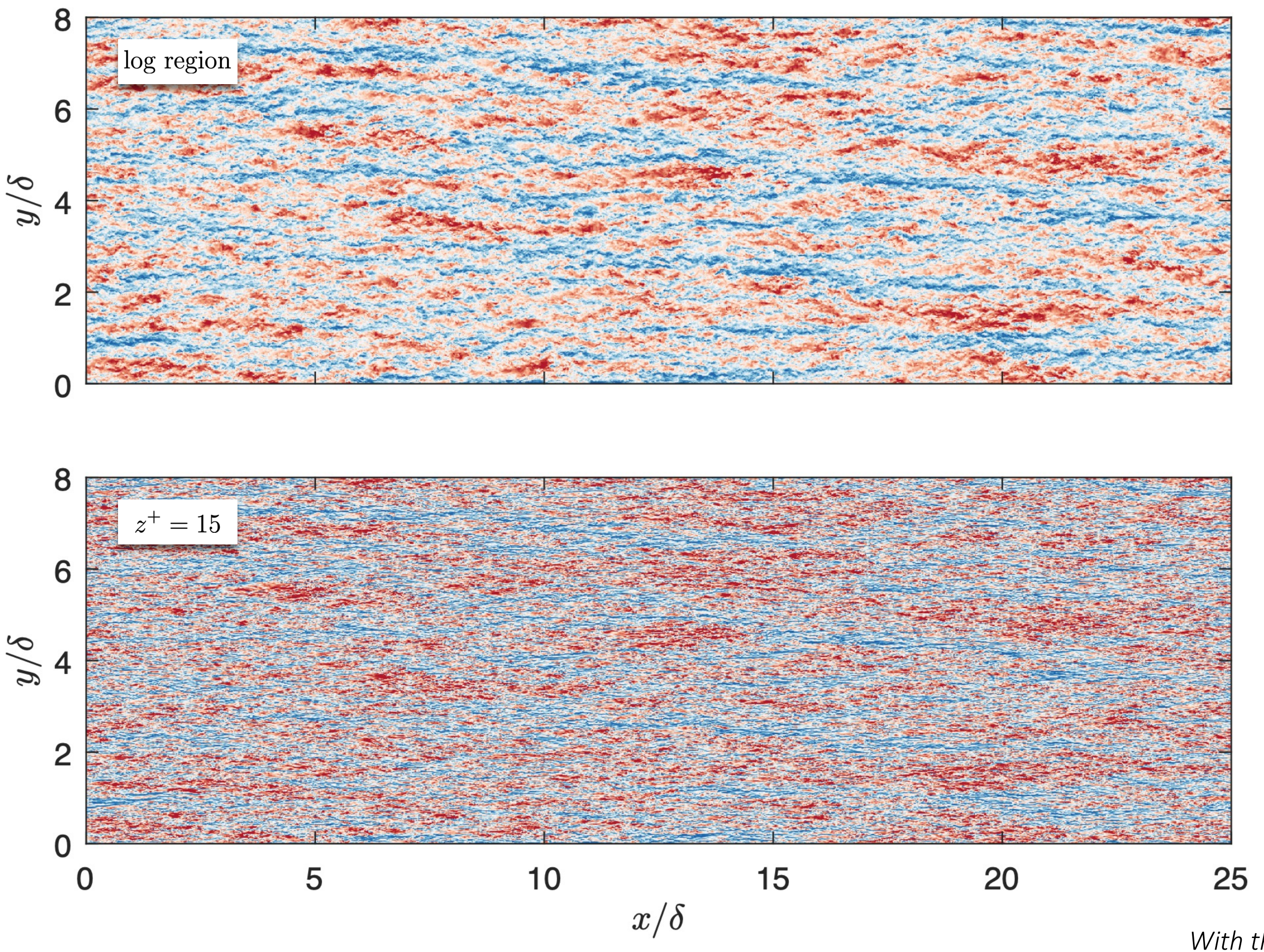

Outer region

Inner region

With thanks to Ivan Marusic

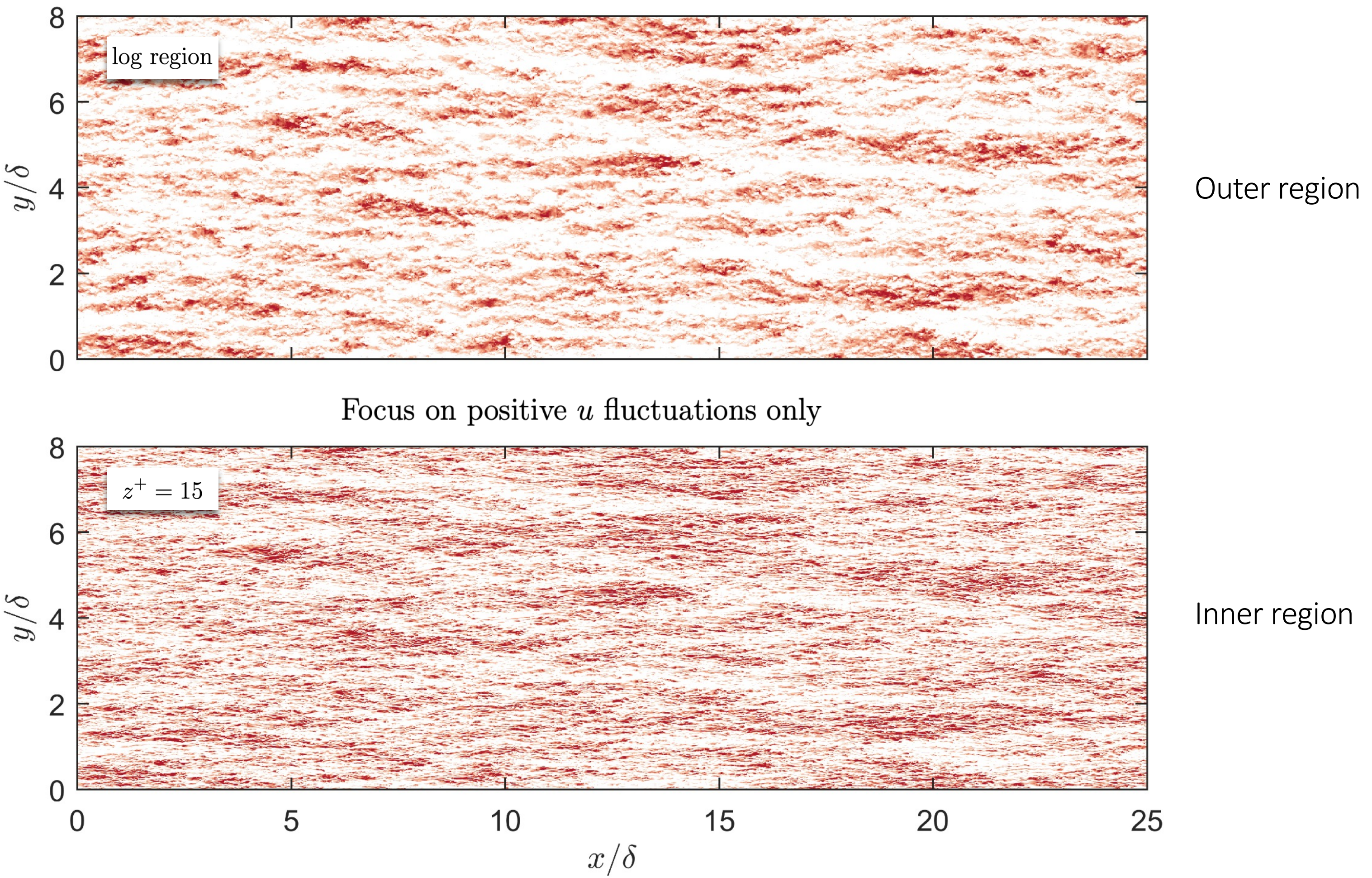
log region
Outer region
Focus on positive u fluctuations only
z+ = 15
Inner region
y/δ
x/δ
0
5
10
15
20
25
0
2
4
6
8

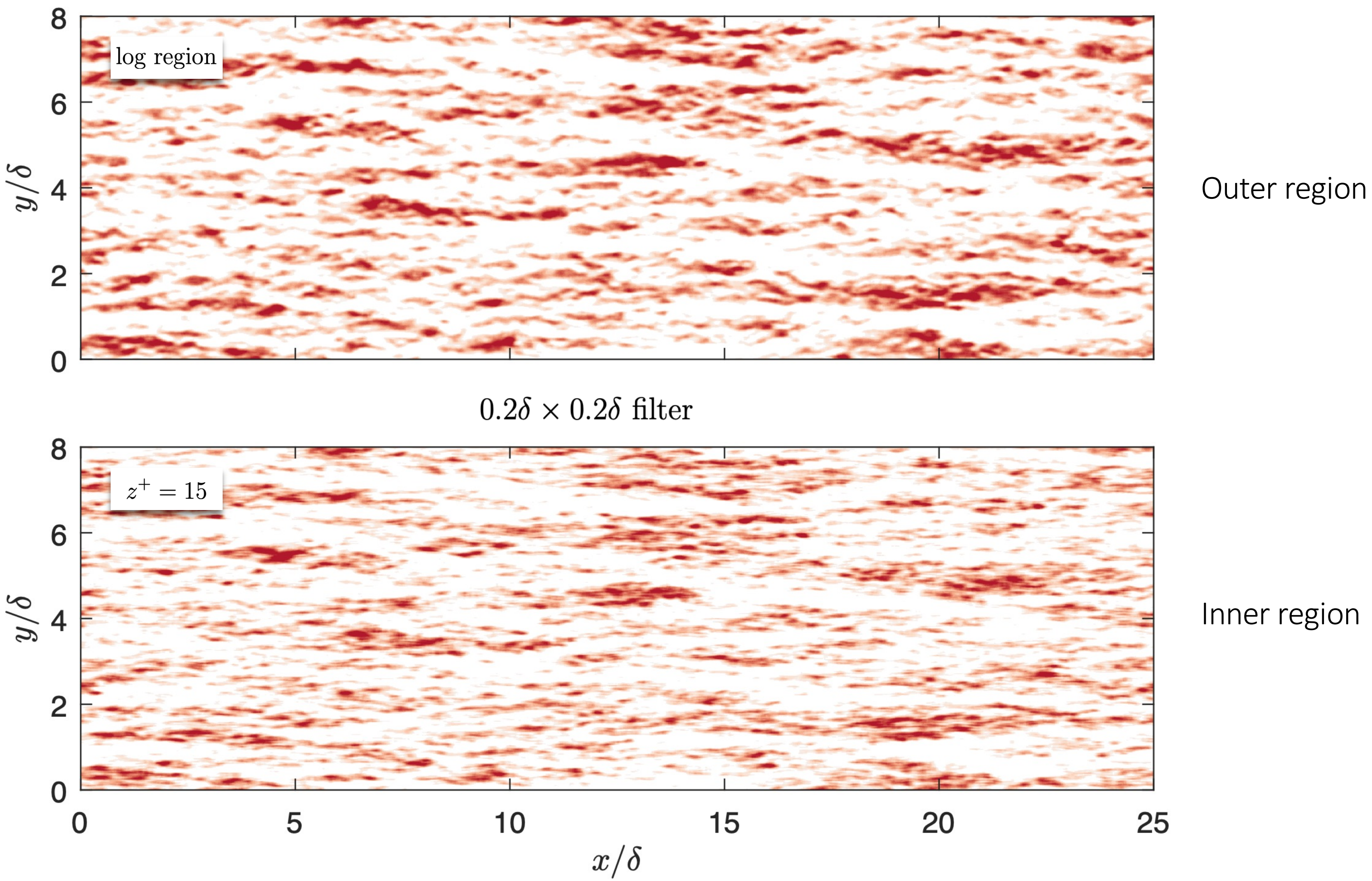

log region
$z^+ = 15$
$0.2\delta \times 0.2\delta$ filter
y/δ
x/δ
0
2
4
6
8
0
5
10
15
20
25
Outer region
Inner region

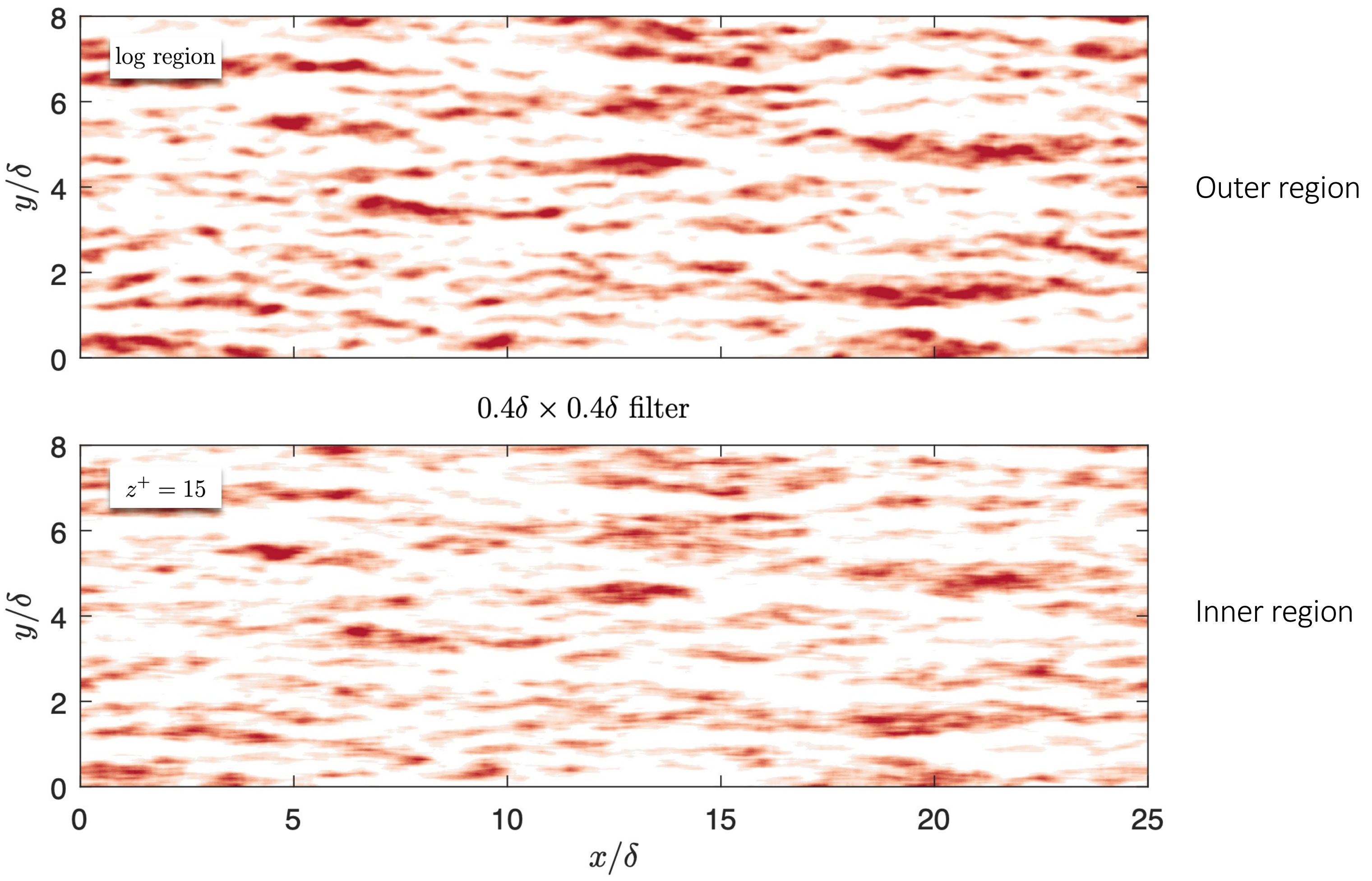
log region
$0.4\delta \times 0.4\delta$ filter
$z^+ = 15$
y/δ
x/δ
0
2
4
6
8
0
5
10
15
20
25
Outer region
Inner region

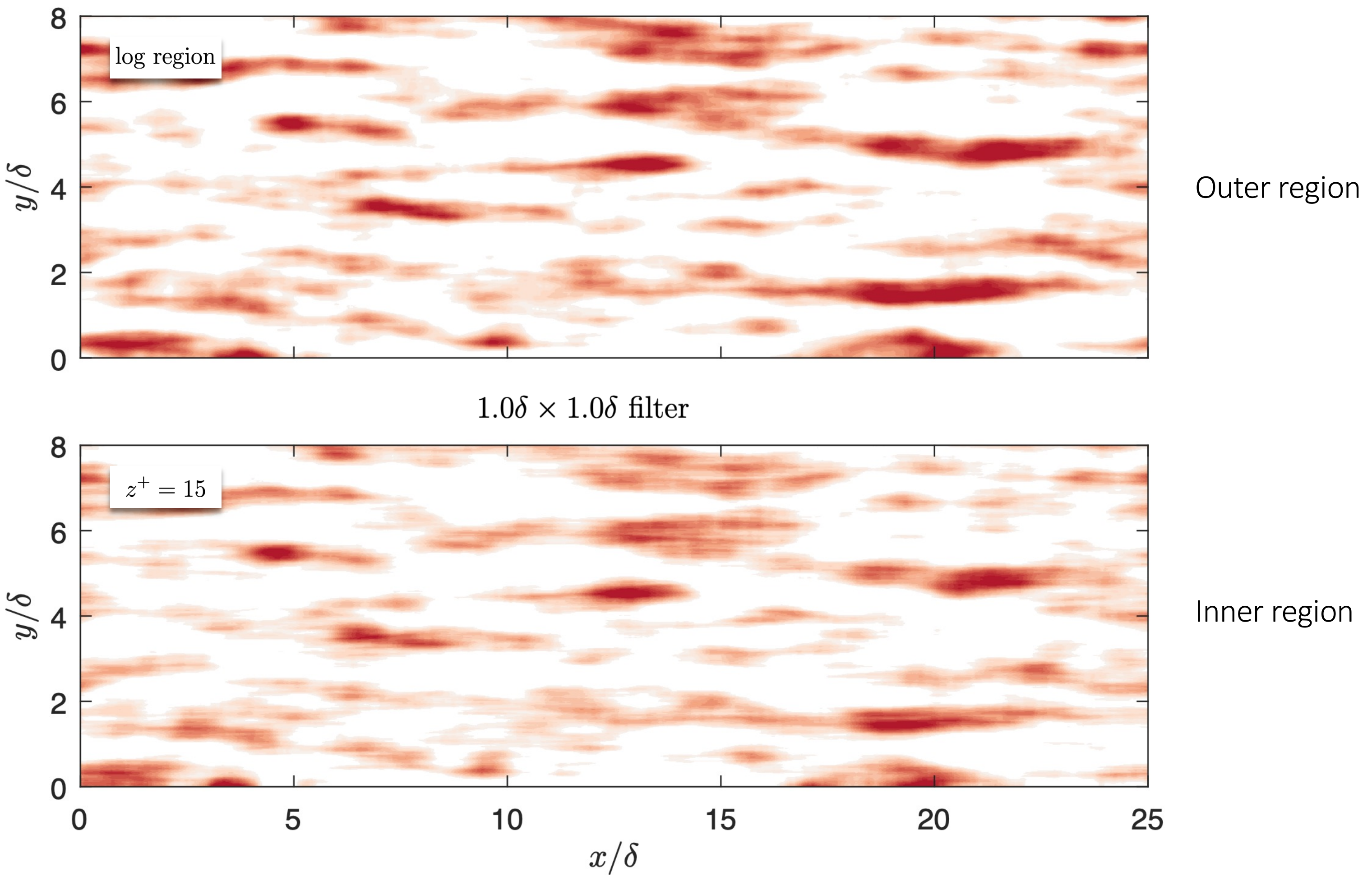
log region
$z^+ = 15$
$1.0\delta \times 1.0\delta$ filter
y/δ
x/δ
0
2
4
6
8
0
5
10
15
20
25
Outer region
Inner region

Wall-shear stress spectra with increasing Reynolds number

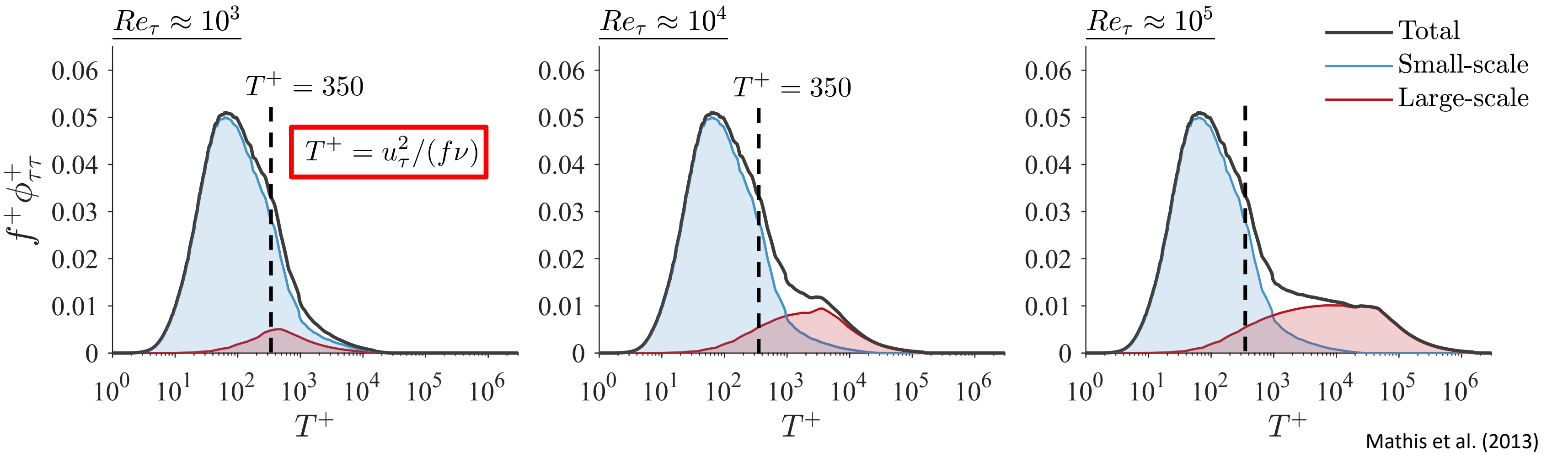

Mathis et al. (2013)
Chandran et al. (2020)

- We consider $T^+ < 350$ to be associated with inner-scaled motions, and $T^+ > 350$ with outer-scaled motions
- Outer-scaled motions contribute more and more to the wall shear stress fluctuations with increasing Re_t
- Targeting outer-scale motions gives new pathway to drag reduction at high Reynolds number (Marusic et al. 2021)

Growth of the inner peak

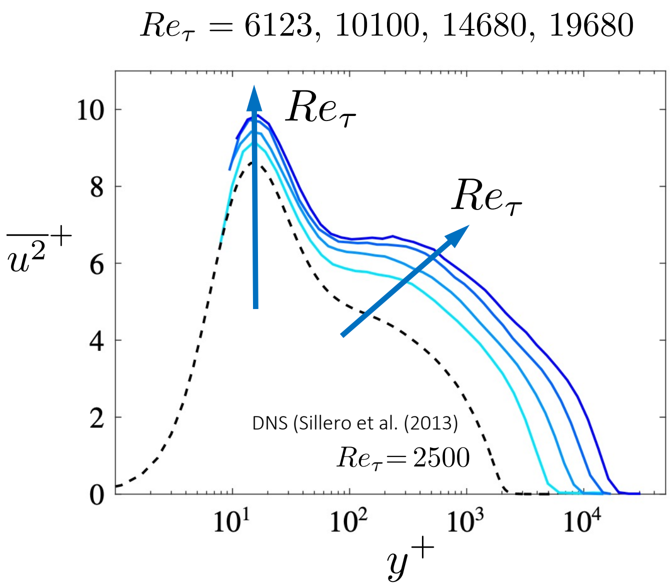

- Superstructures and VLSM
- Growth of the inner peak reflects the influence of the outer layer motions on the inner layer
- Modulation and superimposition
- Outer layer scales on δ
- Inner layer has mixed scaling
- Transition between inner and outer regions often called the meso-layer
- Power law in mean velocity

POD analysis of VLSM

Pipe flow

$Re_\tau = 354$

$y = 0.2$

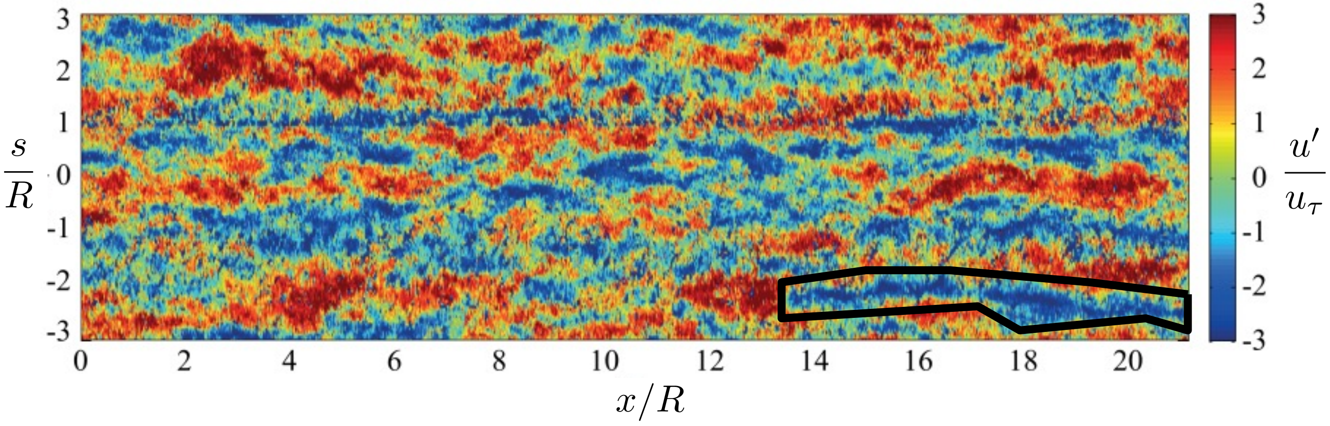

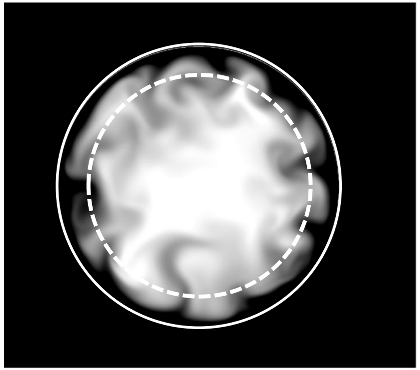

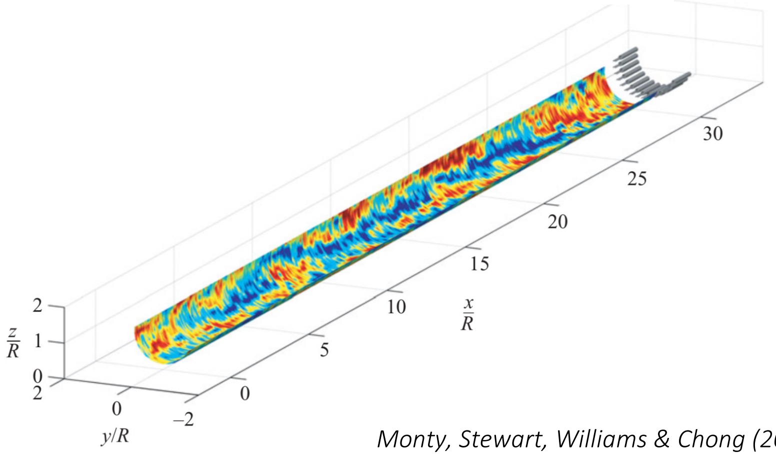

Hellström et al. (2011, 2015, 2016), Hellström & Smits (2014)

Monty, Stewart, Williams & Chong (2007)

Energy distribution among POD modes

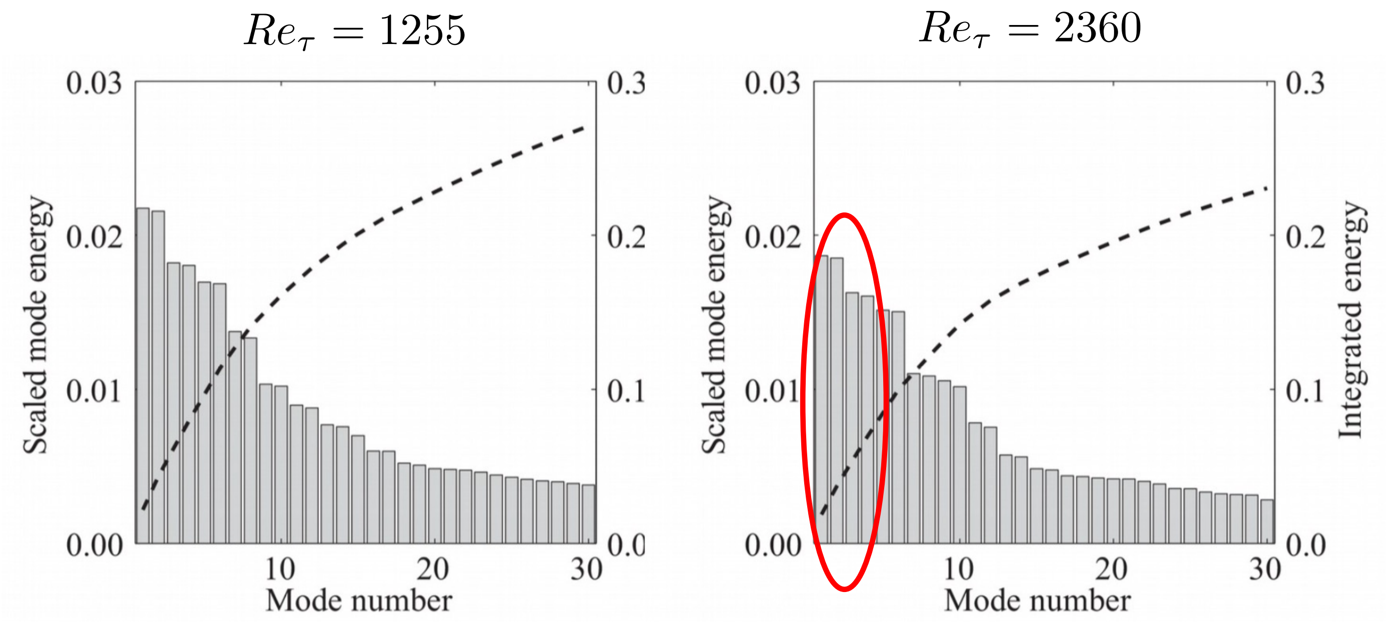

- We expect the VLSM to be the most energetic structures
- First 16 modes come in pairs
- The first 10 modes contain 15% of total energy

POD mode contribution to shear stress

- First 10 most energetic modes also contain 43% of the integrated Reynolds shear stress

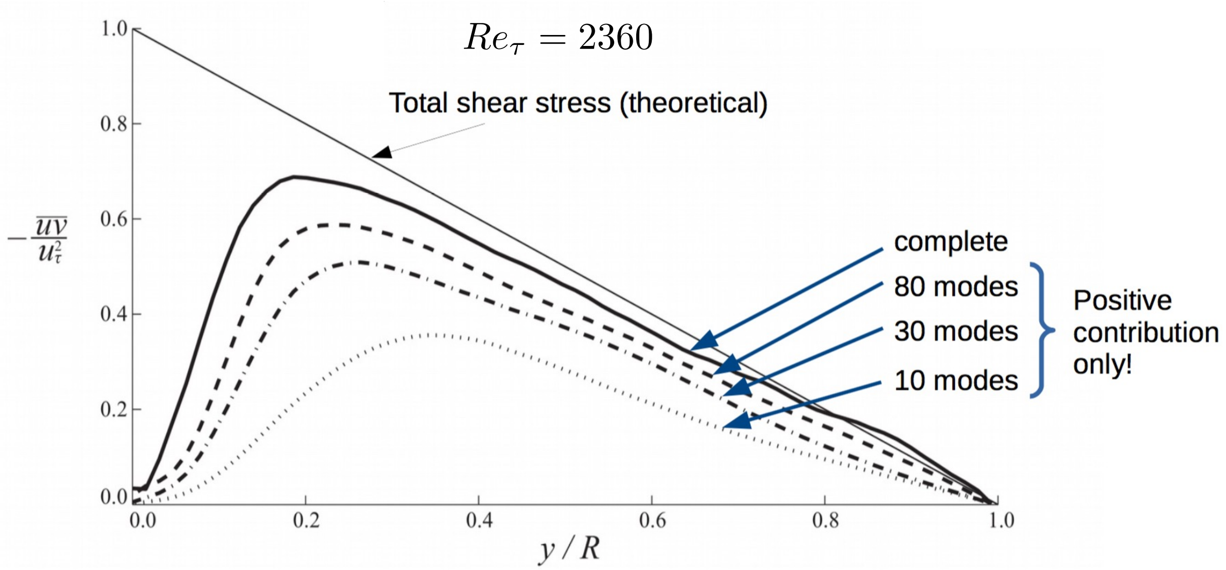

POD mode contribution to shear stress

- First 10 most energetic modes also contain 43% of the integrated Reynolds shear stress
- Superposition of the first few most energetic modes may reconstruct the structures

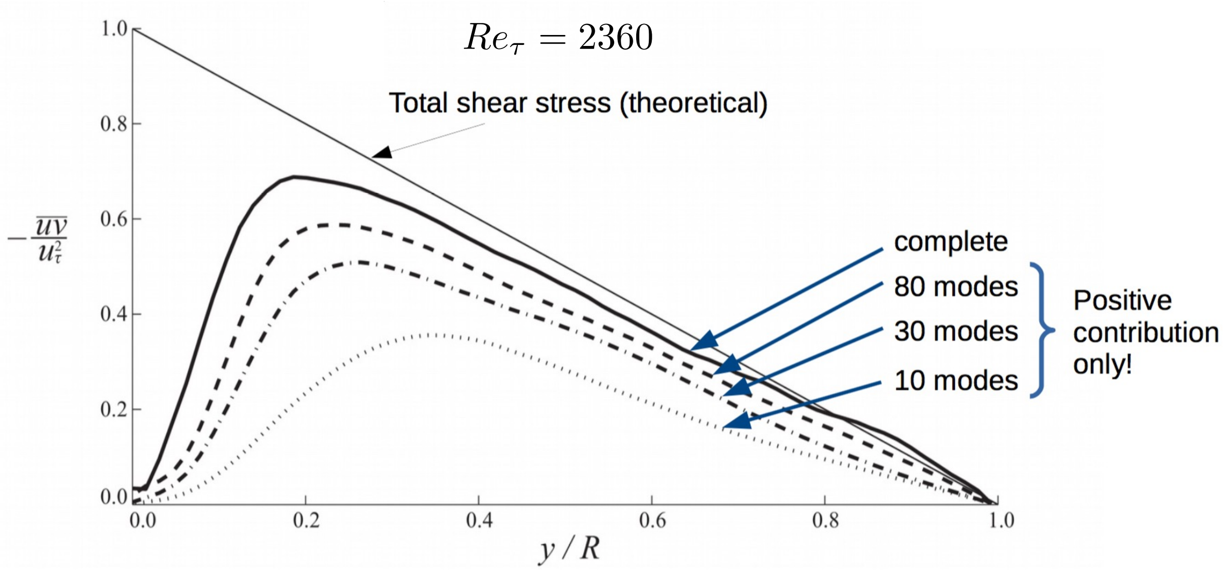

Reconstructed POD modes

Original velocity field

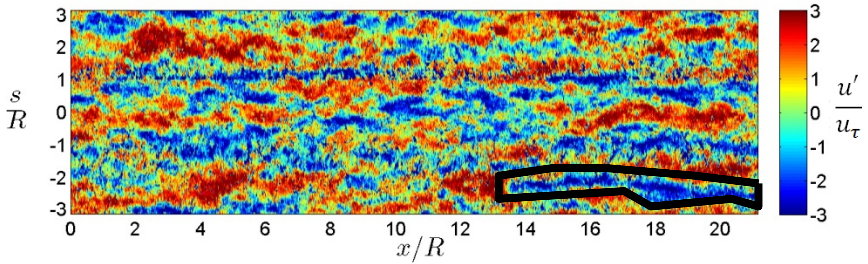

Reconstructed mode 1

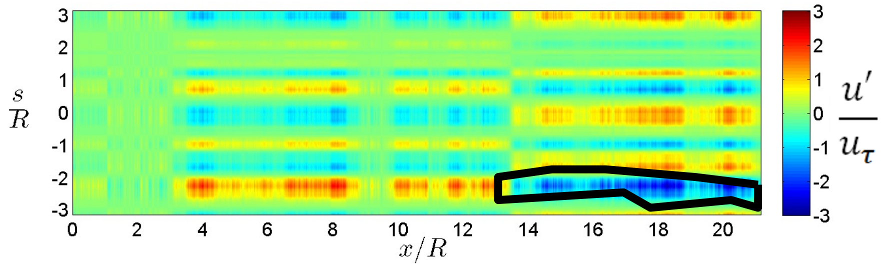

Reconstructed mode 2

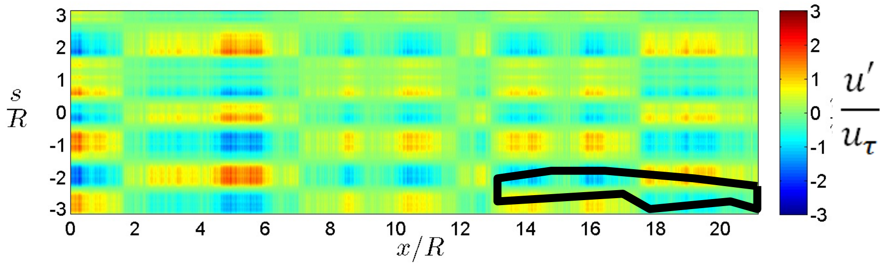

POD mode superposition

Original velocity field

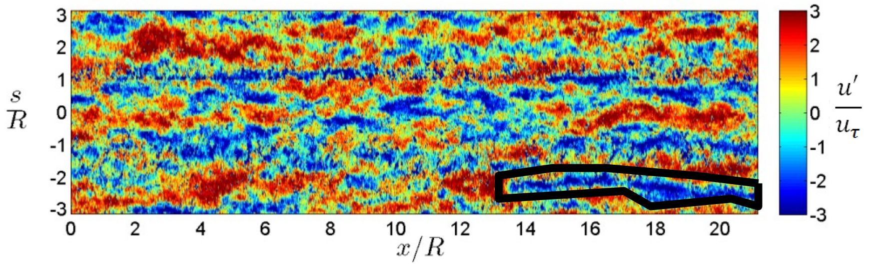

Superimposed 4 modes

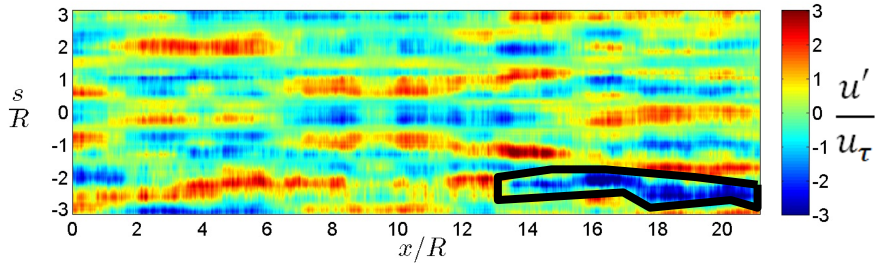

Superimposed 10 modes

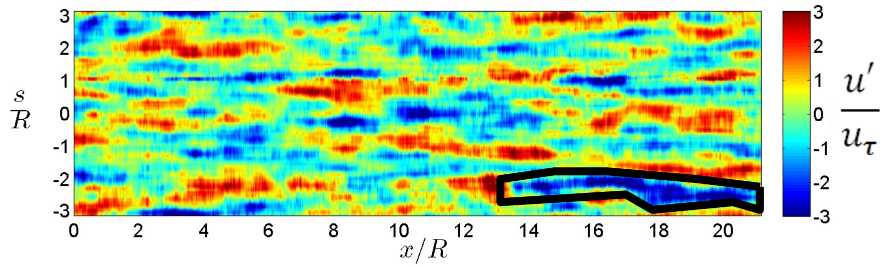

Ordering by azimuthal mode

Energy content of the first 15 azimuthal modes

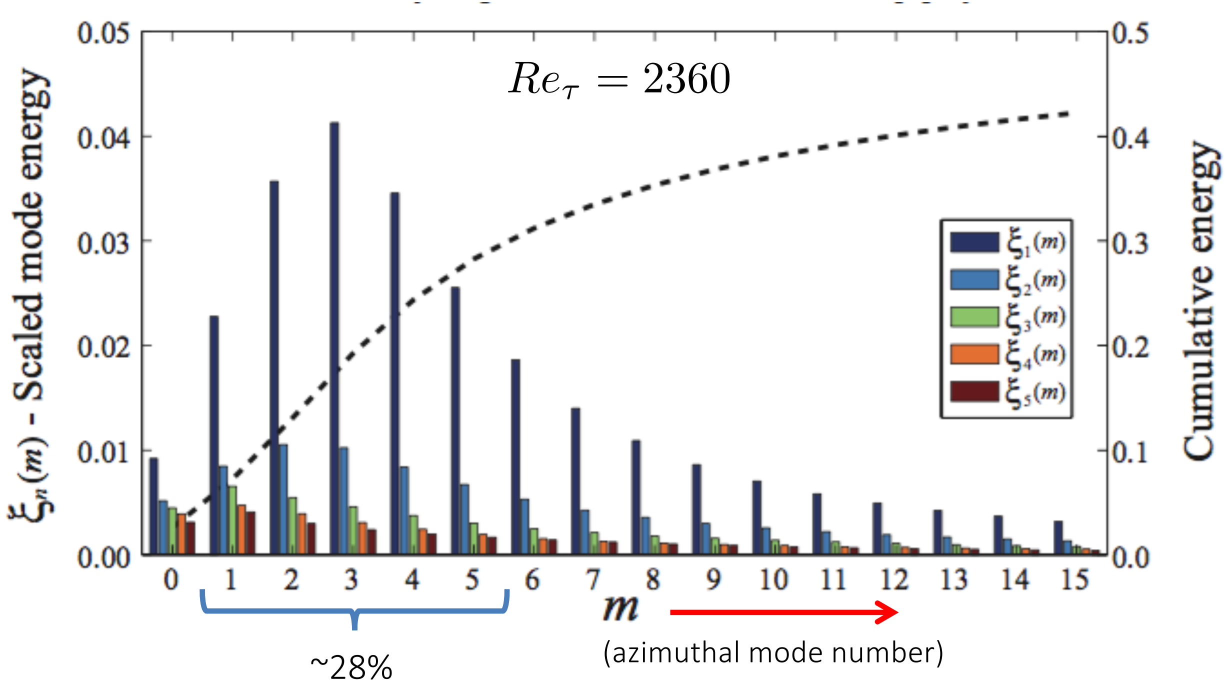

Ordering by azimuthal mode

Energy content of the first 15 azimuthal modes

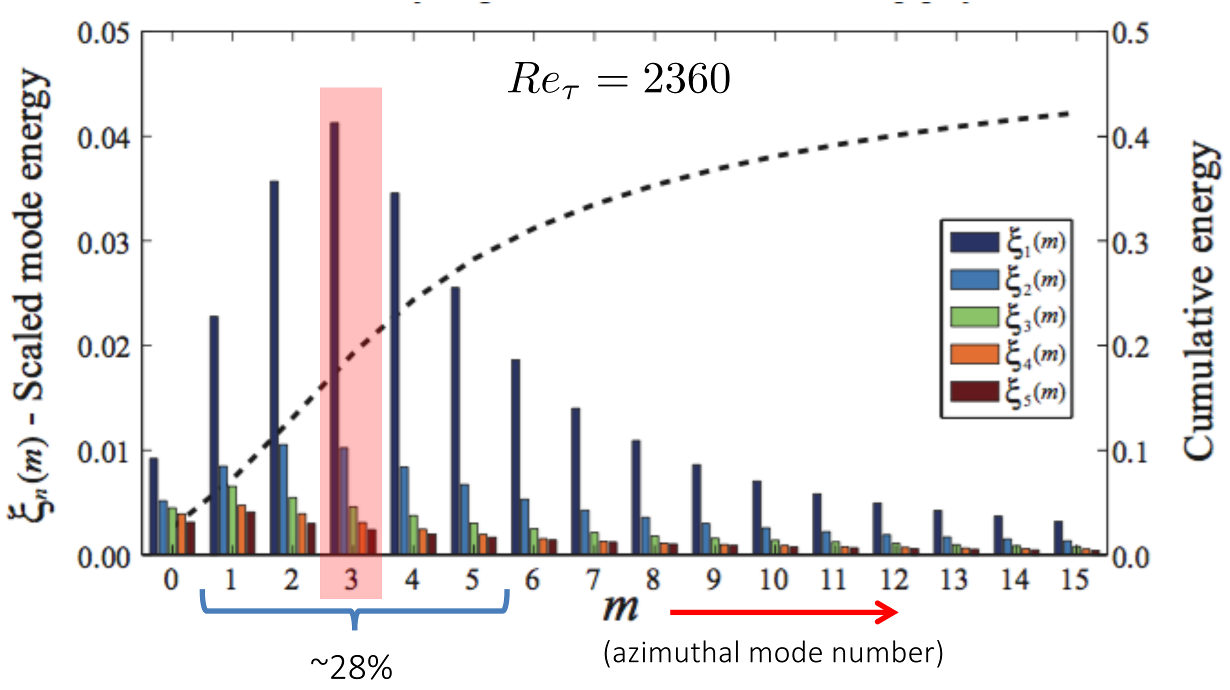

Azimuthal mode m = (3)

Positive contribution to the Reynolds shear stress, (-u'v')

Azimuthal mode number m = (3)

$Re_\tau = 2360$

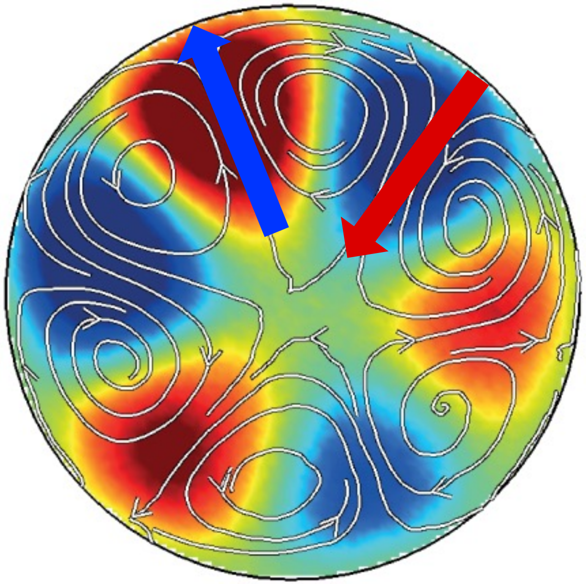

sPOD Mode 1

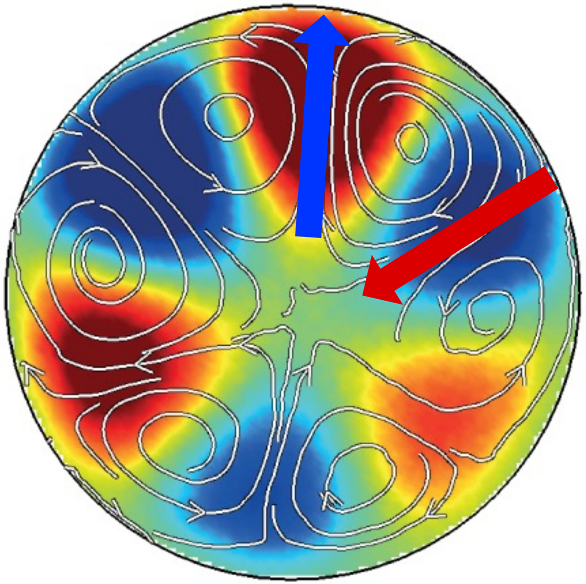

sPOD Mode 2

u' < 0

u' > 0

Azimuthal mode m = (2)

Positive contribution to the Reynolds shear stress, (-u'v')

Azimuthal mode number m = (2)

$Re_\tau = 2360$

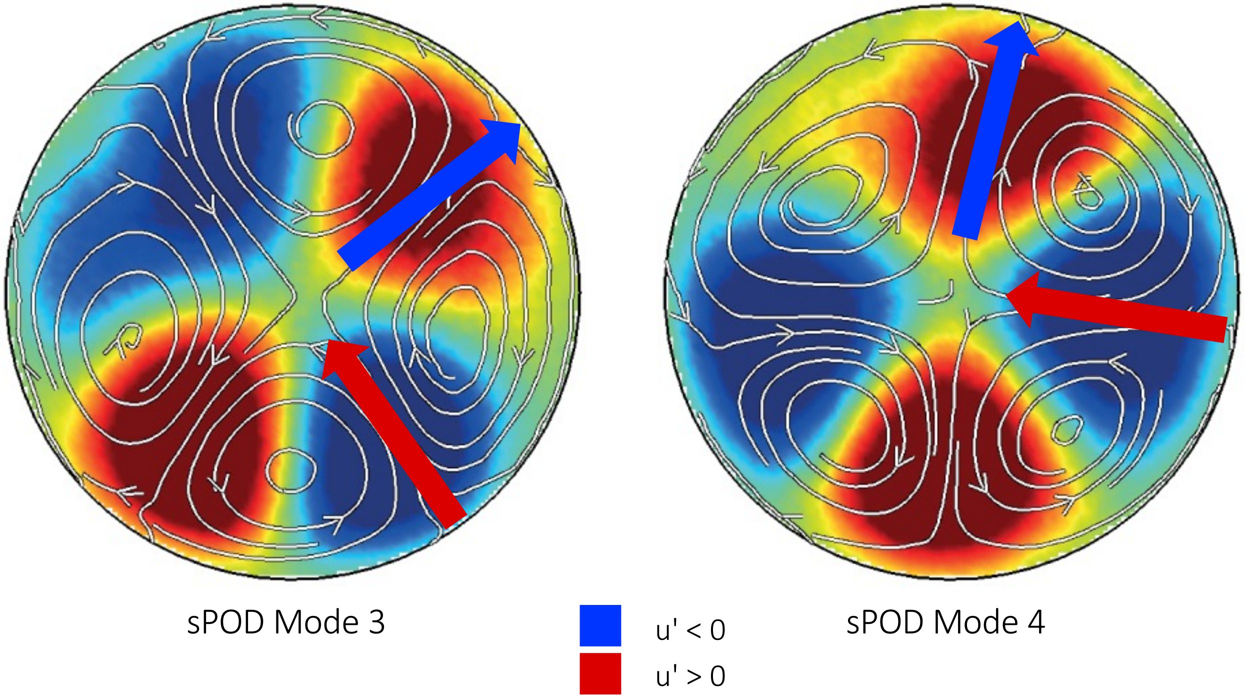

Azimuthal mode self similarity

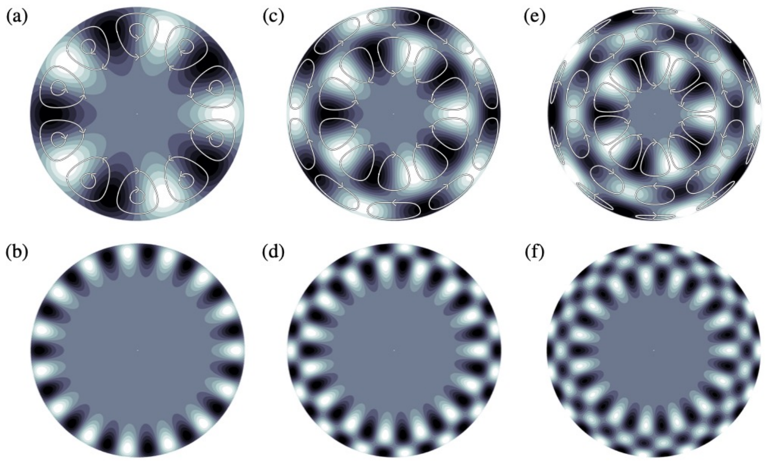

FIGURE 3. Contour plots of the streamwise component of sample POD modes for $Re_\tau = 2460$, where white and black represent positive and negative values, respectively. The streamlines indicate the in-plane component of the POD modes, $\Phi^{(n)}(m;r)$. (a) $\Phi^{(1)}(5;r)$; (b) $\Phi^{(1)}(15;r)$; (c) $\Phi^{(2)}(5;r)$; (d) $\Phi^{(2)}(15;r)$; (e) $\Phi^{(3)}(5;r)$; (f) $\Phi^{(3)}(15;r)$.

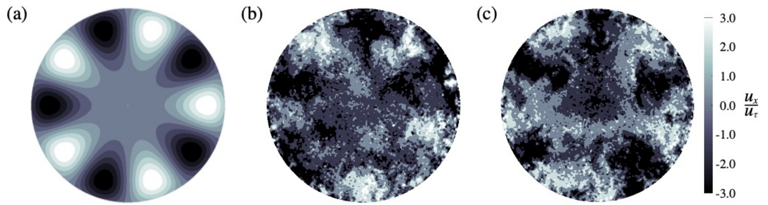

FIGURE 4. Activity of the POD modes in the instantaneous velocity field. (a) the streamwise component of $\Phi^{(1)}(5;r)$. (b) and (c) show the instantaneous streamwise velocity fluctuations at data block 6 and images 900 and 2108, respectively. $Re_\tau = 2460$

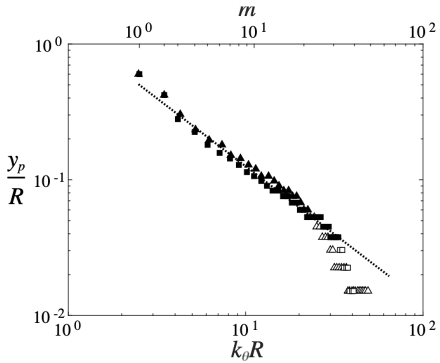

FIGURE 5. Modal peak location for the first POD mode ($n = 1$) and azimuthal modenumbers $m \in [1,\ 64]$. ▲ $Re_\tau = 1330$; ■ $Re_\tau = 2460$; $\cdots\cdots$ $y_p/R = 2\pi C\ (k_\theta R)^{-1}$, with $C = 0.2$. Modes with a peak location $y_p^+ < 75$ are identified with open symbols. The lower abscissa indicates the azimuthal wave number, while the upper abscissa shows the corresponding azimuthal mode number, for $Re_\tau = 2460$.

Two-plane PIV

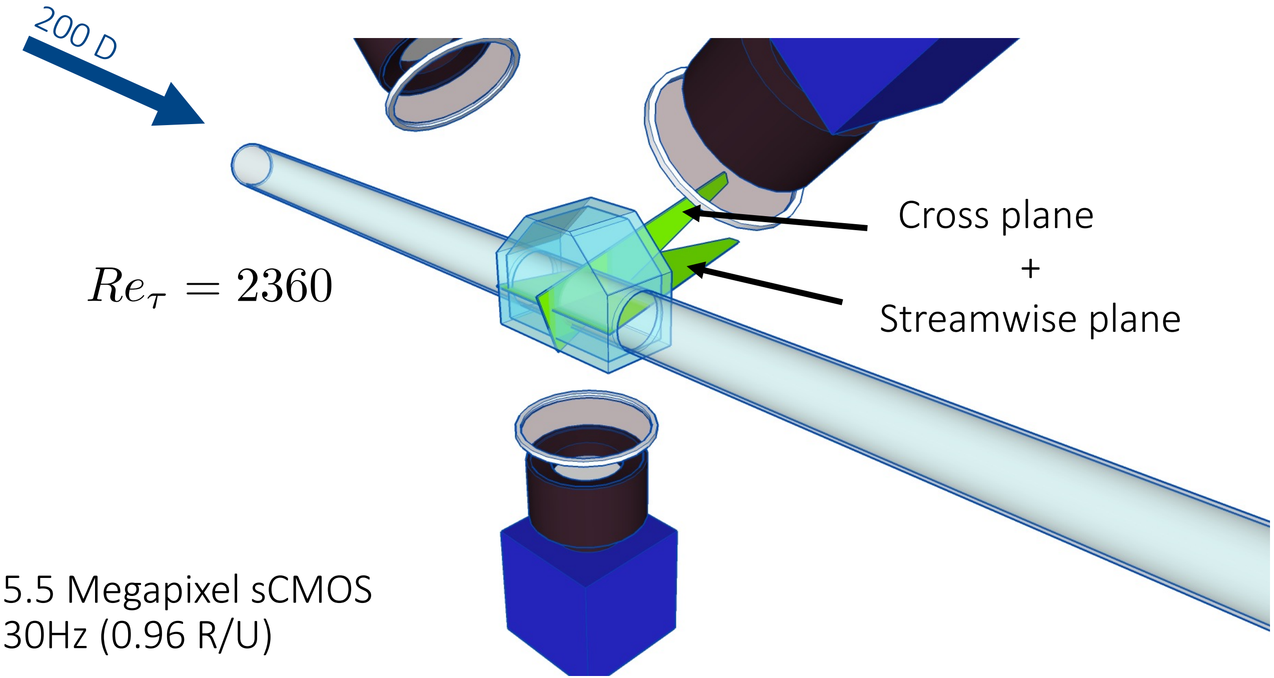

- 5.5 Megapixel sCMOS
  30Hz (0.96 R/U)
- 22000 Snapshots

Hellström, Ganapathisubramani & Smits (2015)

Cross-correlation of $\alpha_1(3,t)$ with all other coefficients

$$\rho(m_1,m_2,n_1,n_2,\tau)=\frac{\left(\alpha_{n_1}(m_1,t)\ ,\ \alpha_{n_2}(m_2,t+\tau)\right)}{\|\alpha_{n_1}(m_1,t)\|\,\|\alpha_{n_2}(m_2,t)\|}$$

Which mode comes before?

(downstream)

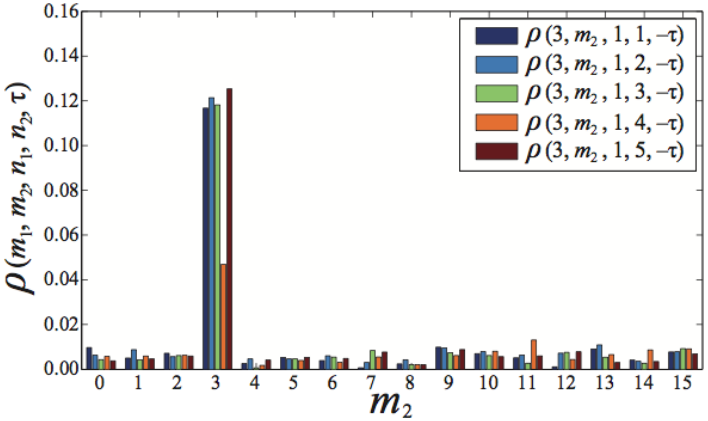

Which mode comes after?

(upstream)

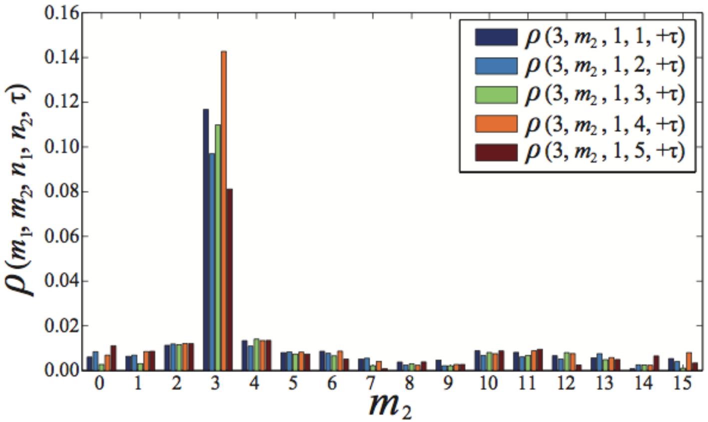

- Within $\pm$ R, the structures either remain the same, or they transition to a higher order POD mode with the same azimuthal mode number but a different radial mode number.

Conditional mode shown for $(m,n) = (3,1)$

Φ^{n}_{cond} = < $u_i(x,r,\theta,t)$ | $\{\alpha^n > \alpha^n_{rms}\}$ >

α^n is the coefficient for Φ^{n}_{SPOD}

(cross-stream plane)

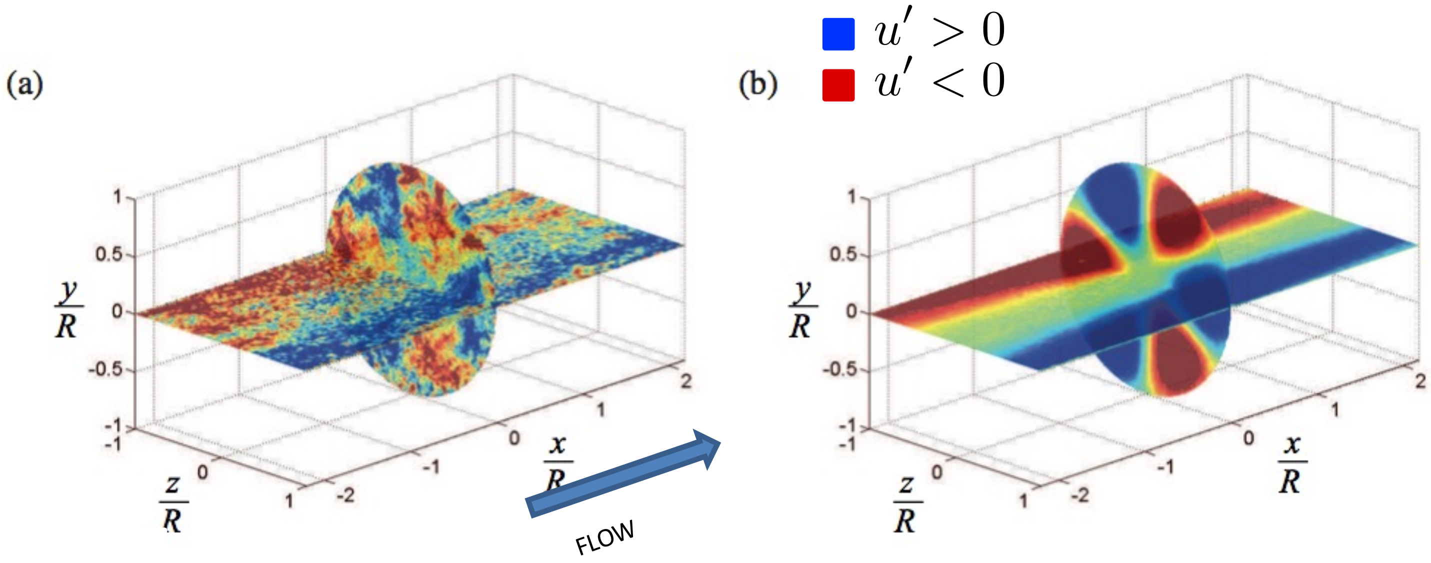

Instantaneous velocity field

Conditional mode

Where do the VLSM come from?

Conditional mode m = *3*

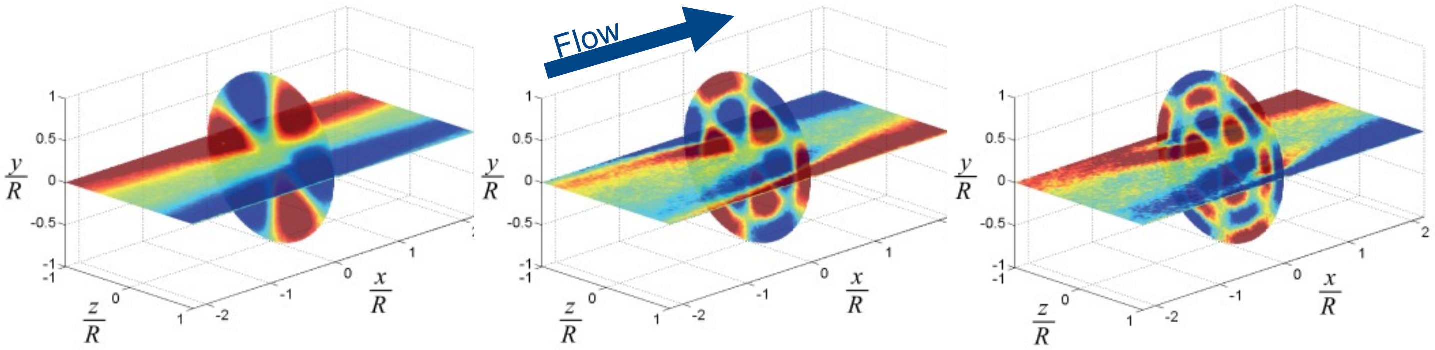

$\Psi_{(3,1)}(x,r,\theta)$ $\Psi_{(3,2)}(x,r,\theta)$ $\Psi_{(3,3)}(x,r,\theta)$

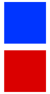

$u' < 0$
$u' > 0$

- Transition between these modes will appear as an azimuthal phase shift but it is caused by a radial displacement

Where do the VLSM come from?

Conditional mode *m = 4*

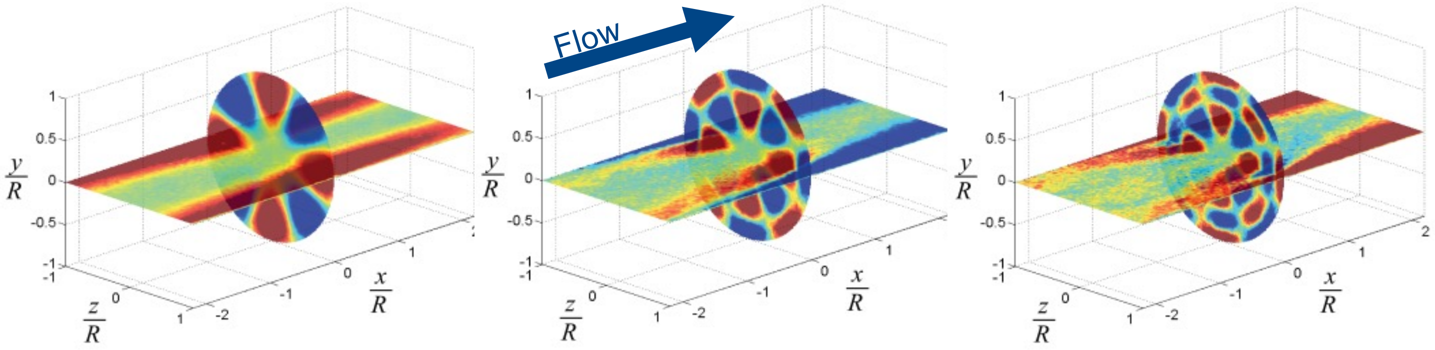

$\Psi_{(4,1)}(x, r, \theta)$ $\Psi_{(4,2)}(x, r, \theta)$ $\Psi_{(4,3)}(x, r, \theta)$

- Blue: $u' < 0$
- Red: $u' > 0$

- Transition between these modes will appear as an azimuthal phase shift but it is caused by a radial displacement

Conclusions

- The dual plane conditional modes show structures starting at the wall, growing towards the wake region, detach and vanish.
- The structure associated with POD mode $\Phi^{(n)}(r,3)$ exist for ≈2R, after which a transition occurs.
- The conditional modes show a radial evolution of the structures.
- The VLSM consist of an alignment of 2-3 structures.
- The long VLSM wavelength is due to a structure repetition, rather than azimuthal meandering.
- The meandering is primarily due to the superposition of structures with different azimuthal mode number (m)

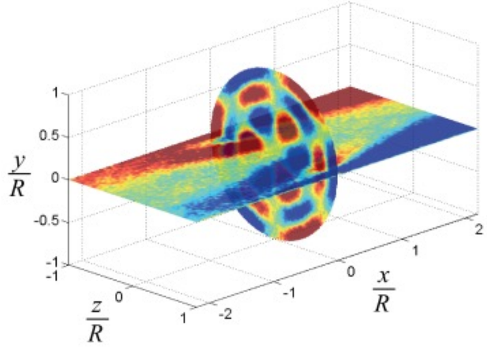

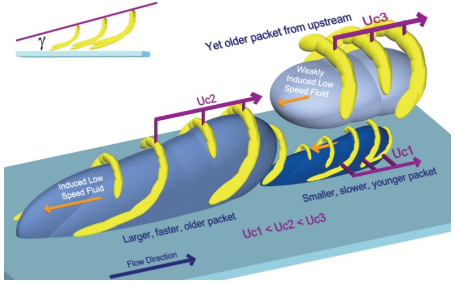

Summary: incompressible pipe and boundary layers

- A log-law in turbulence is found to occur in the same region where the log-law in mean velocity is found, in accordance with AEM, but only for $Re^+ > 10,000$
- Von Karman constant value needs DNS
- A mesolayer exists as a blending region between the wall-scaled region and the y-scaled region (only evident at high Reynolds number)
- Inner peak increases logarithmically with Re_τ, but slower than expected for AEM
- Outer peak appears for $Re_\tau > 10,000$
- Spectra asymptote very slowly to-5/3
- No k^{-1} region at these Reynolds numbers, not in accord with spectral overlap argument
- Number of UMZ's increases logarithmically with Re^+, but slower than hierarchy count

- The increasing dominance of the VLSM may be disrupting the AEM at higher Reynolds number
- New developments in AEM are extending its range

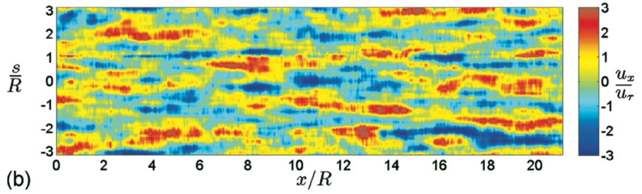

Hellstrom, Sinha & Smits (2011)

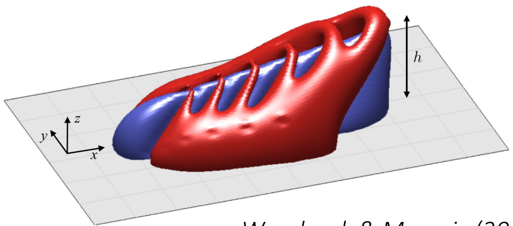

Woodcock & Marusic (2015)

Beyond canonical flows

- Flat plate zero pg flow, or fully developed pipe/channel flows are canonical but singular cases
- Need to move beyond canonical flows
- Wall-bounded turbulence includes roughness, pressure gradients, surface curvature, three-dimensional flows, separation, blowing, suction, etc.
- Much work was done in the past, but the last 20 years or so the basic research community seems to have focused on canonical cases (including me)

- We may have reached a point of diminishing returns in studying canonical flows

Questions?